Technische Universität München
TUM School of Natural Sciences

Sustainable biosynthesis of modified fatty acids for industrial applications using oleate hydratases

Sophia Alice Prem

Vollständiger Abdruck der von der TUM School of Natural Sciences der Technischen Universität München zur Erlangung einer Doktorin der Naturwissenschaften (Dr. rer. nat.) genehmigten Dissertation.

Vorsitz: Prof. Dr. Tom Nilges

Prüfer*innen der Dissertation:

1. Prof. Dr. Thomas Brück
2. apl. Prof. Dr. Wolfgang Eisenreich
3. Prof. Dr. Robert Kourist

Die Dissertation wurde am 13.09.2023 bei der Technischen Universität München eingereicht und durch die TUM School of Natural Sciences am 17.10.2023 angenommen.

I. Abstract

The increasing human population and growing affluence have increased the demand for consumer goods. This has resulted in adverse impacts on nature, including increased land use, chemical pollution, and biodiversity loss. To address these challenges and the need for a sustainable industrial transition for production processes of commodity goods, current research efforts are focused on finding less energy-intensive methods that have reduced impacts on biodiversity and land use.

One example is the biosynthesis of 10-hydroxy stearic acid (10-HSA) from oleic acid, a starting material for other high-value bio-based materials with potential applications in cosmetic and lubricant industries.

Its biosynthesis can be carried out using oleate hydratases (OH), which are hydro-lyases that have shown high expression rates in soluble form. Oleic acid, the main component of sustainable plant oils such as rapeseed, sunflower, and olive oil, can also be readily sourced more sustainably from microbial oil using oleaginous yeasts or bacteria.

This thesis presents the sustainable bioconversion of microbial oils to oleic acid and further to 10-HSA as well as the oxidized form of 10-HSA, 10-keto stearic acid (10-KSA) using tailored reaction cascades. First, a new OH was identified and characterized, termed OhyPp, which was derived from the terrestrial bacterium *Pediococcus parvulus.* This enzyme expands the portfolio of monomeric OHs and allows further insights into their mechanisms. Despite sharing 74% sequence identity and 91% similarity with a reported OH enzyme termed OhyRe from *Rhodococcus erythropolis*, OhyPp exhibited distinct features. Furthermore, it belonged to the same monomeric protein family, Hfam3. The monomeric nature of OhyPp offers advantages for immobilization strategies.

The OhyPp's structure could be predicted using the reported templates as several crystallization attempts failed. Biochemical data indicated that the enzyme showed a higher affinity for flavin adenine dinucleotide (FAD) compared to OhyRe. However, its FAD affinity remains lower than desired. Interestingly, a flexible loop near the FAD binding site may contribute to the disparities in FAD affinities observed between OhyRe and OhyPp, shedding light on the binding properties of FAD and potential critical residues for binding.

In conclusion, further optimization is needed for OH enzymes to be effectively applied in industrial settings. The characterization of OhyPp provides valuable

information on its structural and catalytic features, contributing to the ongoing efforts to enhance OH enzymes for industrial applications.

The second part of the study focused on using OHs in cascade reactions for industrial applications. The analysis optimized the 10-HSA product yields of the reference enzyme OhyRe by exposing it to broad-band white light, which significantly increased activity. The first delineated cascade reaction involved converting triglyceride oils using lipase and OhyRe resulting in varying yields of 10-HSA depending on the triglyceride oil source. A second cascade reaction utilized a secondary alcohol dehydrogenase (secADH) to convert the primary reaction product 10-HSA to 10-keto stearic acid (10-KSA). Optimization and characterization of the cascade reactions and secADH were performed. The data demonstrates the potential of cascade reactions alongside OHs for catalyst optimization and future industrial applications.

In summary, this study presents the sustainable biosynthesis of 10-HSA and 10-KSA by OHs from microbial and plant oils, providing initial steps towards their industrial application.

II. Zusammenfassung

Die steigende Bevölkerungszahl und wachsender Wohlstand haben zu einer höheren Nachfrage nach Konsumgütern geführt. Dies hat negative Auswirkungen auf die Natur zur Folge, darunter erhöhter Flächenverbrauch, chemische Verschmutzung und Verlust der Artenvielfalt. Um diesen Herausforderungen gerecht zu werden, konzentrieren sich Forschungsbemühungen darauf, weniger energieintensive Prozesse zu finden, die geringere Auswirkungen auf die Artenvielfalt und den Flächenverbrauch haben.

Ein Beispiel dafür ist die Herstellung von 10-Hydroxystearinsäure (10-HSA) aus Ölsäure. Diese Säure dient auch als Ausgangsmaterial für hochwertige, bio-basierte Materialien mit möglichen Anwendungen in der Kosmetik- und Schmierstoffindustrie.

Der Herstellungsprozess kann mithilfe von Oleat-Hydratasen (OHs) durchgeführt werden, die eine hohe Expressionsrate in löslicher Form aufweisen. Ölsäure ist die Hauptkomponente nachhaltiger Pflanzenöle wie Raps-, Sonnenblumen- und Olivenöl sowie mikrobieller Öle produziert von Hefen oder Bakterien und damit ausreichend verfügbar.

Diese Studie präsentiert die nachhaltige biochemische Umwandlung von mikrobiellen Ölen in Ölsäure, 10-HSA und die oxidierte Form von 10-HSA, 10-Ketostearinsäure (10-KSA), unter Verwendung von Enzymkaskaden. Zunächst wurde eine neuartige OH namens OhyPp aus *Pediococcus parvulus* eingeführt, um die Palette der verfügbaren OH-Enzyme zu erweitern und Einblicke in ihre Mechanismen zu gewinnen. Obwohl OhyPp eine Sequenzidentität von 74% und eine Ähnlichkeit von 91% mit einem bekannten OH-Enzym namens OhyRe aus *Rhodococcus erythropolis* aufweist, zeigte OhyPp unterschiedliche Eigenschaften. Es gehört allerdings zur gleichen monomeren Proteinfamilie, Hfam3. Die monomere Natur von OhyPp bietet Vorteile für Immobilisierungsstrategien.

Aufgrund fehlgeschlagener Kristallisationsversuche wurde die Struktur von OhyPp mittels des Computeralgorithmus Robetta vorhergesagt. OhyPp zeigte eine höhere Affinität für Flavin-Adenin-Dinukleotid (FAD) im Vergleich zu OhyRe. Dennoch bleibt seine FAD-Affinität geringer als gewünscht für eine adäquate industrielle Anwendung. Interessanterweise kann möglicherweise eine flexible Schleife in der Nähe der FAD-Bindungsstelle zu den beobachteten Unterschieden in der FAD-Affinität zwischen OhyRe und OhyPp beitragen und Einblicke in die Bindungseigenschaften von FAD und potenziellen Bindungsresten liefern.

Zusammenfassend ist eine weitere Optimierung von OH-Enzymen erforderlich, um sie effektiv in industriellen Anwendungen einzusetzen. Die Charakterisierung von OhyPp liefert wertvolle Informationen über dessen strukturelle und katalytische Eigenschaften und trägt zu den laufenden Bemühungen zur Verbesserung von OH-Enzymen für industrielle Anwendungen bei.

Der zweite Teil der Studie konzentrierte sich auf den Einsatz von OHs in Kaskadenreaktionen für industrielle Anwendungen. Die Studie optimierte den Ertrag des OH-Enzyms OhyRe, indem es einer breitbandigen weißen Lichtexposition ausgesetzt wurde, was zu einer signifikanten Steigerung der Aktivität führte. Die erste Kaskadenreaktion umfasste die Umwandlung von Triglyceridölen unter Verwendung von Lipase und OhyRe, wobei die Ausbeuten von 10-HSA je nach verwendetem Öl variierten. In einer zweiten Kaskadenreaktion wurde eine sekundäre Alkoholdehydrogenase (secADH) eingesetzt, um 10-HSA in 10-Ketostearinsäure (10-KSA) umzuwandeln. Es wurden Optimierungen und Charakterisierungen der Kaskadenreaktionen und der secADH durchgeführt. Die Forschung zeigte das Potenzial von Kaskadenreaktionen in Verbindung mit OHs für die Optimierung von Katalysatoren und zukünftige industrielle Anwendungen.

Zusammenfassend präsentiert diese Studie die nachhaltige Biosynthese von 10-HSA und 10-KSA durch OHs aus mikrobiellen und pflanzlichen Ölen und legt damit erste Schritte für ihre industrielle Anwendung dar.

III. Acknowledgements

First, I want to acknowledge and express my cordial gratitude to Prof. Thomas Brück for providing me with the opportunity to pursue this Ph.D. position in his group, which has been pivotal in shaping my scientific and professional journey. I am grateful for the trust and support throughout the years.

I want to thank Prof. Eisenreich, Prof. Kourist and Prof. Nilges for the evaluation and examination of my dissertation.

Additionally, I am very grateful to Daniel Garbe for the great management of the GreenCarbon project, for keeping an eye on due tasks, and for supporting me when questions arose.

Furthermore, I want to express sincere gratitude to Martina Haack for her valuable contributions and support, the fruitful talks about my research, and her creative ideas, which in combination with her expertise, have greatly enhanced the quality of this research.

I want to express sincere gratitude to everyone who contributed to my papers, mentioning our partners from FU Berlin and Marion Ringel.

Also, I want to thank my students, Kateryna Neishsalo, Tim Rheinfrank, Maria Bandookwala, and Atessa Hadawi, who have contributed to this research and with whom I had great scientific conversations.

I am truly grateful to all of my project colleagues, particularly Ayşe Koruyucu, Felix Melcher, Matthias Feigel, and Jonas Breitsameter. Furthermore, I want to express my gratitude towards my group colleagues, particularly Pariya Shaigani, Nadim Ahmad, Nathanael Arnold, Manfred Ritz, and Selina Engelhart-Straub, for their support, patience, and encouragement, which have played a vital role in the successful completion of this project.

Finally, I want to express my greatest gratitude to my beloved family, friends, and my partner for supporting me from day one.

IV. Table of Contents

V. List of Abbreviations

°C	degree Celcius
10-HSA	10-hydroxy stearic acid
10-KSA	10-keto stearic acid
Arg	arginine
ATA	amine transaminase
BVMO	Baeyer-Villiger monooxygenase
CAPS	N-cyclohexyl-3-aminopropanesulfonic acid
CD	circular dichroism
ddH_2O	double distilled water
DTT	dithiothreitol
EDTA	ethylenediaminetetraacetic acid
FabI	bacterial type II fatty acid synthesis enzyme
FAD	oxidized flavin adenine dinucleotide
$FADH_2$	reduced flavin adenine dinucleotide
FAP	fatty acid photodecarboxylase
FID	flame ionization detector
GC	Gas chromatography
Glu	glutamic acid
HEPES	2-[4-(2-Hydroxyethyl)piperazin-1-yl]ethane-1-sulfonic acid
IPTG	Isopropyl-β-D-thiogalactopyranosid
LAH	linoleate hydratase
LCFFA	long-chain free fatty acids
MES	2-(N-morpholino)ethanesulfonic acid
Met	methionine
mM	milli molar
NCBI	The National Center for Biotechnology Information
NTA	nitrilotriacetic acid
OH	oleate hydratase
OhyEm	OH from *Elizabethkingia meningoseptica*
OhyLa	OH from *Lactobacillus acidophilus*
OhyLr	OH from *Lactobacillus rhamnosus*
OhyPp	OH from *Pediococcus parvulus*
OhyRe	OH from *Rhodococcus erythropolis*
OhySa	OH from *Staphylococcus aureus*
OhySt	OH from *Stenotrophomonas sp.* KCTC 12332
Phe	phenylalanine
qPCR	quantitative polymerase chain reaction
RT-PCR	realtime polymerase chain reaction
secADH	secondary alcohol dehydrogenase
STY	space-time yield

TAPS	tris(hydroxymethyl)methylaminopropanesulfonic acid
TB	Terrific Broth medium
Tyr	tyrosine
v/v	volume per volume
Val	valine
WT	wild-type
µM	micro molar

1 Introduction

1.1 Climate change calls for a change in industrial processes

Two of the major challenges facing the twenty-first century lie in the ecological collapse and ongoing climate change, pervasive forces that are already showing their effects across the global expanse. Humankind faces adverse impacts on nature, including increased land use, chemical pollution, and loss of biodiversity [1]. Most of these effects are consequences of intensified resource exploitation of natural goods, where 90% of diversity loss and water-related disturbances and half of greenhouse gas emissions can be attributed to [2]. Furthermore, nearly a third of the worldwide greenhouse gas emissions are directly caused by the industrial sector, with the most significant part for its energy consumption, as shown in **Fig. 1**.

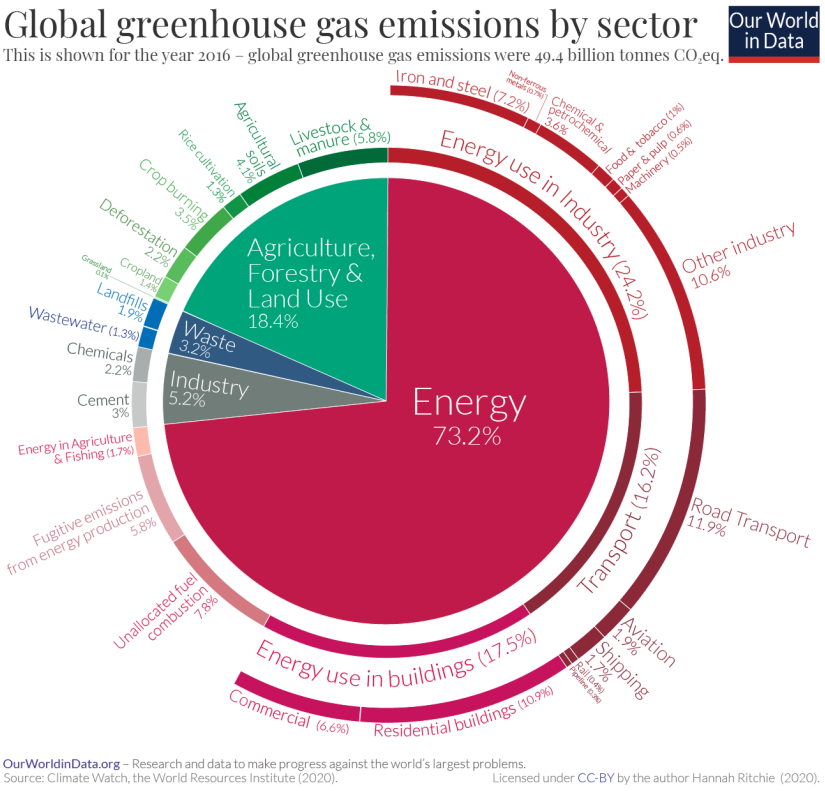

Fig. 1 Global greenhouse gas emissions by sector. A license-free figure, taken from *Our World in data* (accessed on 14.06.2023, https://ourworldindata.org/ghg-emissions-by-sector**).**

However, challenges and pressure for change also entail a surge in novel developments and innovation. Aiming at a decoupling mechanism of economic growth and the release of greenhouse gas emissions, a pronounced research emphasis is being placed on implementing less energy-intensive methodologies, which ideally also include diminished ramifications on biodiversity and reduced land utilization. This can be sustained by biotechnological means, where organisms or biomolecules are applied with lower energy demands than for chemical processes and where cultivation takes place in

bioreactors with less impact by climate or land conditions. However, a current lack of economic feasibility due to paltry yields is hindering the application of many such processes, and extensive scale-up and efficiency optimizations are required to achieve sufficient outcomes in the future.

1.2 Energy-intense route from castor oil to 12-HSA

Modified fatty acids and oil-derived bulk and fine chemicals are applied in large quantities to a variety of industrial applications, including the manufacturing of lubricants [3–5]. Currently, the majority of those are of fossil origin, further fueling the release of greenhouse gases. Additionally, they harm the environment due to toxic effects and low degradability [6]. Consequently, there is a growing demand for lubricants that are both environmentally friendly and sustainable. One example is castor oil, with the main fatty acid being ricinoleic acid, a hydroxylated fatty acid (12R) unsaturated on the C9-position. This oil is not suitable for human consumption, and thus technical applications were established, resulting in a variety of chemical routes for its modification. One is the chemical hydrogenation to saturate the oil, which improves its properties including better heat resistance and oxidative stability, higher melting temperatures, and improved shelf life [5]. This reaction can be followed by hydrolysis to receive 12-(R)-hydroxy stearic acid as a free fatty acid (**Fig. 2**), which is an important, non-toxic additive for the chemical and pharmaceutical industry [7–11]. In Prem et al. 2022 [12], several applications for 12-HSA were mentioned: It is, for instance, used as a surfactant in soaps and body washes. Furthermore, it possesses emollient and thickening characteristics, making it valuable in various applications in the food and pharmaceutical industries, such as skin creams and lotions. It also serves as an additive in grease, lubricating oils, and paints, as well as in the manufacturing of polyvinyl chloride (PVC) and synthetic or natural rubbers.

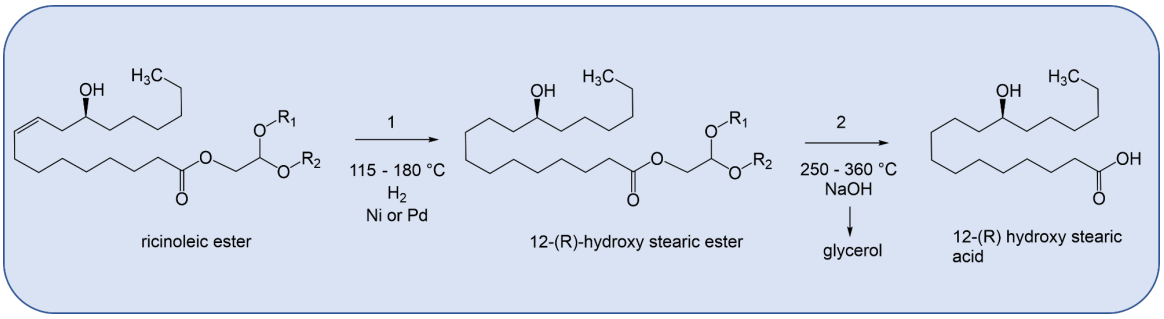

Fig. 2 Process of the production of 12-HSA via chemical hydrogenation of castor oil. In (1), the hydrogenation to saturate the oil at the C9 position using catalysts such as Raney Nickel or Palladium is depicted. (2) Describes the hydrolysis of the hydrogenated castor oil using sodium hydroxide. Reaction conditions were taken from [8].

Despite castor oil being of renewable origin, the current production method follows a chemical route under extreme pressure and temperatures, thus requesting an intense energy demand. The initial hydrogenation step, facilitated by a Nickel or Palladium catalyst, requires less energy compared to the second step. However, it still necessitates temperatures ranging from 115 to 280 °C. The second hydrolysis step requires up to 360 °C and 80% NaOH [5]. Another disadvantage is that castor oil is synthesized by the plant *Ricinus communis*, causing a competition between land use for food versus technical crops, which in regard to an increase in the desertification of land as a result of climate change becomes a salient concern [13]. Also, Lorenzen [14] mentioned that the majority of worldwide castor oil offers emanate from India, resulting in a dependence on fluctuations in demand and quality [5]. He notes that approximately 86% of Indian castor oil is produced in Gujarat, a single state in India, making the production particularly vulnerable to the impacts of seasonality or global warming [5,9].

Consequently, the market aspires for more sustainable options with less energy demand and manufacturable from alternative sources to castor oil.

1.3 10-HSA as an alternative to 12-HSA

One such alternative that sustains most of these demands is the enzymatic biosynthesis of 12-HSA or 10-HSA, an analog of 12-HSA with a hydroxy group on the 10R position of stearic acid, which can be biosynthesized by fatty acid hydratases (EC 4.2.1.53), a class of hydro-lyases [12,15–17]. There is currently one enzyme known to convert cis-vaccenic acid (18:1 *cis*-11) to 12-HSA [18], however, cis-vaccenic acid is not a widely abundant fatty acid [19], hence there is a focus on 10-HSA as it is biosynthesized by OHs from oleic acid as shown in **Fig. 3**.

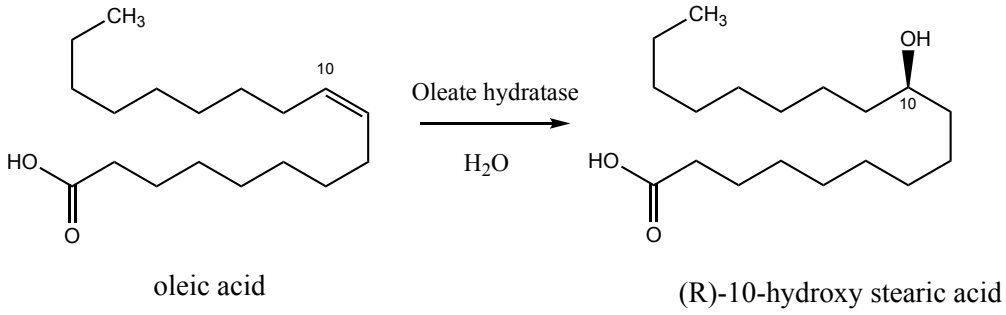

Fig. 3 Enzymatic conversion of oleic acid into (R)-10-hydroxy stearic acid using oleate hydratase.

The high expression rates of OH enzymes in soluble form have generated interest, especially considering that fatty acid-converting enzymes from plants and fungi often lack this characteristic [20–23]. The difficulties associated with soluble protein expression of fatty acid-converting enzymes underlie in their frequent association with cell membranes.

Additionally, they usually solely catalyze the conversion of fatty acids when they are bound to an acyl carrier protein (ACP), CoA, phosphatidylcholine, or other solubilizing molecules, which isn't applicable in an industrial process.

Using enzymes for the production of 10-HSA has several advantages [24]. Firstly, enzymes can be produced from inexpensive materials with low fluctuations in price and they are bio-degradable and non-toxic catalysts. Furthermore, enzymes act under ambient pressure and temperatures making industrial processes more sustainable compared to chemical ones.

Although OHs convert various fatty acids and hence exhibit some degree of low specificity, most demonstrate a particular preference for oleic acid as a substrate [15]. Oleic acid is the main component of many plant oils, such as rapeseed, sunflower, or olive oil [25]. Furthermore, advances have been made in recent years in microbial oil production using oleaginous yeasts or bacteria, where some can use waste streams as substrates solving the problems of the food vs. fuel debate [26]. Additionally, the production of these oils via fermentation is neither seasonal nor location or climate-dependent, has reduced production timelines and high growth rates with high yields of oils [27–29]. An exemplary candidate worthy of mention is the yeast *Cutaneotrichosporon oleaginosus* (ATCC20509), which has garnered attention as a superior choice to produce microbial oil due to its remarkable attributes, including cultivation capabilities at high cell densities and the ability to catabolize a diverse array of substrates [27]. Oleic acid is the predominant species of the produced oil, and with means of media and fermentation parameters adaptation, the fatty acid profile can be altered [26,30,31]. Also, current advances in genetic engineering offer new prospects for the direct targeting of the fatty acid profile [32].

1.4 Elucidation and function of OHs

As discussed in Prem et al. 2022 [12], the presence of hydroxylated fatty acids was initially detected in the steatorrheic feces of humans [33]. There it was stated that these fatty acids are not commonly present in a typical diet and thus it was postulated that their synthesis occurs within the gastrointestinal tract by microorganisms. This hypothesis was confirmed as a specific strain of *Pseudomona*s sp. strain 3266 (later identified as *Elizabethkingia meningoseptica*) was discovered to convert oleic acid into 10-HSA [34]. Further investigations, primarily focusing on human or animal fecal samples, have identified a plethora of other microorganisms capable of producing 10-HSA [35–37]. There was a significant time gap of 47 years between the initial discovery of 10-HSA production by *Pseudomonas* strain 3266 and the first subsequent purification and characterization of the enzyme responsible for this transformation [38].

The function of OHs is of diverse nature, and several theories are currently discussed. They all have in common an evolutionary adaptation to outer environmental stimuli playing a critical role in the survival of living organisms, as has been discussed by a variety of authors [12,39–41].

Many microorganisms have developed strategies to combat toxins by producing detoxifying small molecules or proteins [42]. The same role was attributed to OHs considering them to act as defense factors, as discussed in Prem et al. [12]. This has been suggested after an OH has been identified in *Staphylococcus aureus* (OhySa), which confers resistance against palmitoleic acid [43], the main fatty acid with antimicrobial properties on mammalian skin. In that study, wild-type (WT) *S. aureus* was observed to arrest growth for 2 h upon exposure to palmitoleic acid, whereas the OH-deletion strain wasn't able to recover at all. The hydroxylated form of palmitoleic acid does not exhibit additional toxicity and is not incorporated into the phospholipid membrane but instead exported into the extracellular environment. Saturated fatty acids do not show the same inhibitory effects as unsaturated ones and hydroxy-fatty acids structurally resemble saturated fatty acids more closely, therefore are more likely to be less toxic than their unsaturated equivalents [44].

The reasons why particularly unsaturated long-chain free fatty acids (LCFFA) are reported to be toxic, are most likely diverse, as discussed in Prem et al. 2022 [12]. One of them is that they damage outer membranes, leading to the lysis of protoplasts, leakage of proteins, cell-associated fatty acids, and nucleic acids [45–47,44]. Additionally, the presence of LCFFAs can impede the uptake of proteins and amino acids, particularly in gram-positive bacteria, due to the inherent properties of their cell membranes. It also has been reported that LCFFAs inhibit FabI, which is part of the bacterial type II fatty acid synthesis pathway, as well as other fatty acid-converting enzymes from different organisms [48]. Gram-negative bacteria are inhibited by LCFFAs to a much lesser extent, likely due to the lower permeability of their cell walls to fatty acids [49].

As a result, several microorganisms that reside in close proximity to free fatty acids have been found to hydroxylate LCFFAs, most likely as an adaptive defense mechanism against their external environment [50].

Prem et al. 2023 [51] mention that although there are reports of gram-negative bacteria exhibiting resistance to LCFFAs, it is noteworthy that many of these bacteria still possess fatty acid hydratase genes [16,38]. This suggests the presence of additional functionalities of OHs beyond the explained detoxification. One additional potential function could be an influence on overall cellular stability. Observations have indicated

that bacteria with OH activities exhibit enhanced resistance to heat and solvent stress [52]. For example, it has been documented that marine microorganisms produce 2-OH-hydroxylated fatty acids, and their concentration increases under low pH conditions. This phenomenon is presumed to facilitate control of ion flow into the cell [53].

Additionally, a role of OHs in microbial virulence is discussed. Before OhySa's function was known, its gene was noticed as a virulence factor since anti-myosin antibodies in sera of patients with acute rheumatic fever cross-reacted with OhySa [54]. Recent studies have demonstrated that OhySa is capable of converting cis-9 unsaturated fatty acids derived from the host into their 10-hydroxy derivatives in human serum and at the site of infection in a mouse neutropenic thigh mode [55].

Furthermore, a *Streptococcus pyogenes* strain with the OH gene being deleted showed an increase in survival in the blood and a decrease in human keratinocyte adherence and internalization [56], where the latter might be attributed to a modulation in the cell surface properties [57].

These data suggest that OHs might play a role in immune modulation during *S. aureus* pathogenesis and that they potentially lead to a reduced inflammatory response from the bacteria's host [55].

In addition, hydroxylated fatty acids such as (R)-10-hydroxy-12- octadecenoic acid and (R)-13-hydroxy- 9-octadecenoic acid were found to exhibit antifungal activities [57].

In Prem et al. [12], the location of OHs' activity has been discussed and suggested to reside at several different sites. In varying studies, OHs were observed to function either within the cytoplasm, in the outer environment, or attached to the membrane [12,41,58]. In the case of *Staphylococcus aureus*, OHs have been identified in vesicles that are secreted from the cell when linoleic acid is present [58]. Additionally, an OH from *Lactobacillus plantarum* was found to be a membrane-bound protein, attached electrostatically, and the conversion of linoleate to 10-hydroxy-cis-12-octadecenoic acid was reported to occur at the cell periphery [41]. Additionally, OhySa was observed on the cell surface of *S. aureus* by using immunofluorescence and the protein was found in integral membrane fractions using immunoblotting after purification from the cells [59]. Some microorganisms possess multiple OHs, suggesting a potential complementary defensive effect [60–63]. External membrane-bound hydratases and secreted ones may serve as a primary line of defense, while cytoplasmic fatty acid hydratases could contribute to the overall response mechanism [12].

In summary, OHs provide evolutionary advantages in fatty acid rich surroundings, effect virulence of pathogens and support their host's stress response mechanisms.

However, their places of action might be diverse, is not yet fully clear and remains to be elucidated.

1.5 OH families, structure and mechanism

In Zhang et al. [15], a table presents the few currently available crystal structures of OHs, including one of a linoleate hydratase from *Lactobacillus acidophilus* named LAH [64], and OHs from *Elizabethkingia meningoseptica* (OhyEm) [65], *Rhodococcus erythropolis* [39] (OhyRe), *Stenotrophomonas* sp. KCTC 12332 [40] (OhySt) and *Staphylococcus aureus* [66] (OhySa). All to date characterized OHs carry three core domains but show variations in N- and C-terminal extensions, which are extended in certain subfamilies (**Fig. 4**). Most OHs are dimers, including OhyEm, OhyLa, OhySa and OhySt. At present, the only reported monomeric enzyme is OhyRe [39]. Since the N- and C-terminal extensions don't occur in OhyRe but in all the dimeric OHs, they have been suggested to be involved in dimerization [39]. A monomeric protein structure has several advantages, such as holding superior properties for immobilization strategies for industrial applications and not being prone to subunit dissociation, which is one of the reasons for functional inactivation [67].

Schmid et al.[16] established a classification system and a database of OHs with 11 different homologous subfamilies, which are named HFam1-11, where the average global sequence identity within the families is 62%. The largest homologous family is HFam2, which comprises 1188 sequences, including the fatty acid hydratase 1 from *Lactobacillus acidophilus* (OhyLa) [60]. The fourth largest family is HFam11, comprising 116 sequences. HFam11 is associated with the first reported OH from *Elizabethkingia meningoseptica* (OhyEm) [65]. Additionally, there are two other larger families, HFam1, which consists of 436 sequences, and HFam3, which consists of 191 sequences and contains OhyRe [39].

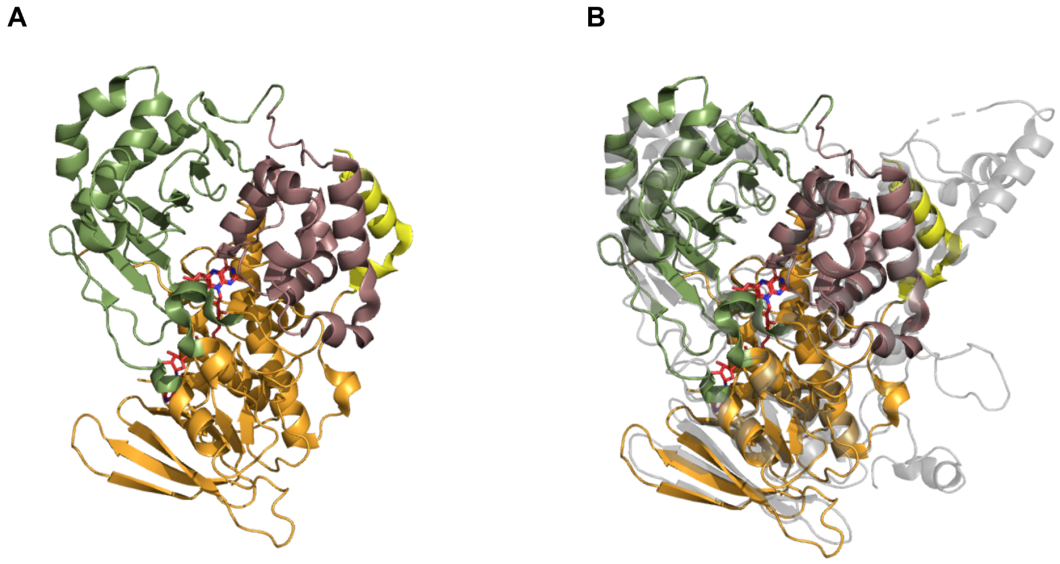

Fig. 4 (A) Crystal structure of OhyRe shown in cartoon representation colored by domains and FAD in stick representation with the following atom color scheme: red: carbon and oxygen, blue: nitrogen. Domains are colored in the following way: orange: domain I, olive: domain II, violet: domain III, yellow: domain IV. The position of FAD in red is derived from the superposition with OhyEm. (**B)** Protomer I of OhyEm (in light grey) is superpositioned with OhyRe in cartoon representation. OhyRe's domains are colored as described in (A). N- and C-terminal extensions of OhyEm on the right have no equivalent in OhyRe. Figure was adapted and modified from [12] and has been prepared with Pymol (Schrödinger Inc.).

One of the biggest challenges in the crystallization efforts is that substrate, product, and FAD can't be resolved with ease as observed by a lack of available structures. Currently, only OhyEm's and OhySa's crystal structures contain FAD, and the latter was additionally predicted to contain substrate and product after slowing down the reaction through mutagenesis, revealing information on the mode of action [66]. It was suggested that the dipole of α-helix 7, Glu82, and oleate hydroxyl stabilize an oxonium-ion ($H3O^+$), whose acidic H^+ subsequently is attacked by the π-electrons of oleic acid. Next, water attacks the formed carbocation and is stabilized through Phe187, Tyr201, and Val505 in OhySa. Glu82, as the main residue suggested to be involved in the reaction, can also be found in OhyEm. It corresponds to Met77 in OhyRe and, consequently, is not able to conduct the same stabilization with its side chain as in OhySa. In Lorenzen et al. [39], Met77 has been exchanged to Glu, however, it led to a 5-fold decrease in activity, suggesting a different mechanism if it actually applies at all as proposed in Radka et al. [66].

1.6 Binding of FAD in OHs

In all OHs, conserved flavin binding sequences can be found. In OhyRe, this sequence follows a GXGXXN, and OhyEm, a GXGXXGX_{21}E/D pattern. Currently, there are two available crystal structures of OHs, where FAD was resolved, namely OhyEm and OhySa [65,66]. Attempts to resolve FAD in OhyRe included the incubation of the enzyme with FAD prior to final purification and crystallization, and soaking of crystals in FAD; however, none of these attempts led to a crystal structure including electron densities reflecting FAD [39]. Nevertheless, as observed by Lorenzen et al. [39], by superpositioning of OhyRe's and OhyEm's crystal structures, enough space could be observed in the cofactor binding region in OhyRe for FAD, and by structural alignments, it was possible to predict the positioning of FAD in OhyRe [12] since own *in silico* docking efforts failed, which was also noticed by Busch et al. [62].

1.7 Function of FAD in OHs

OHs carry FAD upon purification in low occupancy or fully lose it upon purification as observed for OhyRe and LAH [39,64]. The function of FAD is still not fully clear, but Radka et al. [66] proposed that FAD displaces water molecules within the active site, to correctly position the dipole α-helix 7 and Glu82 and, to lead to a flip of Arg81 so that the substrate can enter the cavity.

Using stopped-flow experiments, no reduction or re-oxidation of FAD could be measured in OhyEm but control experiments revealed an 11-fold increase in activity under anaerobic conditions leading to a reduction of FAD as observed by a loss of color [65]. This suggests a structural or stabilizing role for FAD or rather for its reduced form $FADH_2$, which is most likely the actually required stabilizer [65,68]. Whereas a reducing environment is maintained within cells, an oxidizing environment occurs during cell lysis and during the purification of proteins, leading to an oxidization of $FADH_2$ to FAD [69]. That is most likely why purified OHs often are subject to a partial or full loss of function, which can be more or less profound, depending on the protein purification process and the overall affinity of the respective OH to FAD. OhyRe and an OH from *Lactobacillus rhamnosus* (OhyLr), for instance, fully lose their activity upon purification [39,68], whereas OhyEm and OhySa still keep partial functionality [65,66]. This observation can be rationalized by biochemical data, suggesting that OhyEm and OhySa contain small amounts of FAD after purification as opposed to OhyRe, and this remaining FAD might still partially be reduced. OhyLr seems to be an exception, as it is reported to still contain FAD after purification, but no activity was detected [68].

In consequence, for the full functioning of OHs, reduction of FAD is required. However, this is often connected with elaborate means, such as photobleaching, the addition of reducing chemicals, which might also interfere with the enzyme's activity or the use of a cascade reaction with flavin reductase [65,68].

In general, however, a higher occupancy of oxidized FAD in OHs after purification is connected with a higher activity, and a reduction step is only possible if certain amounts of FAD are bound to OH after purification, as has been mentioned in Prem et al. 2023 [51]. Otherwise, additional FAD is needed, which renders an industrial process costly. OhyRe carrying full advantages of a monomeric enzyme still lacks enough FAD after purification for adequate functioning, and thus optimization with protein engineering methods is highly desired.

1.8 Kinetic parameter of OHs

Kinetic parameters play a crucial role in studying the behavior of enzymes in living organisms and simulating conversion processes for industrial scaling [70]. However, as thoroughly discussed in Prem et al. 2022 [12] and 2023 [51], for OHs, special circumstances must be considered. While kinetic parameters have been measured for several OHs, their scientific relevance needs to be carefully evaluated.

Prem et al. note that oleic acid is immiscible in water and thus poses a challenge for OHs, as access to their substrates is crucial. This can be achieved by creating an emulsion, but the formation and quality of the emulsion are dependent on the preparation protocol, potentially leading to unavoidable local and uneven dispersion effects. Additionally, the variation in pH has a significant impact on the dispersion of fatty acids in water, as oleic acid forms a soap at a pH above 7, making it more miscible in water [71]. Therefore, measuring kinetic parameters under different pH conditions may not accurately represent the enzyme's natural behavior.

Furthermore, as already mentioned, $FADH_2$ has previously been identified as the implicated ligand associated with heightened activity [65,68]. The process of FAD and $FADH_2$ undergoing oxidation and reduction is intricately linked to light and oxygen, and these factors exhibit variability based on the prevailing environmental conditions, consequently exerting supplementary influences on kinetic parameters.

In summary, the challenges described above contribute to significant variations in kinetic parameters for the same enzymes, as observed by Zhang et al. [15]. Evaluating kinetic parameters in isolation is of limited utility and does not contribute to a comprehensive understanding of the enzymes' behavior *in vivo*. Consequently, only

when precisely equal and consistent reaction conditions are applied a comparison between kinetic parameters of OHs are of relevance.

1.9 Protein stability of OHs

In Prem et al. 2022 [12], the stability and maintenance of enzymatic activity over an extended period have been discussed. These are crucial factors for efficient processes when using isolated enzymes instead of whole-cell catalysts. Several studies have observed low stability of OHs, with some enzymes losing their activity rapidly [16,72]. In a comparative study on enzyme stability, five different OHs were analyzed and found to start denaturing within lysates after just one day, exposing their hydrophobic sites [16]. As a result, neither the substrate nor the product could be measured, likely due to interactions with the hydrophobic regions of the denatured protein. Buffer optimization showed some improvement in protein stability. Another study reported that OhyEm loses 60% of its activity within 7 days at 4 °C, possibly due to subunit dissociation [72].

However, there is limited published information on the stability of OHs over longer periods, as most studies focus on medicinal than industrial applications. Todea et al. [72] investigated the use of additives to overcome stability issues, testing residual activity after storing the protein for 7 days at 4 °C. Yet, the effects of additives on process stability during multiple re-usage cycles and at elevated temperatures have not been examined [12]. Furthermore, the presence of additives can have negative impacts on the production process as their removal is required before reaction start, increasing process costs.

Prem et al. 2022 [12] discussed the loss of protein activity, which can be attributed to factors such as the disruption of the tertiary structure, dissociation of cofactors, chemical inactivation when reactive chemicals are involved, or subunit dissociation, which is often the initial step in inactivation for multimeric proteins [67]. As a result, multimeric enzymes and those dependent on FAD are more prone to these issues and less advantageous for industrial processes. Monomeric enzymes, on the other hand, can overcome subunit dissociation problems, and enzymes that do not rely on FAD are not subject to cofactor loss. OhyRe is a monomeric OH and loses its activity after purification, which can be associated with a loss of FAD [39]. Therefore, further optimizations are needed for its use in isolated form, as the addition of FAD makes it prohibitively expensive.

1.10 Industrial application of OHs

In Prem et al. 2022 [12], the performance evaluation of catalysts holding paramount importance in industrial processes has been mentioned. There, it was noted that in the context of heterogeneous catalysis, the space-time yield (STY) typically ranges from 1

to 10 kg L^{-1} h^{-1}. However, when considering biocatalysts, the STYs can significantly decrease by up to 1,000 times, reaching levels of approximately 0.001−0.3 kg L^{-1} h^{-1} in comparison to conventional processes [73]. While the pharmaceutical industry, which demands enantiomeric purity and high-quality products, may tolerate such reductions, expensive processes associated with a final product primarily used as an additive, such as 10- or 12-HSA, are unlikely to be applicable. Consequently, significant optimization regarding biocatalysts and the STYs of their processes is required.

It was noted that the enzymatic industrial process for 10-HSA production can be implemented in various modes [12]. Firstly, either wild-type or genetically engineered whole-cells can be employed for the conversion of oleic acid. The advantage lies in the fact that no further purification of the enzyme is required, only the extraction of fatty acids and subsequent purification of 10-HSA are necessary. A disadvantage of whole-cell conversions is the requirement of more elaborate downstream processing steps due to a higher degree of impurities, which also results in more product loss. Whole-cell conversions are commonly used when the production of a specific product involves complex gene clusters and cascades or when enzymes are insoluble or inactive when isolated. In addition, the recycling of whole-cell catalysts presents a greater challenge, especially when the desired product is in solid form and centrifugal forces are not effective in separating the product from the catalyst – as is the case for OHs.

Considering the challenges mentioned, it was suggested that the use of lysates or purified enzymes becomes more desirable in certain cases [12]. Unlike some other fatty acid converting enzymes or hydratases, OHs exhibit high expression rates and solubility. They do not rely on stoichiometric amounts of FAD, which makes them excellent candidates for utilization in their pure form or as part of lysates.

Numerous screenings of OH activities have been conducted using lysates and lyophilized lysates, as documented in the literature [16,68]. Furthermore, a patent describes the large-scale production of 10-HSA using a lysate derived from *R. erythropolis* and *S. maltophilia* [74]. These findings highlight the potential of employing lysates or purified enzymes, as they offer advantages in terms of enzyme stability, scalability, and control over reaction conditions.

Furthermore, Prem et al. 2022 [12] note that pure enzymes also enable the comparison of results under standardized conditions, ensuring greater consistency and reliability for measuring the enzyme's performance and kinetics. Considering the challenges associated with lysates, such as recycling difficulties and weak stability, the use of pure, immobilized enzymes becomes a favorable option in certain cases. Also,

oleic acid and 10-HSA have been found to interact strongly with aggregated proteins during an organic solvent extraction step, which is more profound in lysates since they contain higher amounts of non-converting proteins. This results in losses in yield as up to 50% (own data, not shown). Lastly, immobilization offers advantages such as improved stability, increased enzymatic activity, enhanced stereoselectivity, and efficient recycling, leading to cost savings [75].

1.11 10-HSA as a starting material for high-value fine chemicals

In summary, OHs pose several challenges for their industrial application, while their product 10-HSA remains an industrially attractive compound since it also serves as a starting material for a variety of other high-value fatty acid-based molecules, which has been discussed by Hagedoorn 2021 [76]. These include several applications in different industrial sectors and can be produced by either coupling the enzymes in isolated forms or by using whole-cell catalysts [76,77] as depicted in **Fig. 5**.

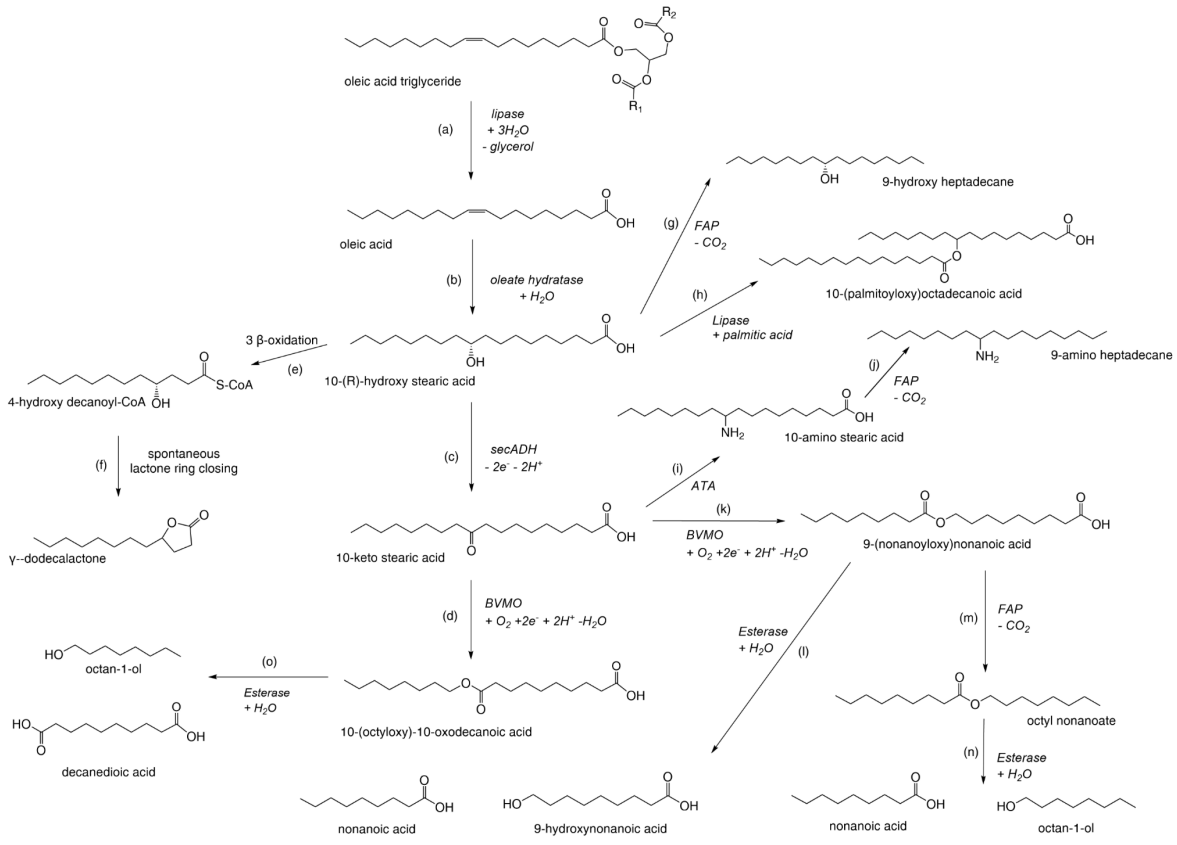

Fig. 5 Catalytic cascades using isolated enzymes or whole-cells producing 10-HSA formed by OHs as starting material for high-value modified fatty acids and fatty acid derived molecules. (a) Triglyceride ester hydrolysis using a lipase leading to free oleic acid. (b) OH hydroxylating free oleic acid into 10-HSA. (c) Secondary alcohol dehydrogenase oxidizing 10-HSA into 10-KSA. (d) BVMO oxidizing 10-KSA into 10-(octyloxy)-10-oxodecanoic acid. (e) Cellular β-oxidation of 10-HSA to 4-hydroxy decanoyl-CoA. (f) Spontaneous lactone ring closing of 4-hydroxy decanoyl-CoA to γ-dodecalactone. (g) Fatty acid photodecarboxylase mediated decarboxylation of 10-HSA

to 9-hydroxy heptadecane. (h) Ester formation of 10-HSA and palmitic acid via lipase to 10-(palmitoyloxy)octadecanoic acid (i) Amine transaminase catalyzed transamination of 10-KSA to 10-amino stearic acid. (j) Decarboxylation of 10-amino stearic acid via fatty acid photodecarboxylase to 9-amino heptadecane. (k) Oxidation of 10-KSA with BVMO to 9-(nonanoyloxy)nonanoic acid (l) Esterase mediated hydrolysis of 9-(nonanoyloxy)nonanoic acid to nonanoic acid and 9-hydroxynonanoic acid. (m) Fatty acid photodecarboxylase mediated decarboxylation of 9-(nonanoyloxy)nonanoic acid to octyl nonanoate. (n) Hydrolysis of octyl nonanoate by esterase to nonanoic acid and octan-1-ol. (o) Esterase mediated hydrolysis of 10-(octyloxy)-10-oxodecanoic acid in octan-1-ol and decanedioic acid. FAP: fatty acid photodecarboxylase, ATA: amine transaminase, BVMO: Baeyer-Villiger monooxygenase, secADH: secondary alcohol dehydrogenase. Figure adapted and modified from Hagedoorn [76].

The initial stage in the biosynthesis of 10-HSA involves the hydrolysis of triglyceride fatty acids (a in **Fig. 5**), resulting in the liberation of free fatty acids. The product of OHs, 10-HSA, then serves as a pivotal precursor for the generation of diverse products with distinct characteristics.

In a recent study, *Yarrowia lipolytica* was engineered to carry an oxidase to control the chain length after β-oxidation and a bacterial OH for the subsequent hydroxylation of the 4-hydroxy decanoyl-CoA fatty acid [78]. This resulted in the formation of γ-dodecalactone, a flavor lactone with milky aromas, which is useful in the food industry (e and f in **Fig. 5**).

Hagedoorn [76] suggests the potential use of lipases and additional fatty acids, to build so-called estolide or fatty acyl esters of hydroxy fatty acids, which have anti-diabetic and anti-inflammatory effects and can be applied as additives in cosmetics [79,80,81] (h in **Fig. 5**). Decarboxylation with fatty acid photodecarboxylase leads to hydroxylated, aminated or internally esterified alkanes (g, j, l in **Fig. 5**).

Additionally, he mentions that 10-KSA, which is oxidized from 10-HSA via a secondary alcohol dehydrogenase, can be a starting point of transaminated and monooxygenated fatty acids (i, k and d in **Fig. 5**), where the latter are candidates for building blocks for bio-based polyesters [76]. In a study, *E. coli* was engineered to carry an OH, a secADH and two different Bayer-Villiger monooxygenases (BVMOs) [77]. A subsequent conversion step with an esterase led to the formation of either n-nonanoic acid and 9-hydroxynonanoic acid or of octan-1-ol and decanedioic acid depending on the applied BVMO.

To summarize, 10-HSA serves as a starting material for a variety of fatty acid-based high-value molecules suitable for industrial applications by biosynthesis using a variety of soluble enzymes.

1.12 In a nutshell

In summary, OHs produce valuable hydroxylated fatty acids, which can serve as precursors for other industrially relevant materials. These have the advantage of being derived from sustainable sources and of possessing non-toxic properties, making them promising alternatives to fossil-based materials. However, the industrial applicability of OHs is still limited due to several challenges. OHs exhibit relatively low stability, slow turnover rates, and low affinity towards FAD, resulting in significant FAD loss during purification processes. To overcome these limitations, a comprehensive understanding of the enzyme's structure and function is necessary, enabling targeted protein engineering strategies. In this study, we present a novel oleate hydratase closely related to OhyRe, which contributes to a deeper understanding of the overall function and structural integrity of the HFam3 enzyme family. Additionally, we demonstrate the potential of sustainable oil conversion by introducing two cascade reactions that showcase the feasibility of producing high-value fatty-based materials in one-pot reaction setups.

2 Material and methods

2.1 Identification of genes

2.1.1 OH from *Pediococcus parvulus*

OhyRe is currently the only known monomeric OH and it loses FAD upon purification. To investigate whether that is specific to the HFam3 family, we aspired to characterize a close relative of OhyRe and its FAD binding capacities. The NCBI database contains a large portfolio of annotated DNA sequences, which have a certain homology to other known OHs, and are predicted to carry the OH function [82]. A blast search with the amino acid sequence of OhyRe revealed a close relative originating from *Pediococcus parvulus*. The OH amino acid sequence was used as a template to order a gene strand (EurofinsGenomics, Germany) with codons optimized for *E. coli.*

2.1.2 Secondary ADH from *Deinococcus radiodurans*

For the cascade reaction with an alcohol dehydrogenase, a wide-range pH- and temperature optimum and high stability are desired. With these properties, a variety of OHs with different optimal parameters can be easily applied without a strong decrease in activity. A secADH from *Micrococcus luteus* is known for the utilization of 10-HSA as a substrate but is predicted to be a L-3-hydroxyacyl-CoA dehydrogenases [83,84]. A blast search on the NCBI database revealed several related structures with the same function prediction, one of them originating from *Deinococcus radiodurans*. It is an organism of great interest due to its extremophile character, with its proteins often exhibiting a higher durability and stability [85]; hence this predicted amino acid sequence was ordered as a gene strand with codons optimized for *E. coli*.

2.2 Protein expression

For protein expression, gene strands were cloned into the multiple cloning site of pet28a(+) and transformed with DH5α cells. After the verification of sequential integrity, plasmids were transformed with the *E. coli* recombinant expression strain BL21DE3. Freshly transformed clones were picked and grown for 16 h in 5 ml of Luria Bertani (LB)-medium, followed by the inoculation of 500 ml of TB to an initial OD_{600} of 0.05 - 0.1 in an Innova44R shaker (Eppendorf, Germany) at 120 rpm and 37 °C. At an OD_{600} of 0.6 - 0.8, the temperature was decreased to 16 °C, and cells were induced with 0.1 mM IPTG (CarlRoth, Germany) for 20 h. Cells were harvested by centrifugation, resuspended into lysis buffer (20 mM Tris-Base pH 7.2, 500 mM NaCl, 20 mM imidazole), and lysed using a high-pressure homogenizer (EmulsiFlex-B15, AVESTIN, Canada) followed by removal of cell debris with centrifugation. The proteins were purified by mixing the cell-free lysates with Ni^{2+}-NTA beads (Thermo Fisher, USA) overnight at 4 °C. Beads were washed with

lysis buffer and eluted using 20 mM Tris-Base pH 7.2, 250 mM imidazol, 500 mM NaCl. After elution, protein solutions were desalted using PD MidiTrap G-25 columns (Cytiva, USA). The final storage buffers were different depending on the application. SecADH was stored in 20 mM Tris-Base, pH 7.2 at 4 °C. OhyRe was stored in 20 mM Tris-Base, pH 7.2 either with or without 200 mM NaCl. OhyPp was stored in 20 mM Tris-Base pH 7.2, 200 mM NaCl and OhyEm in 50 mM MES pH 6, 200 mM NaCl. OhyPp and OhyRe were stored at -20 °C until further usage. SecADH and OhyEm couldn't be stored at -20 °C due to extended aggregation during the thawing process. The protein concentrations were assessed after buffer exchange using ROTI®Quant calibrated with Bovine Serum Albumin (both from CarlRoth, Germany) and diluted to a stock concentration of 30 µM.

2.3 Enzyme assays

Enzyme assays were analyzed either by gas chromatography using GC-FID or GC-MS or by spectrophotometry at 340 nm, when secADH was applied. For the latter, U/ml was calculated using the initial linear slope of the absorbance curve of NADH, its extinction coefficient $\varepsilon = 6.22\ mM^{-1}\ cm^{-1}$ and the plate thickness of 0.59 cm. U is defined as (initial slope·total volume)/(plate thickness·enzyme volume·ε).

2.3.1 OhyPp optimal reaction parameter test

For the evaluation of optimal reaction parameters of OhyPp, high-purity oleic acid (99 %, Alfa Aesar, USA) was emulsified with 148 µl of storage buffer (50 mM MES, pH 6, 200 mM NaCl), resulting in a final concentration of 0.4 % [v/v]. 100 µl of OhyPp protein solution was added, resulting in a final concentration of 6 µM and 1 µl of a 3 mM FAD solution was added. For the reaction, solutions were incubated on an orbital shaker for 2 h. For the optimal temperature evaluation, reactions at 15, 18, 20, 25 and 28 °C were conducted, and the respective conversion was tested. Since Tris-Base changes its pH depending on the temperature, the pH was verified using a pH meter. Reactions were measured using GC-FID.

To obtain the optimal pH, the following buffers were used: pH 5: citrate, pH 5.5-6.5: MES, pH 7-8.5: Tris-Base, pH 9-9.5: TAPS, pH 10: CAPS, (all in a concentration of 100 mM). Since oleic acid is strongly acidic (pk_a of 5.02 (https://pubchem.ncbi.nlm.nih.gov)) and might change the pH, it was verified using a pH-meter. Reactions were measured with a multimode microplate reader (Enspire2, Perkin Elmer, USA) at 340 nm. All reactions were conducted in triplicates.

2.3.2 Substrate specificity test of OhyPp

For the evaluation of substrate specificity, 1 mg of each fatty acid was mixed with 300 µl of buffer (50 mM MES, pH 6, 200 mM) and 200 µl of OhyPp cell-free extract. The conversion was conducted for 24 h at 20 °C. For the evaluation of %conversion, additional reactions were conducted for different fatty acids, which got converted by the cell-free extracts. For that, 1 mg of oleic acid, linoleic acid, linolenic acid and palmitoleic acid were emulsified with 100 µl of storage buffer and 100 µl of 12 µM OhyPp was added. Reactions were conducted for 24 h at 20 °C. Remaining fatty acids and corresponding products were silylated as described in 2.4.2.

2.3.3 Stability test of OhyPp and OhyEm

OhyEm's FAD occupancy was measured with a FAD calibration curve and the same molar amount was added to OhyPp since ligands are known to stabilize proteins. Protein solutions were then stored at 4 °C for in total 27 days. For the reaction, oleic acid was emulsified with 148 µl of 50 mM MES, pH 6, 200 mM resulting in a final concentration of 0.4 % [v/v] and 100 µl of OhyPp or OhyEm (15 µM each) was added. 1 µl of FAD (3 mM) was added and solutions were incubated at 20 °C for 2 h. All reactions were conducted in triplicates.

2.3.4 Light color and intensity test

To test the optimal light color and intensity, 1 µl of oleic acid was emulsified with 149 µl of 20 mM Tris-Base pH 7.2, 200 mM NaCl. 50 µl of OhyRe (30 µM with 30 µM FAD) was added. Reactions were conducted in an incubation shaker with LEDs of adjustable light color and intensity and temperature control (FutureLED, Germany) at 28 °C for 3 h at 100 rpm of horizontal shaking. Reactions were performed under broad-band white, blue (425 nm) and red light (680 nm) and in the dark. Light intensity tests were performed at 48, 243, 364 and 486 µmol/m^2*s. All following reactions, which are part of the cascade reaction study, were conducted under the optimal light exposure (broad-band white light, 364 µmol/m^2*s).

2.3.5 secADH optimal reaction parameter evaluation

To test the optimal pH of secADH, 5 µl of 10 mM 12-HSA in ethanol was mixed with 10 µl secADH (0.2 g/l), 165 µl of each respective buffer, and 20 µl of NAD+ (10 mM), and reactions were measured in a multimode microplate reader.

For the temperature optimum test, 25 µl of 12-HSA (10 mg/ml), 100 µl of secADH (2 mg/ml), 375 µl of 100 mM Tris-Base pH 8 and 20 µl NAD+ (10 mM) were mixed. Samples were incubated at temperatures of 16, 18, 20, 22, 24 and 26 °C for 10 min. Samples were analyzed using GC-FID.

2.3.6 Substrate specificity test of secADH

For the initial substrate specificity test of secADH, primary, secondary, and tertiary alcohol were tested. For that, 10 µl of ethanol, tert-butanol and 2-propanol were added to a 96-well microtiter plate and 10 µl of ADH (2 mg/ml) and 160 µl of 20 mM Tris-Base, pH 7.2 were added. To start the reaction, 20 µl of NAD+ (10 mM) was added and the reaction was monitored in a multimode microplate reader at 340 nm. Since ethanol was observed not to be utilized as substrate by secADH, it was used as a solvent for further substrate analyses. For testing the substrate conversion of diols, 1 M stocks and for secondary alcohols, 10 mM stocks were prepared in ethanol and reactions conducted as just described. Tested alcohols include the following: 2-propanol, 2-pentanol, 3-pentanol, 1,1-dimethoxy-2-propanol, 10-hydroxy stearic acid, 12-hydroxy stearic acid, 2,4-pentanediol, 2,5-hexanediol, 1,3-butanediol, 1,2-butanediol and tert-butanol.

2.3.7 secADH and OH cascade optimal reaction parameter test

A 10 mM emulsion of oleic acid was prepared in 20 mM Tris-Base pH 7.2 and 20 µl were added to 20 µl of OhyRe or OhyEm (30 µM in 50 mM MES buffer pH 6.5 with an equimolar concentration of FAD for OhyRe), 20 µl NAD+ (10 mM), 3 µl ADH (2 mg/ml) and the respective volume of each respective buffer to a total volume of 200 µl. For the temperature optimum, 16, 18, 20, 22, 24, 26 and 28 °C were tested. Reactions were measured using GC-FID.

The following buffers were used for the analysis of the pH-optimum: pH 5: citrate, pH 5.5-6.5: MES, pH 7-8.5: Tris-Base, pH 9-9.5: TAPS, pH 10: CAPS (all in a concentration of 100 mM). Reactions were measured with a multimode microplate reader at 340 nm. All reactions were conducted in triplicates.

2.3.8 Effect of additives on secADH and OhyRe cascading reactions

Ethanol, Tween 80, dimethyl sulfoxide and 1,5-pentanediol at concentrations of 1, 2, 5, 10 and 20 % [v/v] were tested. For that, a stock of 10 mM oleic acid in 50 mM MES buffer pH 6.5 was prepared and 20 µl of that added to 20 µl of OhyRe (30 µM with 30 µM FAD), 20 µl NAD+ (10 mM), the respective volume of the additive and 50 mM MES buffer pH 6.5 to a total volume of 200 µl. Reactions were measured with a multimode microplate reader at 340 nm and were conducted in triplicates.

2.3.9 Testing the light effect on the secADH and OhyRe cascade

For the evaluation of different light intensities for the cascade reaction with secADH and OhyRe, the same concentrations as in 2.3.8 without the additives were applied. The reactions were conducted for 3 h in triplicates and were measured with GC-FID.

2.3.10 Optimal enzyme concentration of secADH and OhyRe cascade

Either secADH's or OhyRe's concentration was varied. A 10 mM oleic acid emulsion in 50 mM MES pH 6.5 was prepared and 20 µl added to different final concentrations of OhyRe or secADH. 1 g/l was used for a fixed OhyRe (concentration stored with an equimolar concentration of FAD) and 0.01 g/l for a fixed secADH concentration. Reactions were monitored at 340 nm and curves were fitted using y=Vmax*x^n/(k^n+x^n) for varying OhyRe and y = Vmax*x/(Km+x*(1+x/Ki)) for varying secADH concentrations.

2.3.11 Long-time conversion of secADH and OhyRe cascade

A 10 mM oleic acid emulsion in 50 mM MES pH 6.5 was prepared and 20 µl added to OhyRe (final conc. 1 g/l stored with an equimolar concentration of FAD), 0.01 g/l secADH, 20 µl NAD+ (10 mM), 1% [v/v] 1,5-pentanediol and 50 mM MES buffer pH 6.5 to a total volume of 200 µl. Reactions were performed in triplicates for 1, 2, 4, 6 and 16 h and were subsequently analyzed using GC-FID.

2.4 Fatty acid esterification

Each reaction was extracted with 1 ml of ethyl acetate by mixing it well and centrifuging the mixture for 3 min at 1000 g. 800 µl of the supernatant were taken, evaporated and the respective esterification protocol was performed.

2.4.1 Fatty acid methyl ester modification

For the quantitative analysis of the conversion of oleic acid to 10-HSA or 10-KSA, a methylation protocol was employed, which was adapted and modified from Griffiths et al. [86]. The reaction was conducted by a liquid handler ((MultiPurposeSampler MPS Robotic, Gerstel). To dry fatty acids, 500 µl of toluene and 10 µl of lauric acid (10 mg/ml) as an internal standard were added and thoroughly mixed. Subsequently, 1 ml of sodium methoxide was added, and the solution was shaken at 80 °C for 20 minutes. Following a cooling step at 5 °C for 5 minutes, 1 ml of methanol-HCl was added, and the reaction mixture was heated again to 80 °C for 20 minutes. After an additional cooling phase, 400 µl of distilled water (ddH_2O) and 1 ml of hexane were added, and the reactions were mixed and centrifuged. Subsequently, 200 µl of the toluene/hexane layer was extracted and utilized for GC-FID measurement.

2.4.2 Silylation protocol

Linoleic and linolenic show better response when silylation is performed as opposed to methylation. Consequently, for the fatty acid specificity of OhyPp, samples were silylated. Dry fatty acids were resuspended in 60 µl pyridine and diluted 1:20 in 50

µl pyridine followed by the addition of 20 µl of N-Methyl-N-(trimethylsilyl)trifluoracetamid (MSTFA)/1 % trimethylchlorosilane. The mixture was incubated for 1 h at 50 °C and measured with GC-MS.

2.5 Gas chromatographic measurements

2.5.1 Fatty acid standards

A mixture of 10-HSA and oleic acid was a kind gift from Jan Lorenzen. To prepare a standard for gas chromatographic analysis, the mixture was purified using preparative liquid chromatography (PLC-2050, Gilson, USA). The resulting standard showed a purity of 97% and was methylated before being used for calibration on GC-FID. Other fatty acids were purchased as standards (either from CarlRoth, Germany, or Sigma Aldrich, Germany) and used for calibration.

2.5.2 Quantitative analysis using GC-FID

For the quantitative analysis of fatty acids, methylated samples were measured using a SHIMADZU GC-2025 (Shimadzu, Japan) with an AOC-20i auto-injector and ZBWAX 13 m/Ø 0.32 mm with a hydrogen flow rate of 14 ml/min, synthetic air flow of 400 ml/min and nitrogen with a flow rate of 30 ml/min and a temperature increase from 150 °C to 240 °C in 5 °C steps per minute. Marine oil mix (Restek, USA) was used as an external standard.

2.5.3 Qualitative analysis using GC-MS

For the qualitative analysis of fatty acids, either methylated or silylated samples were measured on a Trace GC Ultra with a mass spectrometer DSQ2 including a Triplus Autosampler and an SSL Injector (Thermo Fisher, USA). The Temperature ramp was kept at 180 °C for 2.5 min, then increased by 5 °C/min until 285 °C was reached. The used split ratio was 12 and the flow rate 0.8 ml/min. The ion source temperature was 250 °C, the injection volume 1 µl and the mass range 50–650 m/z.

2.6 FAD calibration

For the concentration measurement of FAD, a calibration curve of FAD fluorescence in either 20 mM Tris-Base, 200 mM NaCl, pH 7.2 for OhyRe and OhyPp or 50 mM HEPES, 200 mM NaCl, pH 6 for OhyEm was obtained at an excitation wavelength of 450 nm and at an emission wavelength at 525 nm. The native protein solution was measured for “free” FAD, then proteins were denatured for 15 min at 70 °C and the clear supernatant was measured for “total” FAD. “Bound” FAD was calculated by “total” FAD – “free” FAD.

2.7 K_d-measurement

FAD was removed from OhyEm as described in Engleder *et al.*[21]. FAD (Alfa Aesar, USA) was titrated in 1 µl steps to a 300 µl protein solution with a concentration of 5 µM and with an excitation wavelength of 295 nm and an emission of 335 nm. The fluorescence signal of tryptophan was measured in a Quartz multi-well plate on a plate reader (EnSpire, PerkinElmer, USA). Curves were fitted using the formula Vmax*X/(Kd+X) for OhyPp and OhyRe and BmaxHi*X/(KdHi+X)+BmaxLo*X/(KdLo+X) for OhyEm.

2.8 Melting temperature analysis

Prior to transferring the samples to an RT-PCR cycler (CFX Opus 96, Bio-Rad), the samples were placed on ice. The temperature ramp ranged from 10 °C to 95 °C in 0.5 °C increments, with each cycle holding for 10 seconds. The experiments were performed in quadruplicate.

2.8.1 Melting temperatures of OhyEm, OhyPp and OhyRe

To 5 µl of a 5 µM protein solution of OhyRe, OhyEm or OhyPp 2.5 µl of 10xSYPRO™ Orange (Thermo Scientific, USA) and 16.5 µl of storage buffer were added to optically clear qPCR tubes.

2.8.2 Melting temperatures of secADH

In qPCR tubes with optically clear lids, a mixture was prepared by combining 5 µl of secADH (2 mg/ml) with 2.5 µl of SYPRO™ Orange (Thermo Scientific, USA) (at a dilution of 1:200). Additionally, either 1.3 µl of ethanol as a control or 1.3 µl of 10 mM solutions of each secondary alcohol dissolved in ethanol were added. To complete the mixture, 16.2 µl of buffer was included. For pH 6.5, MES buffer (100 mM) was utilized, while pH 7.5 was achieved with Tris-Base buffer (100 mM), and for pH 9, TAPS buffer (100 mM) was employed.

2.9 Cascade reaction of Lipase and OhyRe

To 329 µl of 20 mM Tris-Base pH 7.2, 1 µl of each respective oil was added and emulsified. Next, 50 µl of OhyRe (2 mg/ml with an equimolar concentration of FAD) and 20 µl of lipase (2 mg/ml) were added. Samples were methylated and measured with GC-FID.

3 Publications

3.1 Publication summaries

3.1.1 Expanding the Portfolio by a Novel Monomeric Oleate Hydratase from *Pediococcus parvulus*

The article 'Expanding the portfolio by a novel monomeric oleate hydratase from Pediococcus parvulus' was published in May 2023 in the journal ChemCatChem. Sophia Alice Prem conceptualized and conducted the study as well as most experiments except for the Robetta model and the size exclusion chromatography - multi-angle light scattering experiments.

The first publication highlights a new oleate hydratase (OH) from *Pediococcus parvulus* (OhyPp) identified by means of genome mining. These types of enzymes are known to functionalize unsaturated fatty acids and are of high potential to one day replace the current production methods of hydroxylated fatty acids for industrial applications. For that, a portfolio of different OHs is desirable to choose from depending on the requirements of the process and to gain more insights into their modes of action. That is why we have characterized the novel OhyPp, thereby reporting only the second monomeric OH with distinct features. The enzyme differs from the reported reference OH from *Rhodococcus erythropolis* (OhyRe) despite a sequence identity of 74% and a similarity of 91%. OhyPp is the second member of the Hfam3 family and, just like OhyRe, occurs as a monomeric protein, which brings potential benefits in immobilization strategies.

As structure elucidation by crystallization failed, the protein's structure was predicted with a Robetta model disclosing a similar one to OhyRe. Sequence-wise, OhyPp contains a strictly conserved methionine in the position of a glutamic acid, which was suggested to be involved in the catalysis of HFam11 members, confirming the theory of a diverging mechanism in HFam3 family members.

OhyPp, similar to OhyRe, relies on FAD for its functioning, but surprisingly, it exhibits a higher affinity for FAD. Nevertheless, OhyEm still maintains significantly stronger affinities, being 200 and 500 times higher than OhyPp and OhyRe, respectively. Generally, OHs display low occupancy of FAD, which currently hampers their utility in industrial processes due to cofactor loss during purification and subsequent reuse cycles. Among the HFam3 family members, which have the lowest binding affinity to FAD, a distinctive feature—a flexible loop—in close proximity to the FAD binding cleft, might play a role. The disparities in FAD affinities observed between OhyRe and OhyPp

provide valuable insights into the binding properties of FAD and the potential residues responsible for the binding process.

In summary, OHs still require optimization before they can be applied in industrial settings and the novel OhyPp helps by providing novel information on the structural and catalytic features.

3.1.2 Two Cascade Reactions with Oleate Hydratases for the Sustainable Biosynthesis of Fatty Acid-Derived Fine Chemicals

The article 'Two Cascade Reactions with Oleate Hydratases for the Sustainable Biosynthesis of Fatty Acid-Derived Fine Chemicals' has been published in August 2023 in Catalysts by MDPI. Sophia Alice Prem conceptualized and conducted the study and performed all experiments.

The second publication comprises the application of the monomeric oleate hydratase OhyRe embedded in two cascade reactions guiding the way towards facile one-pot reaction with less downstream processing for future industrial applications and for the use in high-throughput screening assays. Cascade reactions widely increase the product spectrum of fatty-acid derived fine-chemicals.

First, it was necessary to optimize the yield of OhyRe as OHs often hold low turnovers, which limits the overall outcome of a cascade reaction. It is known that OHs require $FADH_2$, however, the reduction of FAD has so far been conducted under anaerobic conditions using elaborate chemical means or by photobleaching in an oxygen depleted environment. It could be observed, however, that light exposure with broad-band white light at an intensity of 364 µmol/m^2*s led to a 40-fold increase in activity of OhyRe.

The first presented cascade reaction is a one-pot conversion of different types of triglyceride oils, where the first step contained a lipase for lipid hydrolyzation, and the second step contained OhyRe resulting in varying yields of 10-HSA depending on the type of oil. Surprisingly, microbial oil from *Cutaneotrichosporon oleaginosus* showed the highest yield documenting optimal purity and oleic acid content for this reaction, whereas high-oleic sunflower oil showed a rather low yield of 10-HSA despite having the highest ratio of oleic acid, presumably either due to the lipase's preference or the high oleic acid content's effect, inhibiting OhyRe.

A second cascade was introduced with a before unknown secondary alcohol dehydrogenase (secADH), which can oxidize 10-hydroxy stearic acid (10-HSA), the product of OHs with oleic acid as a precursor to 10-keto stearic acid (10-KSA). Since each of the cascade's member has specific requirements regarding the optimal parameters, extensive optimization, and characterization of the cascade reaction and the secADH was needed. As opposed to OHs, the secADH prefers a basic environment leading to compromises in optimal reaction conditions. The optimization of the cascade reaction showed that either OH or the secADH dominate the reaction conditions and that an optimization is required for each applied OH. The secADH has a rather high melting

temperature, which decreases at higher pH-values and with the exposure to fatty acids as a substrate. An increase of the secADH's concentration leads to a decrease in the cascade's yield hinting towards a product inhibition. Furthermore, the effect of additives for substrate emulsification was evaluated, showing only improvements in low concentrations. Lastly, a conversion over 16 h has been conducted with the optimal reaction parameters leading to a maximum of 10-KSA of 30%, reflecting the consequence of the compromise of non-optimal reaction conditions due to varying requirements.

In a broader context, the incorporation of cascade reactions alongside OHs holds the promise of substantially influencing catalyst optimization screenings and finding industrial applications in the future. This potential stems from their capacity to streamline processing steps, resulting in time and cost savings. The data presented in this context represents initial progress towards the practical realization of these cascade reactions.

3.2 Full-length publications

Full-length publication 1

"Expanding the Portfolio by a Novel Monomeric Oleate Hydratase from *Pediococcus parvulus*"

ChemCatChem

Research Article
doi.org/10.1002/cctc.202300478

Chemistry Europe
European Chemical Societies Publishing

www.chemcatchem.org

Expanding the Portfolio by a Novel Monomeric Oleate Hydratase from *Pediococcus parvulus*

Sophia A. Prem,[a] Carl P. O. Helmer,[b] Bernhard Loll,*[b] Daniel Garbe,[a] and Thomas Brück*[a]

Oleate hydratases convert oleic acid into 10-hydroxy stearic acid, a valuable fine chemical, useful in lubricant and surfactant formulations. They are of large interest due to their high expression rates and solubility, however, they differ drastically by their overall stability and pH- and temperature ranges. To expand their portfolio, another oleate hydratase named OhyPp (originating from *Pediococcus parvulus*) was characterized. It is a close relative of the well-known oleate hydratase OhyRe from *Rhodococcus erythropolis*. OhyPp is only the second member of the monomeric oleate hydratase family with some surprising catalytic features. A distinct characteristic is OhyPp's higher affinity towards FAD compared to OhyRe's helping to understand and improve FAD binding in the future, which is a current drawback for the industrial application of oleate hydratases.

Introduction

Driven by climate change and legislative CO_2 capping measures, several industry sectors are developing sustainable process solutions based on renewable feedstocks. In this context enzymes substitute for chemical catalysts, as they can selectively convert renewable feedstocks at ambient temperatures. Specifically, the enzyme family of hydratases selectively catalyze the hydration of C=C bonds resulting in products, which are conventionally manufactured under high pressure and temperatures by chemical methods. Hydratases are usually well expressed in recombinant systems without the need of unstable cofactors, which would need to be recycled. Moreover, hydratases can catalyze sophisticated, asymmetric reactions.[1–3]

Recently, much attention has been drawn to a class of unsaturated fatty acid converting enzymes called oleate hydratases. These enzymes turn unsaturated fatty acids into hydroxylated fatty acids. Most of them have a high prevalence for accepting oleic acid as a substrate,[3] which is a main fatty acid component of many sustainable plant-based and microbial triglycerides such as high-oleic sunflower oil or oil from yeast *Cutaneotrichosporon oleaginosus*.[4]

Hydroxylated fatty acids are predominantly found in a range of microorganisms, in which they are considered to be defense factors against toxic free fatty acids.[5] Free long chain unsaturated fatty acids are known for their antibacterial effects on gram positive bacteria. Originally, they were thought to disintegrate the microbial cell membrane. However, saturated fatty acids don't convey the same inhibiting effects as unsaturated ones. Instead, it has been reported that long chain unsaturated fatty acids inhibit the FabI enzyme, which is part of the bacterial type II fatty acid synthesis. Additionally, other fatty acid converting enzymes derived from other organisms are known to be inhibited by unsaturated fatty acids.[6] Gram negative bacteria show no inhibition from free long chain unsaturated fatty acids, which most likely is connected to their cell wall being less penetrable for fatty acids. Hydroxy-fatty acids functionally resemble more saturated fatty acids and thus most likely are less toxic than their unsaturated counterparts.[7] Even though it is reported that gram negative bacteria are resistant towards free long chain unsaturated fatty acids, many of them are known to carry fatty acid hydratases.[8,9] That is why most likely, there are other functionalities besides the detoxification. One of them might be their effect on the general cellular stability, most likely conveyed through alterations in the membrane. It was observed that bacteria harboring oleate hydratase activities are more resistant towards heat and solvent stress, which was attributed to a modulated membrane composition.[10] Additionally, it has been reported that marine microorganisms produce 2-OH-hydroxylated fatty acids and that their concentration increases upon exposure to a low pH, which presumably leads to a better flow control of ions into the cell.[11] Some organisms are known to carry more than one fatty acid hydratase further complementing their evolutionary advantages.[12–14] Additionally, microorganisms have been found to be more heat and solvent resistant by carrying an oleate hydratase gene.[10]

Oleate hydratases belong to the class of fatty acid hydratases (EC 4.2.1.53) and have great potential to become a useful industrial biocatalyst for the generation of valuable fatty acid derivates such as (*R*)-10-hydroxy stearic acid (10-HSA),

[a] S. A. Prem, Dr. D. Garbe, Prof. T. Brück
TUM School of Natural Sciences
Werner Siemens-Chair of Synthetic Biotechnology
Technical University of Munich (TUM)
Lichtenbergstr. 4, 85748 Garching (Germany)
E-mail: brueck@tum.de
[b] C. P. O. Helmer, Dr. B. Loll
Institute for Chemistry and Biochemistry
Laboratory of Structural Biochemistry
Freie Universität Berlin
Takustr. 6, 14195 Berlin (Germany)
E-mail: loll@chemie.fu-berlin.de

Supporting information for this article is available on the WWW under https://doi.org/10.1002/cctc.202300478

which is considered as a replacement for (*R*)-12-hydroxy stearic acid (12-HSA), an industrial product applied as lubricant and emollient. 12-HSA is currently generated by chemical hydrogenation of castor oil under extreme pressure and temperature with the help of metal catalysts, thus calling for a more eco-friendly alternative process.[5] Furthermore, hydroxylated fatty acids are valuable precursors for flavor lactones, where some fatty acid based lactones convey fruity and milky odors.[15] For instance, γ-dodecalactone is a component responsible for the buttery flavor in milk fat and can be produced from oleic acid with 10-HSA as an intermediate.[16] Compared to chemical synthesis, these natural hydroxy fatty acids have higher value since they are stereospecific.

Oleate hydratases were applied in the form of whole-cell catalysis,[17] isolated as pure enzymes[18] and as cell-free extract.[19] Recently, an oleate hydratase and a linoleate hydratase were used as part of a microbial host process, where their genes were integrated into the genome of *Yarrowia lipolytica* to produce γ- and δ-dodecalactone.[15] Fatty acid hydratases act strictly on free fatty acids, whereas they can't convert fatty acids as part of triacyl glycerides.[20]

So far, a variety of oleate hydratases originating from different organisms were described and characterized. Economical industrial processes ask for distinct requirements, which can be sustained by a large portfolio of enzymes with varying characteristics. These comprise different pH- and temperature profiles, dimeric or monomeric structures, turnover rates and substrate specificity.[3] At present, the only reported monomeric oleate hydratase is OhyRe originating from *Rhodococcus erythropolis*, while all other reported enzyme varieties are functional dimers. Until now, crystal structures of OhyRe,[18] OhyEm (*Elizabethkingia meningoseptica*),[21] OySa (*Staphylococcus aureus*),[22] OhySt (*Stenotrophomonas sp.* KCTC 12332)[23] and OhyLa (linoleate hydratase from *Lactobacillus acidophilus*)[24] are available. The structures of OhyEm, OhySa and OhySt were determined with bound FAD and OhySa is the only structure, where the binding of 10-HSA and oleic acid was observed. FAD dependency is a characteristic of oleate hydratases and in Radka *et al.*,[22] it was suggested that upon binding of FAD a conformational shift allows the substrate oleic acid to enter deep into the inner active site cavity, which prevents water quenching of reactive intermediates, subsequently allowing for substrate conversion to the target product.

It is known that oleate hydratases have a substantially higher activity using $FADH_2$ as a cofactor.[21,25] On the other hand, upon cell lysis and purification, $FADH_2$ gets oxidized immediately to FAD, which makes an industrial application using $FADH_2$ impractical. Depleting oxygen and using additives increases the costs to produce a normally cheap molecule such as 10-HSA and additives also contaminate the final product. But also for small scale measurements and reactions, this causes several issues. The affinity measurement of $FADH_2$ towards the enzyme is elaborate and additives might influence the interaction between enzyme and ligand. In general, oleate hydratases have low affinity towards FAD and many lose it upon purification, hampering current industrial applications.[5]

In this study, a close relative of OhyRe has been identified and characterized. It is an oleate hydratase originating from *Pediococcus parvulus*, (OhyPp) (former name *Pediococcus damnosus*), a lactic acid bacterium, first extracted from ropy Basque Country ciders, which today is used as a starter culture for the fermentation of vegetables, meat and dairy products.[26] We could demonstrate that OhyPp is monomeric and has slightly higher affinity towards FAD than OhyRe. Additionally, this variant offers unexpected insights into the structural features of binding of FAD and expands the portfolio of monomeric oleate hydrases by a new member.

Results and Discussion

OhyPp – a close relative of OhyRe

OhyPp is predicted to be 558 amino acids long with a calculated molecular mass of 66.4 kDa. For protein expression in *Escherichia coli*, a codon-optimized DNA-sequence of OhyPp was cloned into the vector pET28a(+) and expressed with an N-terminal His-tag (Figure S1), (DNA and amino acid sequences see supporting information). After purification via IMAC, the enzyme solution was nearly colorless, which is a similar effect as for OhyRe and can be attributed to a loss of FAD. This subsequently leads to a loss of activity as well. Such an observation has been made for many fatty acid hydratases.[18,20,21,24]

Quaternary structure analysis

We employed size exclusion chromatography coupled to multi-angle light scattering to analyze the oligomerization state of OhyPp in solution. OhyPp can be characterized as a monomeric enzyme as OhyRe (Figure S2).[18] Monomeric oleate hydratases lack N- and C-terminal extensions in their amino acid sequence, which are thought to be responsible for dimerization.

Optimal reaction conditions

The optimal growth temperature of *P. parvulus* is at 30 °C[26] diverting from the optimal temperature of OhyPp at 18 °C (Figure 1(A)). The optimal pH is at 6 with a rather low tolerance for a wide range compared to OhyRe (Figure 1(B)). Furthermore, OhyPp requires a buffer containing 200 mM NaCl (Figure 2), which yielded in the highest activity. Interestingly, OhyPp was not stable at a pH of 6 and 6.5 using 50 mM MES, 200 mM of NaCl and phosphate buffer, observable by instant aggregation during desalting and loss of activity. Therefore, OhyPp was stored in 20 mM Tris/Base and 200 mM NaCl at pH 7.2, where no immediate aggregation was observed, while enzyme activity remained. For the reactions, MES buffer (50 mM MES, 200 mM NaCl, pH 6) was added to the reaction medium so that a final pH of 6 was reached.

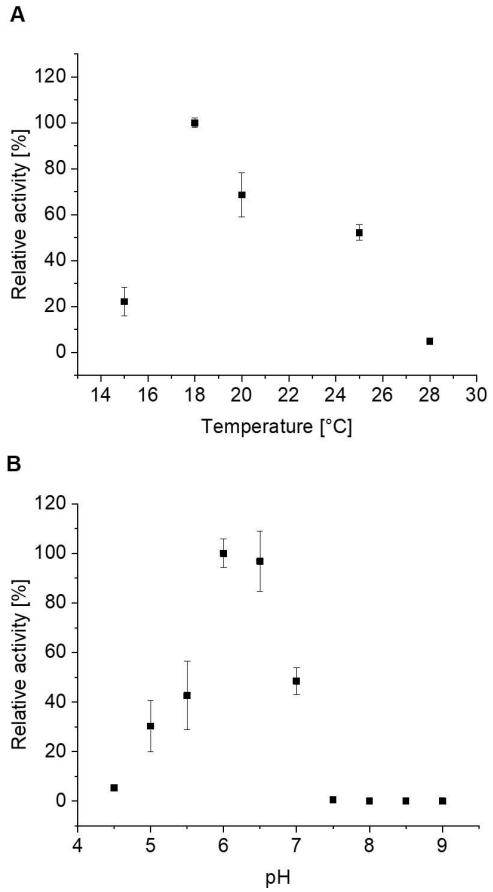

Figure 1. (A) Determination of the optimal reaction temperature. Values are normalized to maximal activity. Enzyme was stored in 20 mM Tris/Base, pH 7.2, 200 mM NaCl and 50 mM MES, 200 mM NaCl buffer was added to reach a pH of 6 in the reaction. Error bars represent the standard deviation of triplicate experiments. **(B)** Determination of the optimal pH. Values are normalized to maximal activity (pH 6). The different buffer types used can be found in the experimental section. Error bars represent the standard deviation of triplicate experiments.

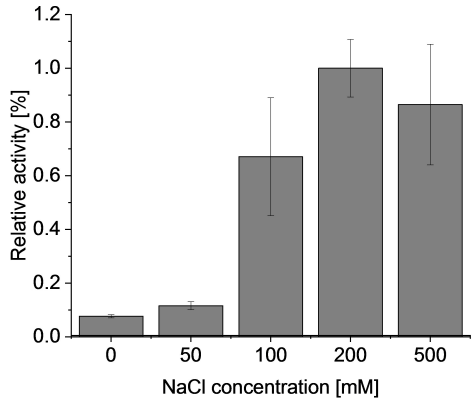

Figure 2. Determination of the optimal NaCl-concentration for activity. Values are normalized to the maximal activity at 200 mM NaCl. Enzyme was stored in 20 mM Tris/Base, pH 7.2, 200 mM NaCl and buffer was adjusted to a pH of 6 with MES buffer for the reaction. Error bars represent the standard deviation of triplicate experiments.

OhyPp having a theoretical pI of 5.33[27] is more active in acidic environments than in basic ones reflecting the strong acidity of both substrate and product. Oleic acid itself has a pK_a of 5.02 (https://pubchem.ncbi.nlm.nih.gov) and thus a strong acidifying effect on buffer systems, which leads to anticipated pHs not being reached. For instance, at experimental conditions with 100 mM Tris/Base, pH 7 and 0.15% oleic acid, the pH dropped down to 6.7. The pH was therefore measured and set to a specific value prior to the experiment. At a pH above 7, oleic acid turns immediately opaque upon mixing with water-based buffers and extended foaming occurs.

At pH-values between 7 to 9, at temperatures below the melting temperature, free fatty acids are known to form crystalline solids consisting of a mixture of acid and soap.[28] These are extremely insoluble in water and consequently only low concentrations of the monomeric fatty acids remains in solution. This monomer stays in equilibrium with the formed crystal. Therefore, this leads to less substrate availability for fatty acid hydratases. Crystals were macroscopically observable. However, the effect was more profound for Tris/Base buffer and thus at a pH above 7.5, N-Tris(hydroxymethyl)methyl-3-amino-propanesulfonic acid (TAPS) buffer was used.

Fatty acid specificity

OhyPp was tested for conversion of a range of different unsaturated fatty acids, which are listed in Table 1. Palmitoleic, linoleic and α-linolenic acid get converted (Figure S3). In general, most fatty acid hydratases have the highest specificity for either linoleic or oleic acid and a rather low tolerance for other substrates.[12,3] A broad substrate spectrum is unique and there is currently just one hydratase known to convert substrates ranging from C16 to C22 unsaturated fatty acids.[12] However, most oleic acid hydratases convert linoleic and linolenic acid as a structural relative.[3]

Table 1. Fatty acids tested for conversion by OhyPp.

Fatty acid		Products	Conversion [%]
palmitoleic acid	C16:1 cis-9	10-hydroxy-hexadecanoic acid	2.3 ± 0.2
petroselinic acid	C18:1 cis-6	n.d.[a]	–
oleic acid	C18:1 cis-9	10-hydroxy octadecanoic acid	34.3 ± 7.7
elaidic acid	C18:1 trans-9	n.d.[a]	–
linoleic acid	C18:2 cis-9,12	10-hydroxy-12(Z)-octadece-noic acid	24.6 ± 7.1
α-linolenic acid	C18:3 cis-9,12,15	10-hydroxy-12(Z), 15(Z)- octa-decadienoic acid	8.9 ± 2.3
gadoleic acid	C20:1 cis-9	n.d.[a]	–
arachidonic acid	C20:4 cis-5,8,11,14	n.d.[a]	–
nervonic acid	C24:1 cis-9	n.d.[a]	–

[a] Not detected.

OhyPp was observed to convert palmitoleic, linoleic and α-linolenic acid besides oleic acid. As most OHs only accept cis-fatty acids for conversion, also OhyPp is not able to convert elaidic acid, the trans-isomer of oleic acid. Furthermore, petroselinic acid is not converted and in linoleic and linolenic acid, only the 9-double bound gets converted leading to the conclusion that OhyPp prefers the 10-position for hydroxylation. Longer fatty acids such as gadoleic and nervonic acid are most likely too large for the inner cavity of OhyPp. In Busch *et al.*,[14] an extensive substrate screening with OhyRe and another *Rhodococcus sp.* OH has been performed showing OhyRe to be the first OH to hydroxylate fatty acids at the 12-position. It will be interesting to investigate whether this is specific for HFam3 family members and compare them to other families leading to more insights into the hydration dynamics.

Sequence comparison

OhyPp is the current closest relative of OhyRe within the NCBI-data base holding a 74% identity and 91% similarity of the sequences. Hydratases were grouped into eleven different classes (HFam1-11) depending on their levels of sequence similarity (HyED, https://hyed.biocatnet.de).[9] OhyEm belongs to HFam11,[21] whereas OhyRe and OhyPp can be categorized into HFam3.[18] Within a class, there is an average global sequence identity of 62%, however, between classes, the identity can be significantly lower. Between OhyEm and OhyRe/OhyPp, there is only a 28/27% identity with a similarity of 56/58% (Table S1).

To gain structural insights in OhyPp, we intended to solve the crystal structure.

Extensive crystallization studies with and without His_6 tag did not lead to crystals diffracting to high resolution, therefore a model for OhyPp was build utilizing Robetta[29] (Figure 3). Compared to the overall structure of OhyRe, the Robetta model of OhyPp is very similar to OhyRe with a root mean square deviation of 1.3 Å for 518 pair of Cα-atoms (Figure S4). OhyPp is organized in four domains, with the FAD binding site composed of domain I and II. Characteristic of members of the HFam3 family, is an extended FAD binding loop, which is extended by about 25 amino acids compared to members of other subfamilies.

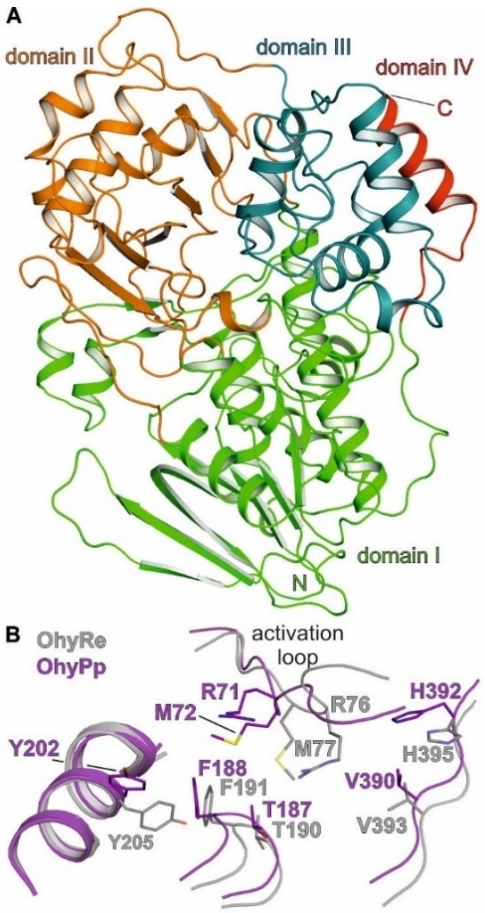

Figure 3. Domain organization of OhyPp with domain I in green, domain II in orange, domain III in deep teal and domain IV in red **(A)**. Superposition of the modelled active site of OhyPp (deep purple) and OhyRe (PDB-ID: 5odo;[18]) coloured in grey **(B)**. Important residues lining the active site are shown in stick representation.

FAD binding

The binding of FAD in comparison to OhyEm and OhyRe was analyzed. To investigate how much FAD is bound to each protein, total FAD concentration was measured by fluorescence after the proteins were denatured with heat and the aggregated protein debris were separated by centrifugation since only unbound FAD returns a fluorescence signal. The occupancy defined as the molar ratio of total FAD per protein is very low in all three proteins. For OhyPp and OhyEm, there is a 15% occupancy after Ni-NTA purification for both and a 6 and 13% occupancy, respectively, after desalting. In contrast, in OhyRe, there is only a 1% occupancy after Ni^{2+}-NTA and no FAD could be detected after desalting. Most FAD was unbound and free in solution of native OhyRe (99%) and OhyPp (78%), whereas in OhyEm most FAD was released only after denaturation. In OhyEm, only 9% of FAD was mobilized after purification. This can either be because parts of the proteins are already denatured or – more likely – that the affinity in OhyRe and OhyPp is so low that most FAD gets released immediately during the purification process. Since there seems to be a diverging behavior on FAD binding, the respective affinities were measured in form of dissociation constants (K_d) by using the quenching of tryptophan fluorescence. Indeed, the K_d of OhyPp was slightly lower than OhyRe's: 83.57 ± 4.11 μM and 204.47 ± 36.75 μM, respectively. Since OhyEm is a dimeric protein, it holds two K_d-values which can be obtained by regression analysis. The first one was measured to be 0.39 ± 0.06 μM, whereas the second one 120.11 ± 2.66 μM (Figure S5). Consequently, OhyEm holds a 500-fold higher affinity than OhyRe and a 200-fold higher one than OhyPp towards FAD. This is also reflected in the activity. After purification, OhyRe and OhyPp lost all activity whereas OhyEm was still active.

Hence, the conversion reaction with OhyPp needs an addition of external FAD.

FAD-binding motive

Characterized oleate hydratases have a commonly conserved FAD binding motive. Specifically, they all harbor a GXG fingerprint (starting at position 8 in OhyPp in Figure S6), which serves as a connecting loop between a β-strand and an α-helix as parts of the Rossman-fold. The first glycine leads to a sharp turn of the structure, whereas the second one allows the FAD's pyrophosphate to bind close to the following α-helix.[30]

The overall FAD binding patterns differ slightly since HFam3-members are having a GXGXXN and HFam11-members comprise the more common $GXGXXGX_{21}E/D$ motif. The latter acid is responsible for binding the 2'-OH of the ADP-ribose. In HFam3-members, the acidic amino acid is replaced by a hydrophobic one being mostly tyrosine, methionine or in the case of OhyPp a phenylalanine.

GGR – a conserved pattern

Oleate hydratases display a strongly conserved RGGREM pattern and has been firstly described by Radka *et al.*[31] It is located in a conserved loop and in proximity of the isoalloxazine ring of FAD and of the suggested substrate binding pocket. Whereas the first arginine is not strongly conserved amongst oleate hydratases, the following sequence "GGR" is. The second arginine and glutamic acid are suggested to bind the isoalloxazine ring in OhySa and additionally, the glutamic acid is described as crucial for activity since it stabilizes a hydronium ion enabling it to attack the oleate π-bond. In OhyRe and in OhyPp, however, the glutamic acid is replaced by a methionine, which is not able to conduct the catalytic reaction in the same way as suggested for OhySa.[22] Interestingly, this is in alignment with an oleate hydroxylase from *Ricinus communis* and the fatty acid desaturase FAD2 of *Arabidopsis thaliana*, as shown in Figure 4. Both are also carrying a methionine at the identical position.

Oleate hydroxylases are different compared to oleate hydratases in a way that they are membrane bound, convert fatty acids that are esterified to phosphatidylcholine and require NADH and cytochrome *b*5 as cofactors.[34] Furthermore, there is a charge-transfer reaction involved in the reaction, defining hydroxylases as oxidoreductases and these hydroxylases carry μ-oxo-bridged diiron cluster making the enzyme dependent on oxygen and iron.[35] Despite the differences between those fatty acid converting enzymes, GGR is a common motive, and it shows a certain degree of evolution between oleate hydratases and plant oleate desaturating enzymes. This sequence most likely is important for fatty acid or cofactor interaction or for activity.

A noticeable structural difference between HFam3 and HFam11 oleate hydratases is the so called "FAD-lid", which contains a conserved GXXXG pattern as opposed to a GGXXXG pattern in the latter. Furthermore, this region is prolonged in HFam3 by 13 amino acids compared to HFam11-type enzymes. This region together with the activation loop is undergoing large conformational changes after FAD interaction in OhySa.[22] These shield the FAD binding site from the solvent.

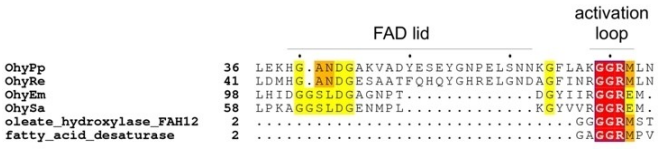

Figure 4. Alignment of the FAD lid and activation loop of two monomeric members of the HFam3 family (OhyRe and OhyPp), two dimeric members of the HFam11 family (OhyEm and OhySa), an oleate hydroxylase from *R. communis* (NP_001310650.1) and a fatty acid desaturase from *A. thaliana* (NP_001319529.1) using the COBALT constraint alignment tool[32] and ESPript from the Endscript-server for visualization (https://espript.ibcp.fr).[33]

Kinetic parameters

Kinetic parameters were measured for OhyPp using oleic acid as a substrate. They resulted in a K_m value of 21.06 ± 5.95 mM and a k_{cat} of 11.46 ± 0.05 min^{-1} (Figure S7). OhyPp is a rather slow enzyme with a half time of 3.7 h, where the maximal conversion could be observed after 24 h (Figure S8).

Kinetic parameters of enzymatic reactions are used to study enzymes' behavior in living organisms or to simulate conversion for industrial upscaling. However, oleate hydratases are a special case. For several oleate hydratases, kinetic parameters were measured. However, their scientific pertinence must be evaluated carefully. Oleic acid is not miscible in water but fatty acid hydratases need access towards their substrates, which can be achieved by creating a emulsion. However, the emulsion formation and its quality are dependent on the preparation protocol. Local and uneven dispersion effects are not avoidable. At a pH above 7, oleic acid forms a soap and is thus more miscible in water. So already the variation in pH has a strong effect on fatty acid dispersion in water and thus the measurement of kinetic parameters is not able to represent the enzyme's natural behavior. In previous experiments, where 10-HSA was enzymatically produced in larger scale and extracted as solid flakes, it could be observed that full conversion was not achieved noticeable by flakes, which still contained significant amounts of oleic acid. Consequently, 10-HSA precipitates together with oleic acid to a solid material even when the former is abundant only in low concentrations. Thus, the more 10-HSA is produced, the more oleic acid leaves the emulsion and is not available for the enzyme for conversion anymore. Also, the way the manual assay is carried out has a strong effect on the reaction's outcome. In summary, all the described challenges are reflected in strongly diverting kinetic parameters for the same enzymes as for example observed by Zhang *et al.*[3] Kinetic parameter assessment out of context meaning not under exactly equal and consistent reaction conditions as used

for upscaling or without a direct comparison are not useful and don't aid in understanding the *in vivo* behavior.

Long-term stability

Long-term stability of OhyPp at 4 °C was assessed and compared with the dimeric enzyme OhyEm. Dimeric enzymes are reported to lose activity due to subunit dissociation amongst other reasons and in an immobilization study, this has been named as a main reason for activity loss for OhyEm.[36] In that study, it has been reported that OhyEm loses 60% of its activity already after 7 days, however, our experiments were contradictory. OhyEm and OhyPp were both stable for a period over 9 days at an equal level and despite some fluctuations still retain 60 and 80% of their initial activity. However, after 27 days, OhyEm still carried 80% of its initial activity, whereas OhyPp only held around 20% (Figure 5).

OhyPp is thus less stable during extended storing than OhyEm, even though the latter is a dimeric enzyme. Consequently, other reasons besides the dissociation of subunits play a role. One might be the higher affinity of OhyEm towards FAD, since FAD binding will stabilize the overall fold of the protein. Whereas at 4 °C enzyme stability is high, during reaction conditions, oleate hydratases are reported to lose activity rather quickly.[9] This is also the case for OhyPp, which during the reaction started to denature forming a white debris. Resolubilization with ethyl acetate was not possible, arguing for protein aggregates, rather than precipitated 10-HSA. One of the reasons might be that free fatty acids can act as soaps and even though the enzymes are evolutionary adapted to these substrates, they still might denature upon exposure to a large excess of free fatty acids. As a result, much more stable enzymes are required for industrial processes.

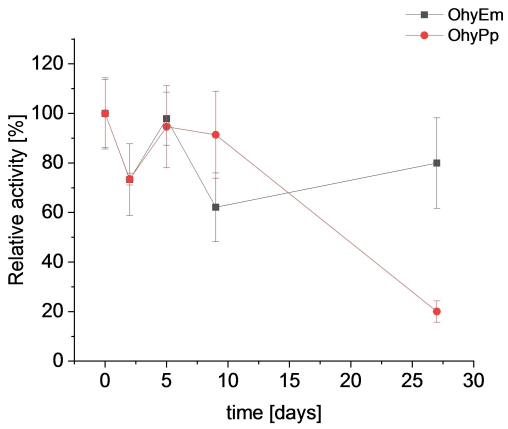

Figure 5. Stability test of monomeric OhyPp compared to dimeric OhyEm over the course of 27 days. Enzyme solutions were stored at 4 °C in each enzyme's respective optimal buffer. Error bars represent the standard deviation of triplicate experiments.

Melting temperatures

Additionally, the melting temperatures of OhyPp, OhyRe and OhyEm were analyzed and compared with each other. OhyPp has a lower long-term stability than OhyEm and this is also reflected in differences in the melting temperatures of these enzymes. OhyEm showed the highest melting temperature with 52.5 ± 0.2 °C. OhyRe's melting temperature was determined with 45.0 ± 0.0 °C and OhyPp has the lowest one with 41.1 ± 0.2 °C. The significant higher melting temperature of OhyEm could be explained by the dimeric occurrence of the protein. The protein-protein interface confers additional stabilization to the dimer. The lowest melting temperature of OhyPp could at least in parts explain the difficulties in the crystallization of the protein.

Conclusion

An oleate hydratase from HFam3 named OhyPp was identified, which is closely related to the already known OhyRe. OhyPp lacks N- and C-terminal extensions, which most likely are responsible for dimerization in agreement with our SEC-MALS experiments confirming OhyPp being monomeric in solution. Despite its high sequence similarity with OhyRe, OhyPp has different characteristics. Its optimal pH is at 6, however, the enzyme is much more stable at a pH of 7.2. Its temperature optimum is differentiating to OhyRe's but also to the organism's optimal growth temperature. OhyPp is able to convert palmitoleic acid and the structural relatives of oleic acid linoleic and linolenic acid. It prefers cis-configuration and doesn't accept substrates with carbons above 20.

Most FAD is lost upon purification, which appears to be typical for monomeric oleate hydratases belonging to the HFam3 subfamily. This low affinity towards FAD currently limits their application in industrial applications. Optimizing this characteristic by using means of protein engineering is thus desirable as OhyPp's sequence and structure might help due to its higher affinity towards FAD compared to OhyRe's.

OhyPp has a similar amino acid sequence structure as OhyRe with a methionine on the position where HFam11 subfamily members carry a glutamic acid, which is thought to be an active residue in conversion. As a result, the proposed reaction mechanism may not be transferable to OhyPp as well. Furthermore, a strongly conserved amino acid motif "GGR" could be observed, which not only exists in all characterized oleate hydratases but also in other fatty acid dehydrogenating enzymes originating from plants.

Finally, stability of OhyPp is given to a minimum of nine days at 4 °C but it is lower compared to dimeric OhyEm. During the reaction, however, strong aggregation was observed. Its low stability might in part explain why no crystals could be obtained for assessing the structure. Instead, a model was designed showing a similar structure compared to OhyRe.

Oleate hydratases belong to one of the few soluble and high expression rate exhibiting fatty acid converting enzymes. They create the valuable industrial product 10-HSA, however,

major challenges remain for a successful adaption of large-scale industrial process and they mainly comprise low FAD binding and process stability. This new enzyme expands the portfolio by a new member and helps to further understand their function.

Experimental Section

Chemicals

Chemicals were mostly purchased from Sigma-Aldrich and Carl Roth at the highest available grade.

Cloning

The sequence of the novel putative oleate hydratase OhyPp (WP_057784965.1) has been derived from the National Center for Biotechnology Information[37] as closest relative of OhyRe in the data base and was synthesized with codons optimized for *E. coli* by EurofinsGenomics. The gene was subsequently cloned into pET28a(+) using Gibson Assembly® Cloning Kit (NEB). For PCR and subsequent cloning, Phusion High-Fidelity Polymerase (Thermo Scientific) was used. After PCR, open vectors were treated with Fast digest *Dpn*I and circularized with T4 DNA Ligase (both from Thermo Scientific). Plasmids were transformed into DH5α and sequenced.

Protein expression

BL21DE3 chemical competent cells were transformed with pET28a(+) containing OhyPp and resulting colonies were used to inoculate an LB overnight-culture, where all liquid cultures contained 50 μg/ml Kanamycin. 500 mL of TB-medium was inoculated with the overnight-culture and grown to an optical density OD_{600} of 0.6–0.8 at 37 °C. Temperature was decreased to 16 °C and cells were induced with isopropyl β-D-1-thiogalactopyranoside (IPTG) with a final concentration of 0.1 mM. After 16 h, cells were harvested, resuspended in buffer (20 mM Tris/Base, 20 mM imidazole, 500 mM NaCl, pH 7.2) using a high pressure homogenizator (EmulsiFlex-B15, AVESTIN). Cell debris were removed by a centrifuge at 20.000xg for 40 min at 4 °C. Protein was purified by incubating cell-free lysate using Ni^{2+}-NTA beads (Thermo Fisher) at 4 °C overnight, washed with buffer and eluted with elution buffer (20 mM Tris/Base, 250 mM imidazol, 500 mM NaCl, pH 7.2). The protein solution was dialyzed into "storage buffer" (20 mM Tris/Base, 200 mM NaCl, pH 7.2). Protein concentration was assessed using ROTI®Quant (Roth) with Bovine Serum Albumine (Roth) as standard. OhyEm was prepared as described in Engleder *et al.*[21] and OhyRe according to Lorenzen *et al.*[18]

Size exclusion chromatography – multi-angle light scattering (SEC-MALS)

SEC-MALS experiments were performed at 18 °C. OhyPp was loaded onto a Superdex 200 increase 10/300 column (Cytiva) previously equilibrated with SEC buffer (20 mM Tris/Base pH 7.5, 150 mM NaCl, 5 mM $MgCl_2$). The column was coupled to a miniDAWN TREOS three-angle light scattering detector (Wyatt Technology) in combination with a RefractoMax520 refractive index detector. For calculation of the molecular mass, protein concentrations were determined from the differential refractive index with a specific refractive index increment (dn/dc) of 0.185 ml g^{-1}. Data was analyzed with the ASTRA 6.1.4.25 software (Wyatt Technology).

Enzymatic assays

High-purity oleic acid (99%, Alfa Aesar) resulting in a final concentration of 0.4% was vortexed with 148 μl of storage buffer until emulsified. 100 μl of protein solution (15 μM) and 1 μl of FAD (3 mM) were added and solutions were incubated at their optimal temperatures with orbital shaking for 2 h. Reaction was stopped, and fatty acids were extracted using 1 mL of ethyl acetate. Reactions including ethyl acetate were vortexed, centrifuged at 15'000xg for 3 min and the upper ethyl acetate layer was transferred to a new vial. After drying off the ethyl acetate, fatty acids were methylated in a liquid handler (MultiPurposeSampler MPS Robotic, Gerstel) using a modified protocol originating from Griffiths *et al.*[38] with HCl methanol (Merck) instead of BF_3 methanol. In our modified protocol, 500 μl of toluene and 10 μl of the standard in toluene is added to the sample and mixed. Then 1 mL of sodium methoxide is added and incubated for 20 min at 80 °C. Afterwards, 1 mL of HCl methanol is added and the solution is incubated again for 20 min at 80 °C. After derivatization, 400 μl of water and 1 mL of hexane is added, the sample mixed, centrifuged and the upper toluene/hexane layer is taken for GC-FID (flame ion detector) analysis. As internal standard, lauric acid (Sigma–Aldrich) was used. Samples were analyzed on a SHIMADZU GC-2025 with an AOC-20i auto injector and ZBWAX 13 m/Ø 0.32 mm with a hydrogen flow rate of 14 ml/min, synthetic air flow of 400 ml/min and nitrogen with a flow rate of 30 ml/min and a temperature increase from 150 °C to 240 °C in 5 °C steps per minute.

Enzyme characterization

To measure the optimal temperature of OhyPp, reactions were conducted at 15, 20, 25 and 28 °C. The enzyme solution was preheated for 5 min to adjust to each respective temperature and the reaction was conducted for 20 min. For pH-tolerance, a pH-range of 4.5–9 was tested. 50 mM Citrate buffer was used for pH 4.5–5.5, 50 mM MES-buffer for pH 5.5–6.5 and 50 mM Tris/Base-buffer for pH 7–9. Reaction was performed for 2 h.

Fatty acid specificity and mass determination

1 mg of each fatty acid was mixed with 300 μl of storage buffer und 200 μl of OhyPp cell-free extract was added. Reactions were incubated for 24 h at 20 °C. For calculating the % conversion of oleic acid and linoleic acid, 1 mg of oleic acid and linoleic acid were mixed with 100 μl of storage buffer and 100 μl of 11.8 μM OhyPp for 24 h at 20 °C. Fatty acids were extracted with 1 mL of ethyl acetate and 1 mL of hexane. After the solvents were evaporated, the fatty acids were resuspended in 60 μl pyridine and diluted in a 1:20 ratio in 50 μl pyridine. To this, 20 μl of N-Methyl-N-(trimethylsilyl)trifluoracetamid (MSTFA) and 1% trimethylchlorosilane was added. Following incubation for 1 h at 50 °C, the samples were measured on a Trace GC Ultra with a mass spectrometer DSQ2, Triplus Autosampler and SSL Injektor. Temperature ramp started at 180 °C for 2.5 min, then 5 °C/min until 285 °C was reached. Used split ratio was 12 and the flow rate 0.8 ml/min. The ion source temperature was 250 °C, injection volume 1 μl and the mass range 50–650 m/z.

Measurement of FAD concentration

A calibration curve of FAD fluorescence in either 20 mM Tris/Base, 200 mM NaCl, pH 7.2 for OhyRe and OhyPp or 50 mM HEPES, 200 mM NaCl, pH 6 for OhyEm was measured using 450 nm as excitation and 525 nm as emission wavelength. For "free" FAD, the native protein solution was measured, for "total" FAD, proteins were denatured for 15 min at 70 °C and the clear supernatant was measured. "Bound" FAD was calculated by "total" FAD – "free" FAD.

K_d-measurement

OhyEm was depleted of FAD as described in Engleder *et al.*[21] FAD (Alfa Aesar) was titrated in 1 μl steps to a 300 μl protein solution with a concentration of 5 μM and the fluorescence signal of tryptophane was measured in a Quartz multi-well plate on a plate reader (Inspire) with an excitation wavelength of 295 nm and an emission wavelength of 335 nm. Curves were fitted using the formula Vmax*X/(Kd + X) for OhyPp and OhyRe and BmaxHi*X/(KdHi + X) + BmaxLo*X/(KdLo + X) for OhyEm.

Stability tests

For stability tests, the FAD concentration of OhyEm was measured using fluorescence after protein purification and to OhyPp the same molar amount of FAD was added to avoid any effect of a difference in FAD concentration. The protein solutions were stored without additional additives at 4 °C for a duration of 27 days in total and for each time step, the required amount of said solution was used. Assays were conducted as described under "enzymatic assays". For each enzyme, its optimal buffer and reaction temperature was used.

Melting temperature analysis

2.5 μl of 10 × SYPRO™ Orange (Thermo Scientific) was added to 5 μl of protein solution (5 μM) and 16.5 μl of storage buffer into qPCR tubes with optically clear lids. Samples were put on ice before transferring them to the RT-PCR cycler (CFX Opus 96, Bio-Rad). Ramp went from 10–95 °C in 0.5 °C steps holding for 10 s per cycle.

Acknowledgements

Carl P. O. Helmer was supported by the RTG 2473 graduate school, funded by the Deutsche Forschungsgemeinschaft (project number 392923329). Sophia A. Prem was supported by the German Federal Ministry of Education and Research (project: GreenCarbon, project number 03SF0577A). We also want to thank Martina Haack for her excellent technical support in the analytics. Open Access funding enabled and organized by Projekt DEAL.

Conflict of Interests

The authors declare no conflict of interest.

Data Availability Statement

Research data are not shared.

Keywords: oleate hydratase · enzyme catalysis · FAD · *Pediococcus parvulus* · fatty acids

[1] B. S. Chen, L. G. Otten, U. Hanefeld, *Biotechnol. Adv.* **2015**, *33*, 526–546.
[2] M. Engleder, H. Pichler, *Appl. Microbiol. Biotechnol.* **2018**, *102*, 5841–5858.
[3] Y. Zhang, B. E. Eser, P. Kristensen, Z. Guo, *Chin. J. Chem. Eng.* **2020**, *28*, 2051–2063.
[4] M. A. Masri, D. Garbe, N. Mehlmer, T. B. Brück, *Energy Environ. Sci.* **2019**, *12*, 2717–2732.
[5] S. Prem, C. P. O. Helmer, N. Dimos, S. Himpich, T. Brück, D. Garbe, B. Loll, *Microb. Cell Fact.* **2022**, *21*, 1–15.
[6] S. V. Pande, J. F. Mead, *J. Biol. Chem.* **1968**, *243*, 6180–6185.
[7] C. J. Zheng, J. S. Yoo, T. G. Lee, H. Y. Cho, Y. H. Kim, W. G. Kim, *FEBS Lett.* **2005**, *579*, 5157–5162.
[8] L. E. Bevers, M. W. H. Pinkse, P. D. E. M. Verhaert, W. R. Hagen, *J. Bacteriol.* **2009**, *191*, 5010–5012.
[9] J. Schmid, L. Steiner, S. Fademrecht, J. Pleiss, K. B. Otte, B. Hauer, *J. Mol. Catal. B* **2016**, *133*, S243–S249.
[10] E. Rosberg-Cody, A. Liavonchanka, C. Göbel, R. P. Ross, O. O'Sullivan, G. F. Fitzgerald, I. Feussner, C. Stanton, *BMC Biochem.* **2011**, *12*, 9.
[11] F. Bajerski, D. Wagner, K. Mangelsdorf, *Front. Microbiol.* **2017**, *8*, 1–11.
[12] A. Hirata, S. Kishino, S. B. Park, M. Takeuchi, N. Kitamura, J. Ogawa, *J. Lipid Res.* **2015**, *56*, 1340–1350.
[13] W.-R. Kang, M.-J. Seo, K.-C. Shin, J.-B. Park, D.-K. Oh, *Appl. Environ. Microbiol.* **2017**, *83*, 1–11.
[14] H. Busch, F. Tonin, N. Alvarenga, M. van den Broek, S. Lu, J. M. Daran, U. Hanefeld, P. L. Hagedoorn, *Appl. Microbiol. Biotechnol.* **2020**, *104*, 5801–5812.
[15] E. R. Marella, J. Dahlin, M. I. Dam, J. ter Horst, H. B. Christensen, S. Sudarsan, G. Wang, C. Holkenbrink, I. Borodina, *Metab. Eng.* **2020**, *61*, 427–436.
[16] H. Zia, U. von Ah, Y. H. Meng, R. Schmidt, J. Kerler, P. Fuchsmann, *Food Chem. X* **2022**, *13*, 100220.
[17] E. Y. Jeon, J. H. Lee, K. M. Yang, Y. C. Joo, D. K. Oh, J. B. Park, *Process Biochem.* **2012**, *47*, 941–947.
[18] J. Lorenzen, R. Driller, A. Waldow, F. Qoura, B. Loll, T. Brück, *ChemCatChem* **2018**, *10*, 407–414.
[19] T. Brück, J. Lorenzen, *A Process for the Cell-Free Enzymatic Production of 10-Hydroxystearic Acid (10-HSA) from Bio-Based Oils for Lubricant Formulation* **2019**, EP3461901 A1.
[20] A. Volkov, A. Liavonchanka, O. Kamneva, T. Fiedler, C. Goebel, B. Kreikemeyer, I. Feussner, *J. Biol. Chem.* **2010**, *285*, 10353–10361.
[21] M. Engleder, T. Pavkov-Keller, A. Emmerstorfer, A. Hromic, S. Schrempf, G. Steinkellner, T. Wriessnegger, E. Leitner, G. A. Strohmeier, I. Kaluzna, D. Mink, M. Schürmann, S. Wallner, P. Macheroux, K. Gruber, H. Pichler, *ChemBioChem* **2015**, *16*, 1730–1734.
[22] C. D. Radka, J. L. Batte, M. W. Frank, B. M. Young, C. O. Rock, *J. Biol. Chem.* **2021**, *296*, 100252.
[23] A. K. Park, G. H. Lee, D. W. Kim, E. H. Jang, H. T. Kwon, Y. M. Chi, *Biochem. Biophys. Res. Commun.* **2018**, *499*, 772–776.
[24] A. Volkov, S. Khoshnevis, P. Neumann, C. Herrfurth, D. Wohlwend, R. Ficner, I. Feussner, *Acta Crystallogr. Sect. D* **2013**, *69*, 648–657.
[25] S. Serra, D. De Simeis, S. Marzorati, M. Valentino, *Catalysts* **2021**, *11*, 1–14.
[26] T. Immerstrand, C. J. Paul, A. Rosenquist, S. Deraz, O. B. Mårtensson, Å. Ljungh, A. Blücher, R. Öste, O. Holst, E. N. Karlsson, *J. Food Prot.* **2010**, *73*, 960–966.
[27] E. Gasteiger, A. Hoogland, Chr. Gattiker, S. Duvaud, M. R. Wilkins, R. D. Appel, A. Bairoch, *Protein Identification and Analysis Tools on the Expasy Server* **2005**.
[28] D. M. Small, *Polyunsaturated Fat. Acids Hum. Nutr. Nestlé Nutr. Work. Ser.* **1992**, *28*.15–39.
[29] M. Baek, F. DiMaio, I. Anishchenko, J. Dauparas, S. Ovchinnikov, G. R. Lee, J. Wang, Q. Cong, L. N. Kinch, R. D. Schaeffer, C. Millán, H. Park, C. Adams, C. Glassman, R. A. DeGiovanni, J. H. Pereira, A. V. Rodrigues, A. A. van Dijk, A. C. Ebrecht, D. J. Opperman, T. Sagmeister, C. Buhlheller,

T. Pavkov-Keller, M. K. Rathinaswamy, U. Dalwadi, C. K. Yip, J. E. Burke, K. C. Garcia, N. V. Grishin, P. D. Adams, R. J. Read, D. Baker, *Science* **2021**, *373*, 871–876.
[30] R. K. Wierenga, P. Terpstra, W. G. J. Hol, *J. Mol. Biol.* **1986**, *187*, 101–107.
[31] C. D. Radka, J. L. Batte, M. W. Frank, B. M. Young, C. O. Rock, *J. Biol. Chem.* **2021**, *296*, 100252.
[32] J. Papadopoulos, R. Agarwala, *Bioinformatics* **2007**, *23*, 1073–79.
[33] X. Robert, P. Gouet, *Nucl. Acids Res.* **2014**, *42*, W320–W324.
[34] F. J. Van De Loo, P. Broun, S. Turner, C. Somerville, *Proc. Natl. Acad. Sci. USA* **1995**, *92*, 6743–6747.
[35] T. Galliard, P. K. Stumpf, *J. Biol. Chem.* **1966**, *241*, 5806–5812.
[36] A. Todea, A. Hiseni, L. G. Otten, I. W. C. E. Arends, F. Peter, C. G. Boeriu, *J. Mol. Catal. B* **2015**, *119*, 40–47.
[37] "National Center for Biotechnology Information (NCBI). Bethesda (MD): National Library of Medicine (US), National Center for Biotechnology Information.," can be found under http://www.ncbi.nlm.nih.gov/, **1988**.
[38] M. J. Griffiths, R. P. Van Hille, S. T. L. Harrison, *Lipids* **2010**, *45*, 1053–1060.

Manuscript received: March 29, 2023
Revised manuscript received: May 23, 2023
Accepted manuscript online: May 23, 2023
Version of record online: June 22, 2023

ChemCatChem

Supporting Information

Expanding the Portfolio by a Novel Monomeric Oleate Hydratase from *Pediococcus parvulus*

Sophia A. Prem, Carl P. O. Helmer, Bernhard Loll,* Daniel Garbe, and Thomas Brück*

Nucleotide sequence of recombinant OhyPp

ATGGCAAAGGCATATATGATTGGCAGCGGCATTGGCAACCTGGCGGCAGGCATTTATCTGATTCGCGATGGCGGCTGG
AGCGGCGATCAGATTACCATGTTTGGCCTGGAAAAACATGGCGCGAACGATGGCGCGAAAGTGGCGGATTATGAAAGC
GAATATGGCAACCCGGAACTGAGCAACAACAAAGGCTTTCTGGCGAAAGGCGGCCGCATGCTGAACGAAGAAACCTAT
GAGAACCTGTGGGATGTGCTGCGCAGCGTGCCGAGCCTGGATAACCCGGGCCAGAGCGTGACCGATGATATTCTGAA
CTTTGATCATGCGCATCCGACCCATGATGTGGCGCGCCTGATGGATCGCACCGATGGCATTCGCAACAAAGGCGATCA
GAAAGATTATAACCACATGCAGTTTAACAACCAGGATCGCTTTCTGCTGACCAAACTGATGATGATGCCGGAAAGCAAAG
AACCGCAGCTGAACGATGTGAGCATTGAACAGTGGTTCGCGAAGAGCCCGCATATCTTCACCACCAACTTCTGGTATAT
GTGGCAGACCACCTTTGCGTTTAAGAAGGAGAGCAGCGCGATGGAACTGCGCCGCTATATGAACCGCATGATTCTGGA
ATTTAGCCGCATTAACACCCTGGCGGGCGTGACCCGCACTCCGTATAACCAGTATGAGAGCATTATTCTGCCGATGCGC
AAATATCTGACCGATCATGGCGTGAACTTCGTGAACAACCGCAAGATTACCGAATTTGTGTTTAAAGATACCCCGCTGCG
CGATGATATTATTGTGACCGGCCTGAAATATGAAGAAGTGGATAACGATAACAAACCGGGCGAAATTGAAATTGGCGAG
AACGATTTTGTGTTTGATACCAACGGCGCGATTACCGATAGCAGCAGCATTGGCGATCTGAACACTCCGATTAAAGAGA
ACATGGAATATGCGCCGAGCGCGGCGCTGTGGAAACAGGCGACCGAACATTTCTATAACCTGGGCAACCCGGATAAAT
TCTTCGCGGATCGCAAACAGAGCGAATGGCTGAGCTTTACCGTGACCACCAACAACCATTTTCTGCTGAACGAAATTAG
CCGCATTACCCAGCAGGAACCGGGCAACGCGCTGAACACCTGGGTGGATAGCAACAACCTGATGAGCATTGTGGTGCA
TCATCAGCCGCATTTCCATGTGCAGAAGGAGAACGAAACCGTGTTCTGGGGCTATGTGATGTATCCGCGTCGCAAAGGC
GATTATGTGGATAAACCGTTTATTGAAATGACCGGCAAAGAGATGCTGGAAGAACTGCTGGGCCATCTGGCAGCGGTGG
ATCCGGCGCGCGATAACATTGCGGATCATACCGAAGAGATTATGGATAGCATTGTGAACGTGATTCCGGCGTATATGCC
GTATGCGAGCGCGCTGTTTAACCGCCGCGCGGTGGGCGATCGTCCGGCGGTGGTGCCGAAGAACAGCAAGAACCTGG
CGTTTATTAGCCAGTTTGCGGAAATGCCGTTTGATATGGTGTTTACCGAACAGTATAGCTTTCGCTGCGCGCAGGTGGC
GGTGTATCACTTTATGGGCATTCCGGATAGCGAACTGACCCCGCTGCATCATTATGAGAAACAGCCGAAAGTGCTGGCG
CGCGCGACTAAGACTATGTTCCGT

Amino acid sequence of expressed OhyPp

MAKAYMIGSGIGNLAAGIYLIRDGGWSGDQITMFGLEKHGANDGAKVADYESEYGNPELSNNKGFLAKGGRMLNEETYENL
WDVLRSVPSLDNPGQSVTDDILNFDHAHPTHDVARLMDRTDGIRNKGDQKDYNHMQFNNQDRFLLTKLMMMPESKEPQLN
DVSIEQWFAKSPHIFTTNFWYMWQTTFAFKKESSAMELRRYMNRMILEFSRINTLAGVTRTPYNQYESIILPMRKYLTDHGVN
FVNNRKITEFVFKDTPLRDDIIVTGLKYEEVDNDNKPGEIEIGENDFVFDTNGAITDSSSIGDLNTPIKENMEYAPSAALWKQATE
HFYNLGNPDKFFADRKQSEWLSFTVTTNNHFLLNEISRITQQEPGNALNTWVDSNNLMSIVVHHQPHFHVQKENETVFWGYV
MYPRRKGDYVDKPFIEMTGKEMLEELLGHLAAVDPARDNIADHTEEIMDSIVNVIPAYMPYASALFNRRAVGDRPAVVPKNSK
NLAFISQFAEMPFDMVFTEQYSFRCAQVAVYHFMGIPDSELTPLHHYEKQPKVLARATKTMFR

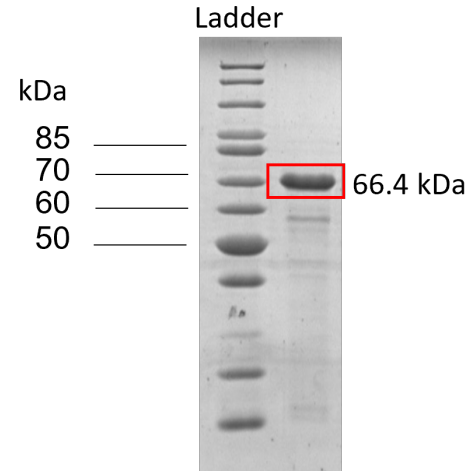

Figure S1. SDS-page of OhyPp after IMAC and desalting as described in the experimental section. OhyPp was measured to be 66.4 kDa large.

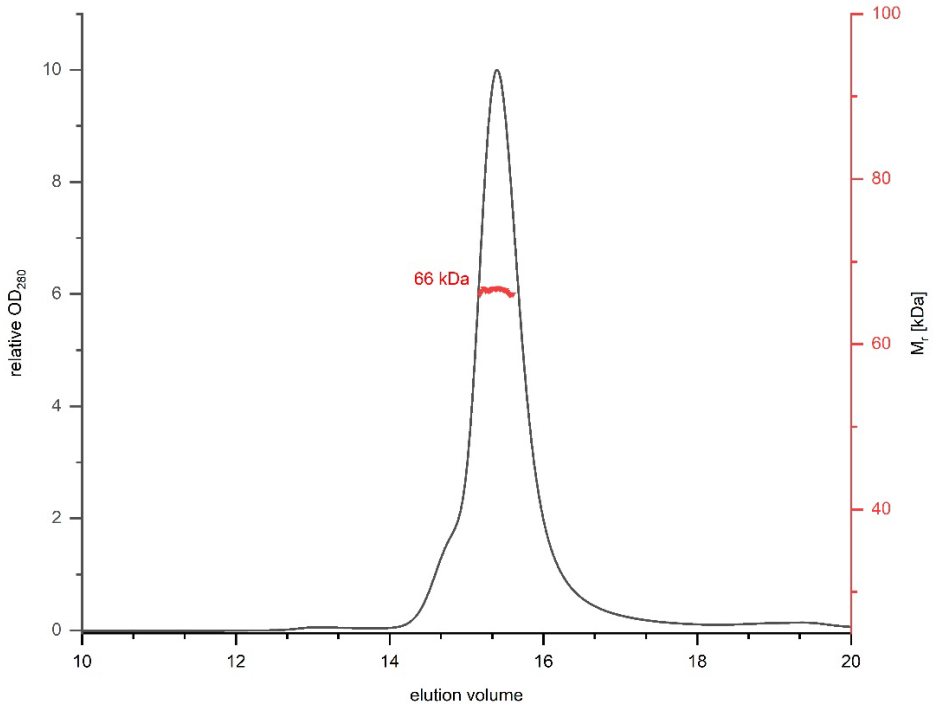

Figure S2. Enzyme characterization of OhyPp. SEC/MALS of OhyPp (grey) resulted in a single peak. This is consistent with a monomer (theoretical Mr 66.4 kDa). The red curve reflects the refractive index signal.

A

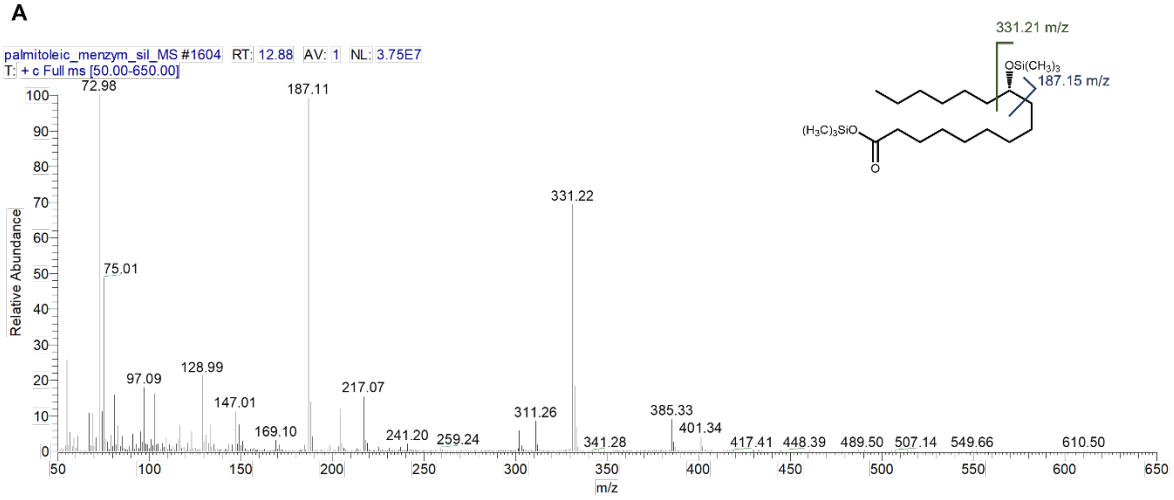
palmitoleic_menzym_sil_MS #1604 RT: 12.88 AV: 1 NL: 3.75E7
T: + c Full ms [50.00-650.00]
Relative Abundance
m/z
72.98
187.11
331.22
75.01
97.09
128.99
147.01
169.10
217.07
241.20
259.24
311.26
341.28
385.33
401.34
417.41
448.39
489.50
507.14
549.66
610.50
331.21 m/z
OSi(CH3)3
187.15 m/z
(H3C)3SiO
O

B

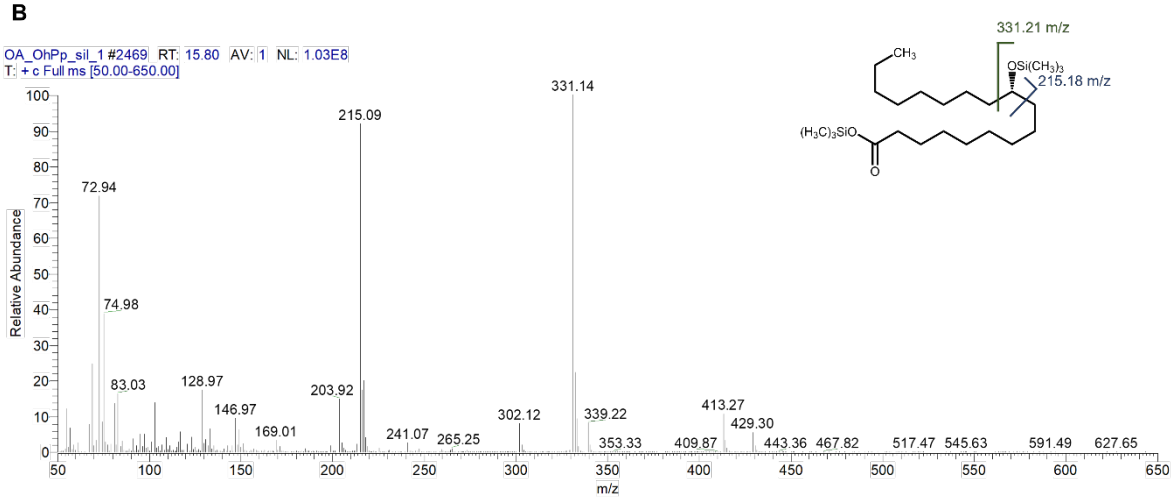
OA_OhPp_sil_1 #2469 RT: 15.80 AV: 1 NL: 1.03E8
T: + c Full ms [50.00-650.00]
Relative Abundance
m/z
331.14
215.09
72.94
74.98
83.03
128.97
146.97
169.01
203.92
241.07
265.25
302.12
339.22
353.33
409.87
413.27
429.30
443.36
467.82
517.47
545.63
591.49
627.65
331.21 m/z
CH3
OSi(CH3)3
215.18 m/z
(H3C)3SiO
O

C

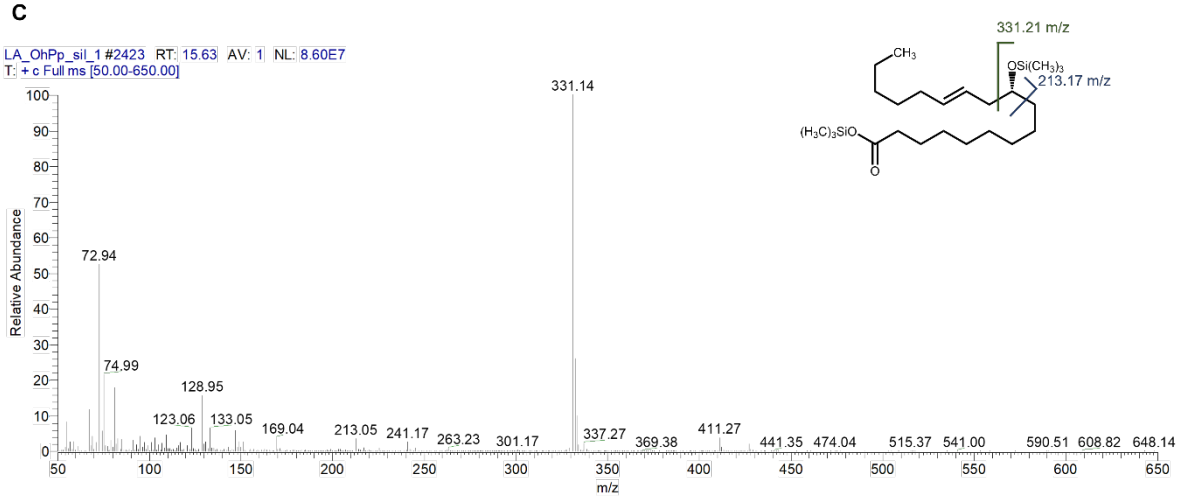
LA_OhPp_sil_1 #2423 RT: 15.63 AV: 1 NL: 8.60E7
T: + c Full ms [50.00-650.00]
Relative Abundance
m/z
331.14
72.94
74.99
128.95
123.06
133.05
169.04
213.05
241.17
263.23
301.17
337.27
369.38
411.27
441.35
474.04
515.37
541.00
590.51
608.82
648.14
331.21 m/z
CH3
OSi(CH3)3
213.17 m/z
(H3C)3SiO
O

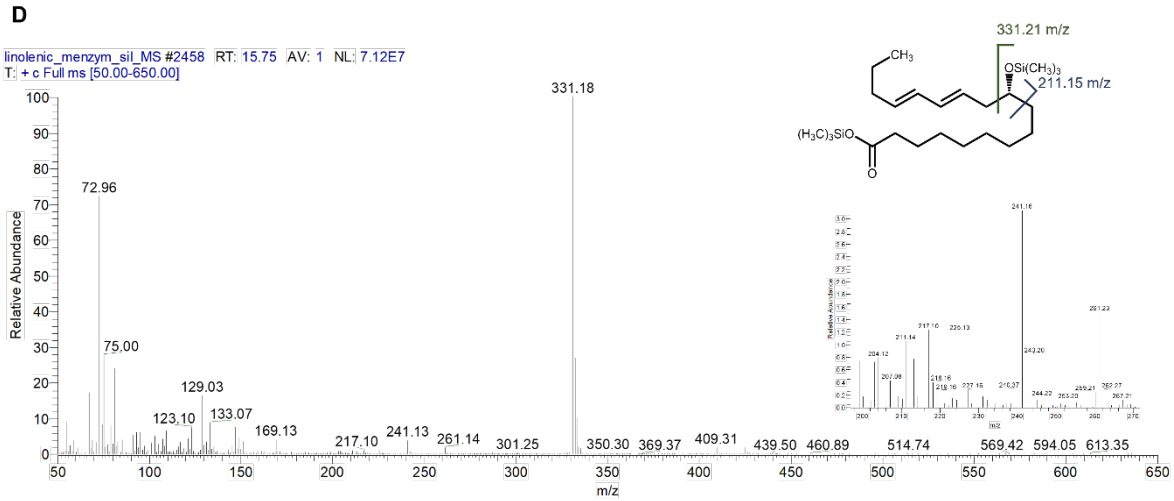

Figure S3. MS spectra of silylated enzymatically hydroxylated palmitoleic, oleic, linoleic and α-linolenic acid. **(A)** MS spectrum of silylated hydroxylated palmitoleic acid. Specific fragment ions: 331.21 and 187.15 *m/z*. **(B)** MS spectrum of silylated hydroxylated oleic acid. Specific fragment ions: 331.21 and 215.18 *m/z*. **(C)** MS spectrum of silylated hydroxylated linoleic acid. Specific fragment ions: 331.21 and 213.17 *m/z*. **(D)** MS spectrum of silylated hydroxylated α-linolenic acid. Specific fragment ions: 331.21 and 211.15 *m/z*.

Table S1. Sequence identities (A) and sequence similarities (B) between the three different variants of oleate hydratases, OhyRe, OhyPp and OhyEm. Percentages were calculated using Geneious (https://www.geneious.com).

A.

	OhyRe	OhyPp	OhyEm
OhyRe		74.2 %	27.8 %
OhyPp	74.2 %		27.2 %
OhyEm	27.8 %	27.2 %	

B.

	OhyRe	OhyPp	OhyEm
OhyRe		91.3 %	55.7 %
OhyPp	91.3 %		57.5 %
OhyEm	55.7 %	57.5 %	

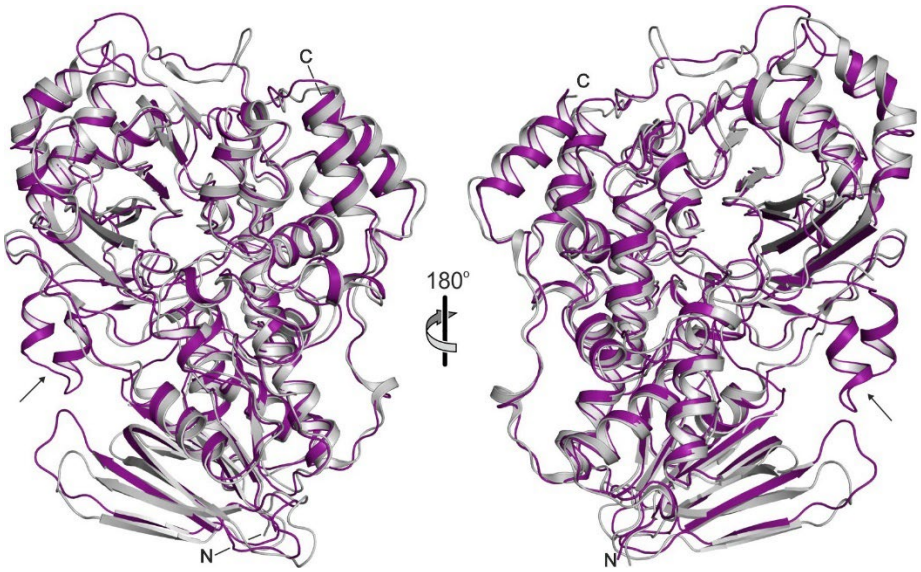

Figure S4. Superposition of the overall structure of OhyPp (deep purple) and OhyRe (PDB-ID: 5odo [18]). The extended FAD binding loop of OhyPp is indicated by an arrow.

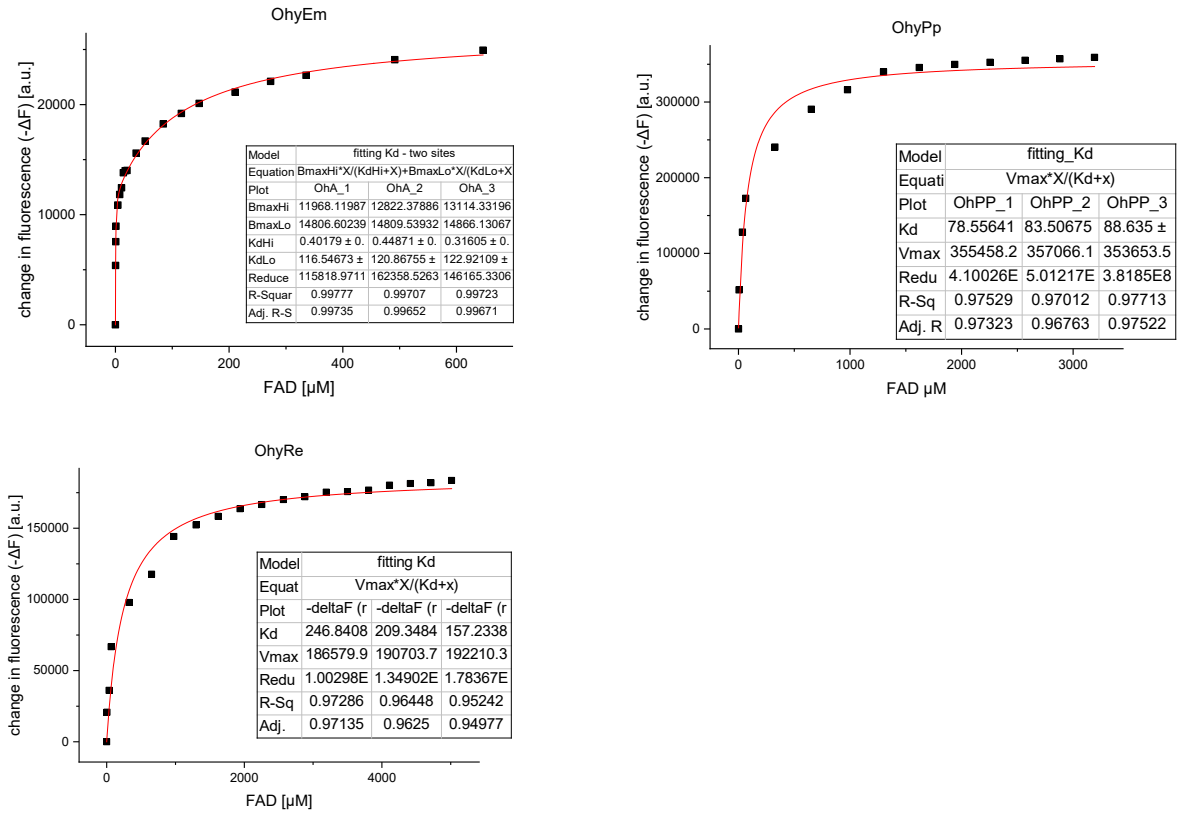

Figure S5. Non-linear curve fit of the change of fluorescence upon FAD titration to 0.5 μM of OhyEm and 5 μM of OhyPp and OhyRe.

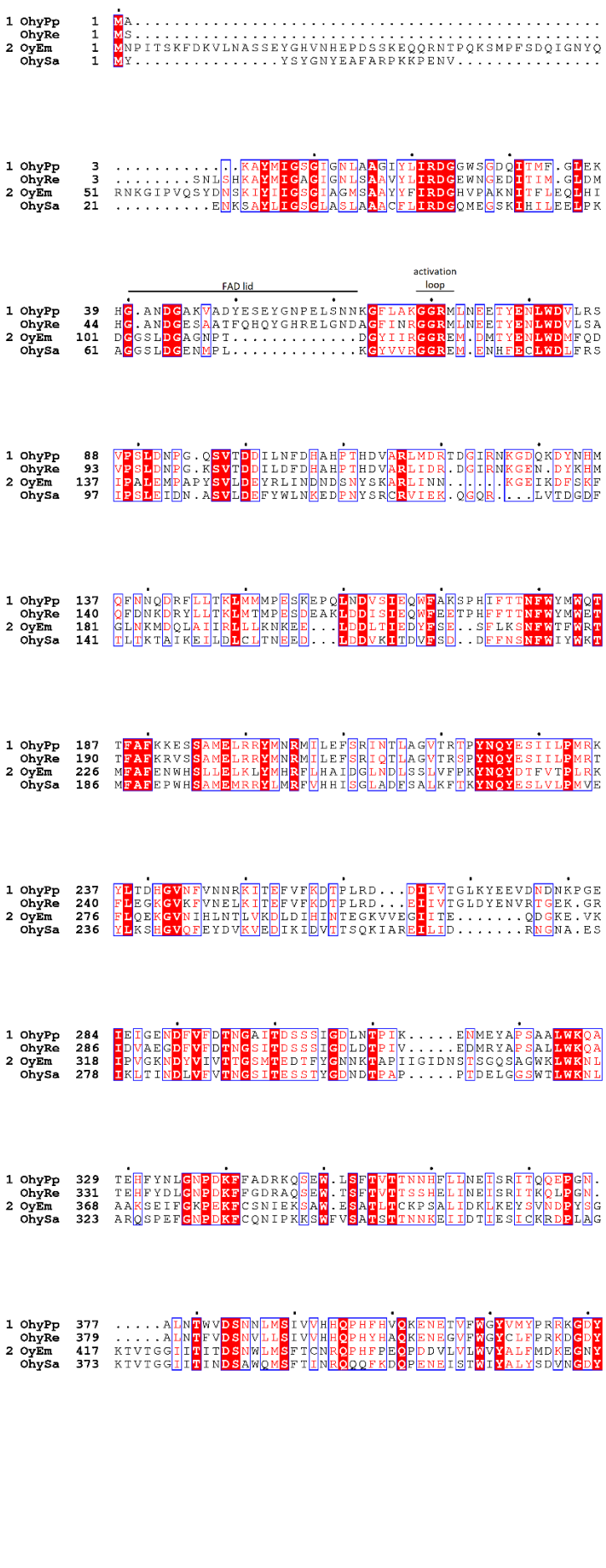
FAD lid
activation loop

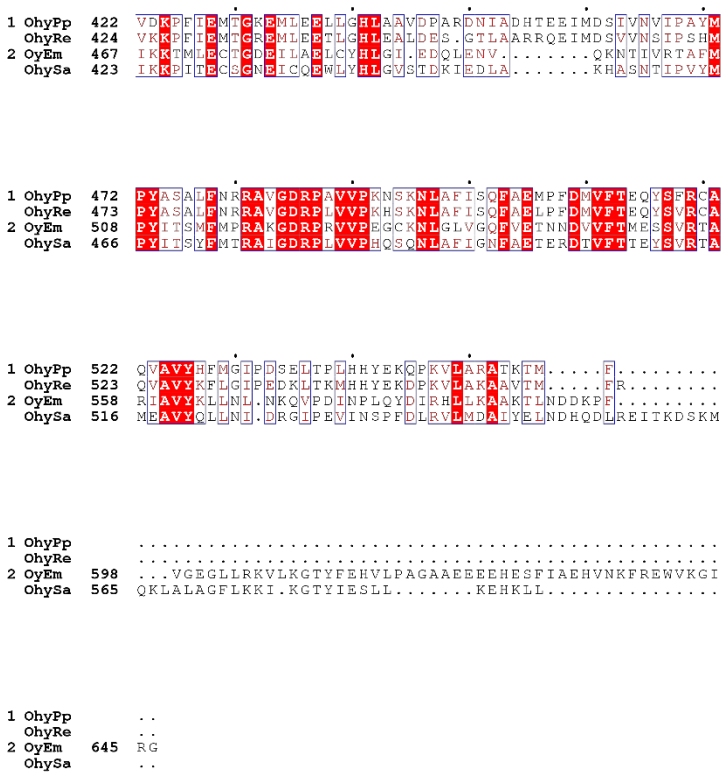

Figure S6. Alignments between two groups (monomeric and dimeric OHs). Each group contains two monomeric members of the HFam3 family (OhyRe and OhyPp) and two dimeric members of the HFam11 family (OhyEm and OhySa) using the COBALT constraint alignment tool and ESPript from the Endscript-server for visualization. Red box, white character represents strict identity. Red character represents similarity in a group and a blue frame represents similarity across groups.

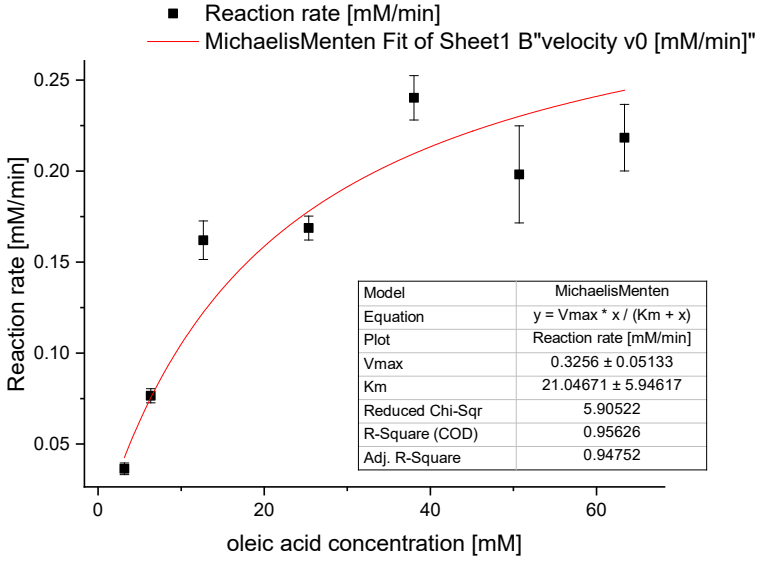

Figure S7. Michaelis-Menten saturation curve of 28.42 µM of OhyPp using oleic acid as substrate. Curve was fitted using y = Vmx*x / (Km+x) in OriginLab. Reactions were performed in triplicates.

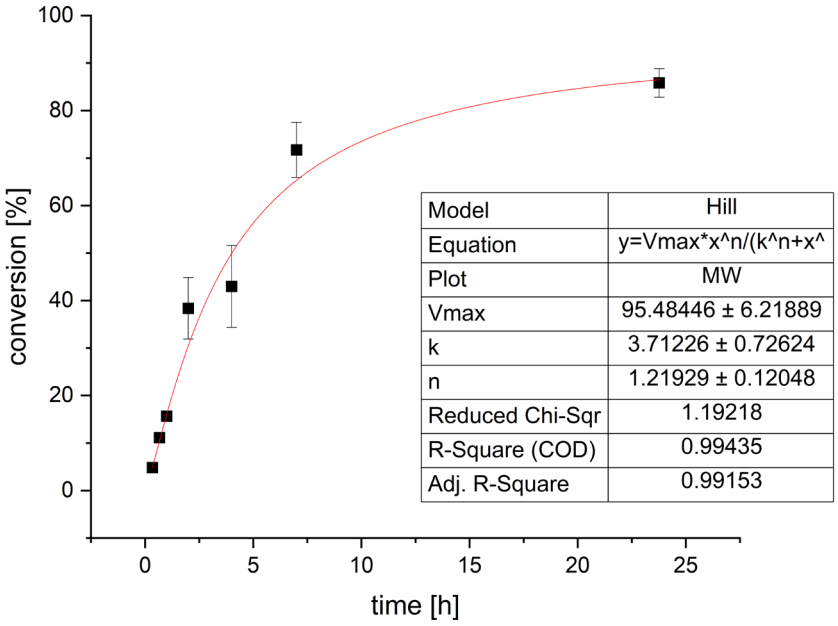

Figure S8. Conversion test of OhyPp over time fitted with y=Vmax*x*x^n/(k^n+x^n). Reactions were performed in triplicates.

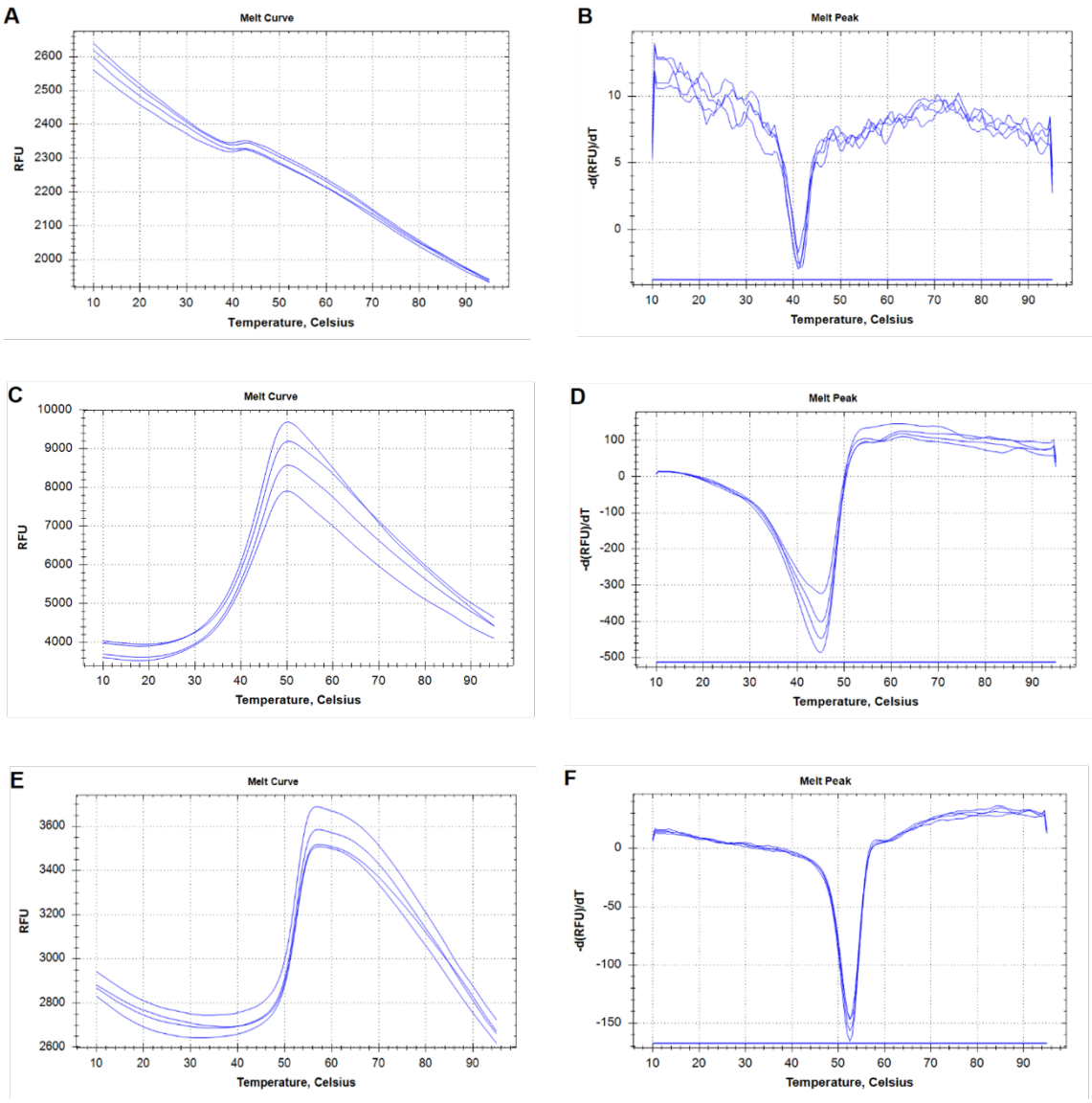

Figure S9. Thermal melting curves of each respective oleate hydratase in four replicates monitored with SYPRO™ Orange. (A) Melt curve of OhyPp. (B) First-order derivative of OhyPp melt curve as a function of the temperatures showing a minimum at 41.1 ± 0.2 °C. (C) Melt curve of OhyRe. (D) First-order derivative of OhyRe melt curve as a function of the temperatures showing a minimum at 45.0 ± 0.0 °C. (E) Melt curve of OhyEm. (F) First-order derivative of OhyEm melt curve as a function of the temperatures showing a minimum at 52.5 ± 0.2 °C.

Full-length publication 2

"Two Cascade Reactions with Oleate Hydratases for the Sustainable Biosynthesis of Fatty Acid-Derived Fine Chemicals"

catalysts

MDPI

Article

Two Cascade Reactions with Oleate Hydratases for the Sustainable Biosynthesis of Fatty Acid-Derived Fine Chemicals

Sophia A. Prem, Martina Haack, Felix Melcher, Marion Ringel, Daniel Garbe and Thomas Brück *

Werner Siemens-Chair of Synthetic Biotechnology, School of Natural Sciences, Technical University of Munich, Lichtenbergstr. 4, 85748 Garching, Germany; sophia.prem@tum.de (S.A.P.); martina.haack@tum.de (M.H.); felix.melcher@tum.de (F.M.); marion.ringel@tum.de (M.R.); daniel.garbe@tum.de (D.G.)
* Correspondence: brueck@tum.de

Abstract: Oleate hydratases (OHs) are of significant industrial interest for the sustainable generation of valuable fine chemicals. When combined with other enzymes in multi-step cascades, the direct formation of fatty acid congeners can be accomplished with minimal processing steps. In this study, two cascade reactions are presented, which can be applied in one-pot approaches. The first cascade was placed "upstream" of an OH derived from *Rhodococcus erythropolis* (OhyRe), where a lipase from *Candida rugosa* was applied to hydrolyze triglycerides into free fatty acids, a crucial step for OH conversion. Further, we tested the lipase–OhyRe cascade with various types of renewable triglycerides of plant and microbial origin. In this context, the most efficient conversion was observed for microbial oil from *Cutaneotrichosporon oleaginosus* leading the way toward its industrial application. In contrast, the second cascade was placed "downstream" of OhyRe, where a novel secondary alcohol dehydrogenase (secADH) was applied to oxidize the hydroxylated fatty acid into a fatty acid ketone. Optimal reaction parameters for the cascade with the secADH were established, which allows this to be applied to high-throughput screens. Moreover, we describe a light-dependent route, thereby extending the catalytic efficiency of the OH enzyme system.

Keywords: oleate hydratase; secondary alcohol dehydrogenase; cascade reactions; lipase; screening; 10-hydroxy stearic acid; 10-keto stearic acid; oleic acid; triglycerides; microbial oil; *Deinococcus radiodurans*; *Candida rugosa*; *Cutaneotrichosporon oleaginosus*; *Rhodococcus erythropolis*

Citation: Prem, S.A.; Haack, M.; Melcher, F.; Ringel, M.; Garbe, D.; Brück, T. Two Cascade Reactions with Oleate Hydratases for the Sustainable Biosynthesis of Fatty Acid-Derived Fine Chemicals. *Catalysts* **2023**, *13*, 1236. https://doi.org/10.3390/catal13091236

Academic Editor: Wei Du

Received: 11 July 2023
Revised: 26 July 2023
Accepted: 8 August 2023
Published: 25 August 2023

1. Introduction

In nature, metabolic pathways are realized by cascading enzyme-driven reactions within cells, ensuring cell growth and viability. The concept of these cellular cascade reactions can also be transferred into extracellular matrices, which allows targeted reactions to be more easily controlled. Further, fewer side-products are generated [1], and simplified downstream product recovery is achieved compared to complex systems present in a microbial cell factory [2]. The application of enzyme cascade reactions has enabled the formation of the sustainable in vitro biosynthesis of fine chemicals and the advent of efficient screening methods in the fields of biotechnology, enzymology, and other related areas. In this context, one-pot enzyme reaction cascades combined with simplified cofactor regeneration systems, the application of enzyme co-immobilization, scaffolding, or encapsulation leads to the targeted design of effective chemical production systems [3].

The advantages of in vitro enzyme cascades for the industrial biosynthesis of target molecules are reduced downstream processes, leading to lower production costs, and in the case of enzyme recycling, less product and catalyst extraction and purification steps, enabling higher space-time yields given the optimized conversion parameters. Furthermore, less organic solvent and energy consumption are needed, making the process more sustainable. Lastly, reduced end- or side-product inhibition occurs, which can be the case for whole-cell biocatalysts containing enzyme cascades [4,5].

In general, there are several routes to how cascade enzyme reactions can be applied. This might be either by the application of enzymes originating from different organisms in the form of synthetic cascades or the extraction of naturally occurring catalysts contained within an existing metabolic pathway. However, the non-natural enzyme coupling efforts might lead to severe incompatibilities regarding reaction parameters such as side reactions, varying temperature or pH profiles, substrate access, and solubility issues, as well as substrate promiscuity, leading to side reactions [2]. Consequently, in most cases, intensive optimization efforts are required to achieve satisfying reaction outputs, and usually trade-offs are to be expected when applying non-optimal parameters for each biocatalyst component.

So far, enzyme cascade reactions have been applied in industrial processes to generate platform chemicals, such as chiral alcohols [6], and are considered for the production of complex pharmaceutical molecules [7], thereby showcasing the immanent relevance of in vitro catalytic systems.

Additionally, enzyme cascades can be applied to design high-throughput assays as they allow for the rapid and facile screening of biological targets. With regard to the former, a plethora of variations regarding the output signals are available, of which the most common ones are spectrophotometric, including but not limited to absorbance [8–10], fluorescence [11,12], and bioluminescence [13,14] signals.

At present, there have been only minor efforts to develop relevant reaction cascades revolving around oleate hydratases (OH), which predominantly convert free oleic acid into 10-(R)-hydroxy stearic acid (10-HSA), a fatty acid-derived fine chemical in the lubricant and cosmetic industry [15]. Naturally, this class of enzymes is considered to be involved in defense measures against free fatty acids, which are reported to be toxic for many microorganisms. Consequently, OHs are not able to convert fatty acids with a protected carboxy group, such as methyl esters or acyl glycerides.

Besides their substrates, OHs exhibit the binding of FAD as a cofactor during catalysis. This cofactor, despite not participating in a redox reaction, has been proposed to have structural significance during the catalytic process [16]. Additionally, it has been observed that an environment with reducing conditions leads to a significant enhancement in activity. This finding suggests that $FADH_2$ is likely the preferred cofactor in the catalytic process. Upon cell lysis, $FADH_2$ is oxidized to FAD, and in many OHs, only low FAD occupancy can be measured after protein purification, thus making the direct proof of $FADH_2$ binding preferences considerably challenging. For instance, OhyRe [17], OH from *Pediococcus parvulus* (OhyPp) [18], and a linoleate hydratase (LAH) [19] have been observed to fully lose FAD upon purification [18,19].

One of the main goals for the sustainable biosynthesis of 10-HSA is the use of plant and microbial as well as waste oils. The OH substrate oleic acid is the main fatty acid component of many plant and microbial oils, such as high-oleic sunflower oil (HOSO) or yeast triglycerides sourced from the oleaginous yeast *Cutaneotrichosporon oleaginosus* [20]. The latter provides a new, sustainable substrate for OH-centered reactions due to higher yields and reduced land use compared to conventional plant-based resources. Additionally, the fatty acid profile of *C. oleaginosus* can be altered by adapting fermentation and media parameters [21,22]. Furthermore, a novel genetic engineering process paves the way for tailored fatty acid profiles, thus prospectively allowing for the efficient production of sustainably sourced 10-HSA [23].

Currently, the analogue 12-HSA is solely produced from castor oil via hydrogenation under extreme pressure and temperature, leading to exposure to fluctuations in quality and demand. To this end, plant and microbial oils with high oleic acid content are more diversely available on the market, and biocatalysts convert under moderate conditions with low energy demand. However, to date, the low stability and performance of the available biocatalysts, resulting in rather low yields, have led to high prices compared to conventional production methods. This is where fewer processing steps are advantageous, resulting in time and material savings and ultimately enhancing the economic viability.

10-HSA, furthermore, is a solid material, and thus, no in-between liquid–liquid separation steps are required. The utilization of customized enzyme cascade reactions has the potential to steer closer to achieving this objective.

Several OHs with varying properties are already described and characterized [17,18,24,25], however, monomeric OHs exhibit the greatest potential for an industrial application, as subunit dissociation can be neglected and immobilization strategies can be adopted easier [26]. Hence, this study focuses on an OH from *Rhodococcus erythropolis* (OhyRe) as the first identified member of monomeric OHs.

A variety of cascades centered around OHs are reported by Hagedoorn et al. [27], and they would significantly broaden the product and application portfolio. This can, for instance, be achieved by applying different enzymes such as alcohol dehydrogenases, amine transaminase, or lipases, exploiting their esterification capabilities.

For the cascade reaction of 10-HSA into its oxidized product, called 10-keto stearic acid (10-KSA), an alcohol dehydrogenase (ADH) is required, which exhibits substrate preference for longer carbon chain alcohols over short ones. To date, several organisms, such as *Rhodococcus erythropolis* [28] and *Nocardia cholesterolicum* NRRL 5767 [29], are reported to convert 10-HSA into 10-KSA, and an isolated ADH from *Micrococcus luteus* has already been applied in screenings [30].

In this study, we first optimized OhyRe's conversion efficiency by using broadband white light and subsequently applied two different cascade reactions involving OHs. These reactions are of relevance for the one-pot production of 10-HSA from triglyceride oils and 10-keto stearic acid (10-KSA). The latter reaction might additionally be useful for screening purposes due to its absorbance response.

Since some OHs [24], as well as OhyRe [17], have low turnover numbers, they were considered to be the limiting components in the enzyme cascade reactions. Consequently, prior optimization was required to achieve appropriate outputs, which is why the effect of light on the conversion of OhyRe was investigated.

Next, the first cascade was investigated as depicted in Figure 1a, which is the combination of OhyRe with a lipase from *Candida rugosa* for the direct conversion of triglyceride oils into 10-HSA without the need for the prior hydrolysis of oils into free fatty acids. Lipases are widely studied enzymes [31], and thus, there are several reports about their application in cascade reactions [32–34]. However, to our knowledge, there is no report demonstrating the combination of lipase and OHs in vitro.

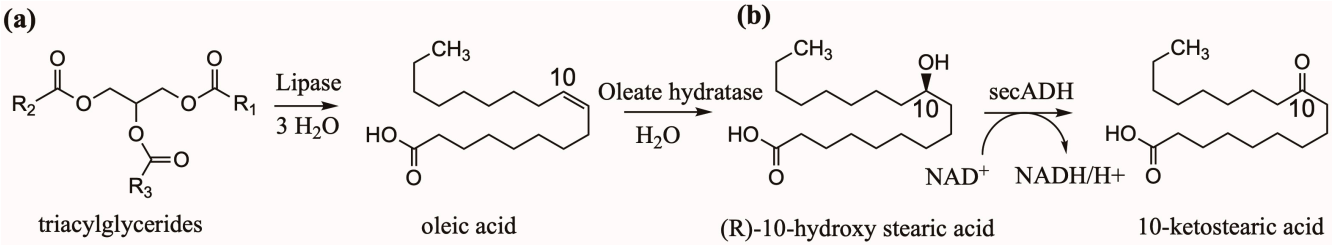

Figure 1. (**a**) "Upstream" cascade reaction, with the combination of a lipase and an OH to produce 10-HSA without the need for prior hydrolysis of oils into free fatty acids. (**b**) "Downstream" cascade reaction, with the combination of an OH and a secondary alcohol dehydrogenase to produce 10-KSA.

The second cascade reaction, as depicted in Figure 1b, comprises the conversion of oleic acid into 10-HSA, followed by the biosynthesis of 10-KSA using a novel secondary alcohol dehydrogenase. Furthermore, the reaction parameters were optimized for this cascade reaction to be able to produce 10-KSA as a fine chemical, and secondly, also to prospectively use it in high-throughput screening assays. Despite an uncharacterized secondary ADH being applied already in a high-throughput screen [30], a detailed characterization of the reaction parameters has been lacking so far, which is required for an adequate application.

2. Results and Discussion

2.1. Optimization of OhyRe Using Light

Before applying the above-mentioned cascade reactions, it was necessary to maximize OH's activity due to the observed slow turnovers. It was reported that a reducing environment strongly enhances OH's activity, which before has been achieved in vitro by applying elaborate means, such as employing a cascade involving a flavin oxidoreductase [35], by photobleaching, or with the addition of DTT under anaerobic conditions, as described by Engleder et al. [16].

For this study, a more rapid method for the generation of a reducing environment was needed, and this was achieved by using a light source, where the FAD can be partially reduced without the addition of chemicals and without maintaining an anaerobic environment. Since OhyRe loses most FAD upon purification, an equimolar concentration of FAD was added. The effect of light on the OhyRe conversion was tested, and indeed, it could be observed that the addition of broadband white light during the reaction led to a 40-fold increase in activity compared to when the reaction was conducted in the dark, as depicted in Figure 2a.

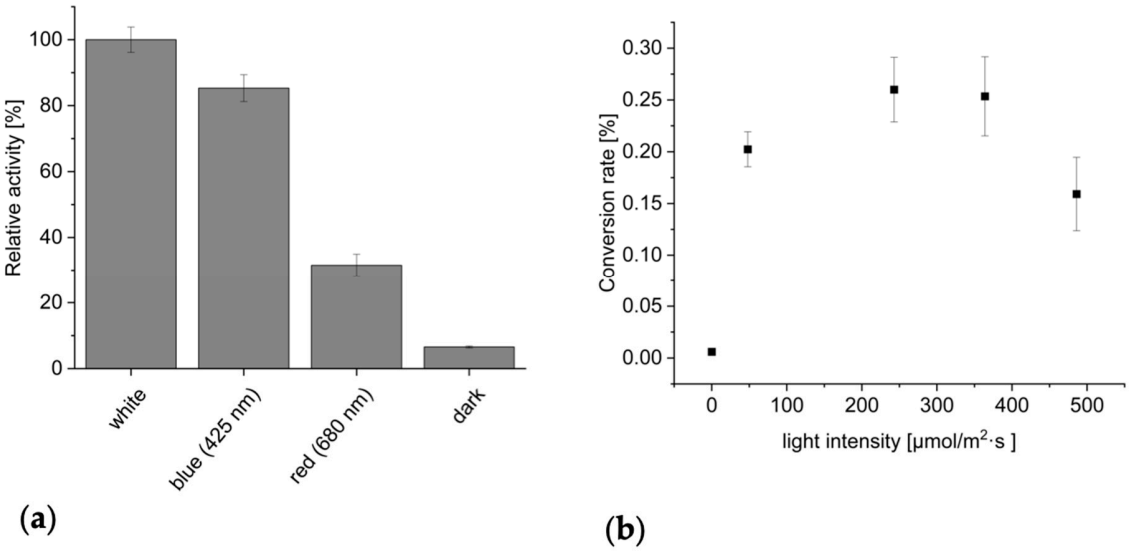

Figure 2. (**a**) Effects of different light colors (broadband white, blue (425 nm), red (680 nm), and no light (dark)) on the conversion of oleic acid into 10-HSA by OhyRe. Conversions are presented relative to the highest yield, which was observed under broadband white light. The photosynthetic active radiation was 191 µmol/m^2·s or each condition. (**b**) Conversion rates of the biosynthesis of 10-HSA by applying varying light intensity in µmol/m^2·s using broadband white light. Reactions were conducted in triplicates.

Also, specific light colors were tested, and blue light showed a similar positive effect, leading to the conclusion that blue light is indeed responsible for the improved activity of OhyRe. Blue light is known to act as an activator for blue-light-sensing proteins via the excitation of FAD [36,37]. Most likely the reduction of FAD, leading to $FADH_2$, the preferred cofactor of OhyRe, is responsible for the enhanced activity. Next, the optimal light intensity was tested, and a broad optimal range between 243 and 364 µmol/m^2·s was observed (Figure 2b). Based on the outcomes of these experiments, the subsequent reactions were conducted using broadband white light at an intensity of 364 µmol/m^2·s.

OHs are likely the limiting enzymes in coupled reactions due to their low turnover numbers, making them the primary focus in optimization efforts. Therefore, the improvement of activity through blue and broadband white light illumination is a first step towards the optimization of OhyRe's catalytic activity within cascade reactions.

2.2. A Cascade Reaction Using a Lipase and OhyRe

Next, by applying the broadband light activation, a cascade reaction using a lipase and OhyRe, the conversion of sustainable microbial and plant oils with varying oleic acid concentrations was analyzed. Commercially available olive, linseed, and rapeseed oils were applied and compared to high-oleic sunflower oil (HOSO) and triglyceride oil from *C. oleaginosus*. For the first step of the cascade reaction, the commercially available lipase from *Candida rugosa* was used since it is known as a high-fidelity enzyme for the hydrolysis of triglycerides into free fatty acids and glycerol and is also active over a wide temperature and pH range [38,39]. Additionally, a recent screening experiment showed that *Candida rugosa* lipase was most efficient for rapeseed oil and HOSO conversion [40].

It has to be considered that oils contain small amounts of free fatty acids originating from the processing and storage conditions [41]. To evaluate whether OhyRe can convert any residual free fatty acids from crude oil, and thus, to determine the background activity, first, the conversion of the oil was tested with OhyRe but without lipase. However, as desired, no production of 10-HSA was observed, thereby pointing towards the fact that the amount of free fatty acids in the tested oils can be neglected.

Instead, when the *C. rugosa* lipase was added in combination with OhyRe, conversion at different yields was observed depending on the type of oil used. The highest yield was achieved for rapeseed oil, with a conversion of 35% of oleic acid, and the least for linseed oil, with 6% (Figure 3a), which was expected since it also contains the lowest amount of oleic acid amongst all oils tested (Table 1).

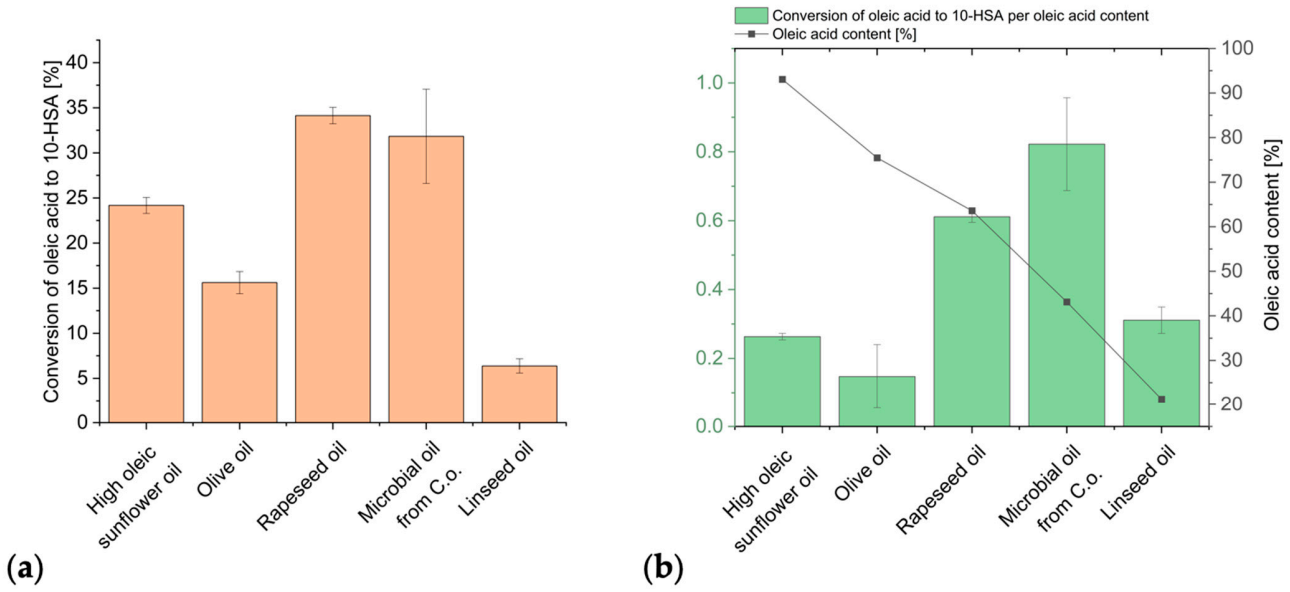

Figure 3. Conversion of different types of oils to free fatty acids and 10-HSA using a lipase from *C. rugosa* and OhyRe. Experiments were conducted in triplicates. (**a**) Conversion of oleic acid to 10-HSA in (%) for high-oleic sunflower oil, olive oil, rapeseed oil, microbial oil from *C.o.*, and linseed oil. (**b**) Conversion of oleic acid to 10-HSA in (%) per oleic acid content of each oil type and the oleic acid content in (%).

To evaluate the effect of the oleic acid content, we calculated the converted 10-HSA per oleic acid content in each respective oil and observed that now the microbial oil from *C. oleaginosus* showed the highest conversion, while olive and HOSO showed the lowest conversion (Figure 3b). Strikingly, the performance of HOSO was one of the lowest regarding the converted 10-HSA per oleic acid content of oils. In general, there was a decrease in yield with increasing oleic acid content, which might be a sign of substrate inhibition. Also, the types of oils were processed differently, and the remaining ingredients most likely can influence the enzymes' activities. However, the used HOSO is for for

technical applications, and thus, well purified, leading to the depletion of contaminants, yet it still showed low yields. Additionally, the composition of the triglycerides might affect the yield due to the preferences of the lipase [42,43]. Linseed oil contains large amounts of C18:2 and C18:3, which are also substrates for OhyRe [17] and other OHs [18], and thus, could bind and might lead to side reactions, resulting in a lower yield, whereas in *C. oleaginosus* oil, the most abundant fatty acid after oleic acid is C16:0 (Table 1). Thus, this oil might be beneficial regarding the oleic acid content relative to other C18 species. Recently, our research group successfully utilized CRISPR/Cas to genetically engineer *C. oleaginosus*, resulting in oil without any polyunsaturated fatty acids [23]. For upcoming experiments, it will be intriguing to investigate if the conversion yield can be further improved using this type of oil.

Table 1. Fatty acid profiles of the oils used for the cascade reaction of a lipase (from *Candida rugosa*) and OhyRe in (%).

Fatty Acid	High-Oleic Sunflower Oil	Olive Oil	Rapeseed Oil	Microbial Oil from C.o.	Linseed Oil
C16:0	2.64	11.82	4.14	36.48	5.40
C16:1	-	0.65	0.20	0.49	0.11
C18:0	1.50	2.75	1.66	17.50	3.92
C18:1 (oleic acid)	93.07	75.02	62.57	43.14	20.71
C18:2	2.21	8.51	21.50	1.28	15.44
C18:3	-	0.71	9.24	-	54.27
C20:0	0.18	0.54	0.58	0.15	0.16
C20:1	0.40	-	0.11	0.96	-

For the assay applied here, the oil was emulsified with buffer. Even though lipases prefer an aqueous–oil bilayer [44] as opposed to emulsified oil, which is the exact opposite of OHs strictly requiring emulsified oil, there was up to 35% of conversion. Still, further optimizations can be applied to tackle the tradeoffs of the two varying specifications of lipases and OHs regarding the emulsification of oil. This can, for instance, be achieved by testing the effect of surfactants or by applying a two-step conversion with an intermediate emulsification step.

In summary, the conducted experiments show that the lipase from *Candida rugosa* and OhyRe can indeed be used in a cascade reaction, thus allowing for the efficient conversion of triacyl glycerides-based oils into 10-HSA. However, the conversion efficiency is largely dependent on the used oil substrate and there is room for optimization to further increase the yield.

2.3. Functional Expression of secADH

Subsequently, we opted for the implementation of the second step in the aimed downstream cascade reaction involving an alcohol dehydrogenase to convert 10-HSA into 10-KSA (cf. Figure 1b). Apart from the large-scale production of this potential fine chemical for further downstream reactions, it can be used for high-throughput screening purposes. An alcohol dehydrogenase from *M. luteus* was already reported to be active on secondary alcohol substrates [45]. However, to expand the toolbox for this reaction, we decided to further search the NCBI database for genes that are related to the one from *M. luteus* and are also predicted to be L-3-hydroxyacyl-CoA dehydrogenases.

An ADH from *Deinococcus radiodurans* was identified (NCBI Reference Sequence: WP_027479748.1), which is an extremophile organism, and thus, its proteins are expected to hold superior properties regarding their optimal range of pH and temperature and overall durability and stability [46]. The gene was codon optimized for *E. coli* and cloned into pet28a(+). SecADH could be expressed in soluble form (Figure S1), which is predicted to be a homo-dimer [47], with one monomer being 32.4 kDa large [48].

2.4. Substrate Spectrum of secADH from Deinococcus radiodurans

To test whether the newly identified secADH was suitable for the cascade together with OHs, the substrate spectrum was investigated (Figure 4).

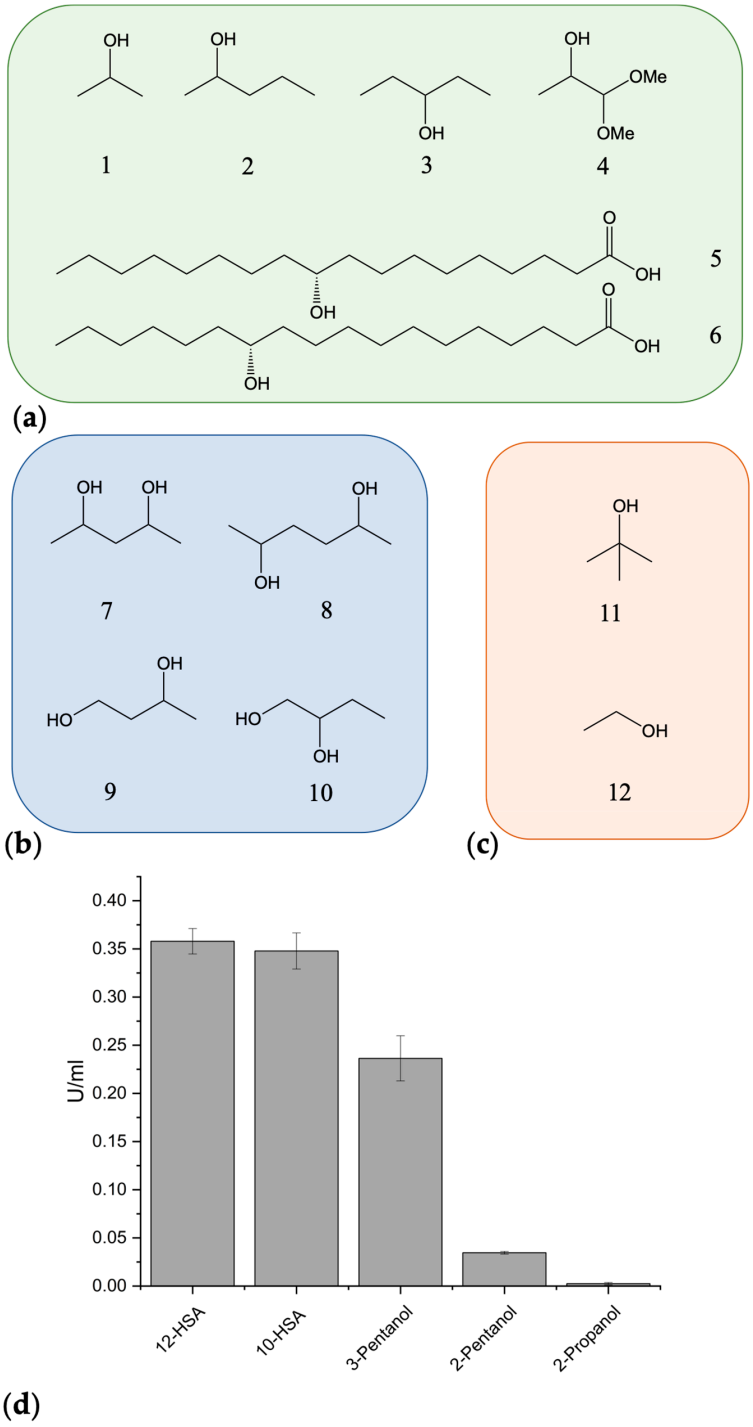

Figure 4. Structures of different substrates tested for conversion by secADH. (**a**) Secondary alcohols, (**b**) diols, (**c**) primary/tertiary alcohols. The substrates were 2-propanol (1), 2-pentanol (2), 3-pentanol (3), 1,1-dimethoxy-2-propanol (4), 10-HSA (5), 12-HSA (6), 2,4-pentanediol (7), 2,5-hexanediol (8), 1,3-butanediol (9), 1,2-butanediol (10), tert-butanol (11), ethanol (12). (**d**) Conversion of the main substrates 12-HSA, 10-HSA, 3-pentanol, 2-pentanol, and 2-propanol in U/mL.

First, the class of alcohols that can be used as substrate was investigated, testing ethanol (12), 2-propanol (1), and tert-butanol (11), which resulted in the conversion of only (1), indicating that neither primary nor tertiary alcohols are substrates for secADH.

Furthermore, we tested the reaction with diols (Figure S2). SecADH could convert diols when both alcohols were secondary ((7) and (8) in Figure 4), albeit at low conversion rates and only with an excess of each respective substrate. Diols, with one of the hydroxy groups being a primary alcohol, were not converted ((9) and (10) in Figure 4).

The enzyme preferred longer carbon chain substrates compared to short ones and can oxidize hydroxylated fatty acids besides alkanols, which we investigated by testing (2) and (3), and (5) and (6). The enzyme had a similar activity towards (5) and (6), and consequently, there was no discrimination between the two different alcohol positions within these alkyl chains. However, when comparing (2) and (3), there was a clear difference, with (3) being preferred. The used (2) was racemic, indicating that secADH prefers R-configurated alcohols—as 10- and 12-HSA are R-configurated as well—and/or alcohols that are not located at the rim of the alkane. There was no conversion observed for 1,1-dimethoxy-2-propanol (4).

A challenging aspect during the measurement was the general insolubility of longer alkanes and fatty acids in water. All substrate stocks were dissolved in ethanol; however, the enzyme reaction has to be performed in a buffer due to the enzyme's stability. 10- and 12-HSA are highly insoluble in water. Only at a concentration of 500 µM in 5% (*v*/*v*) aqueous ethanol in the final reaction, the two long-chain fatty acids were stable in the buffer.

We could thus demonstrate that the newly identified secADH from *Deinococcus radiodurans* can be used in the desired cascade reaction.

2.5. ADH-Coupled Assay Reaction Parameter Optimization

One of the challenges in coupled assays is the diverging reaction parameters, which usually results from the different originating organisms of the involved catalysts or their varying place of action within the cell. In addition to OhyRe, other OHs were tested in combination with the secADH from *Deinococcus radiodurans* to investigate which one of the cascade members dominates the reaction parameters. The different tested OHs originated from *Rhodococcus erythropolis*, *Pediococcus parvulus* (OhyPp), and *Elizabethkingia meningoseptica* (OhyEm). Each of them has specific requirements for their optimal reaction activity.

First, we analyzed the optimal reaction parameters of secADH using 12-HSA as a substrate, and we could observe that it preferred basic environments over acidic ones, with an optimal pH of around 9 (Figure 5a). In addition to the overall optimum being in a basic environment, there was a second smaller optimum at a pH of around 7. Since fatty acids usually show unique behavior in basic environments as opposed to alkane-based alcohols, we performed a pH screening of secADH with 3-pentanol as the substrate (Figure S3). Surprisingly, the first pH optimum shifted towards a more basic environment compared to when 12-HSA was used as the substrate. Since oleic acid has a pk_a of 5.02 [18], we investigated the effect on the pH and whether this might be the reason for the activity shift. We indeed observed that the pH was shifted when 12-HSA was present in the reaction buffer, but it could not explain the change in the optimum (Table S1), thus indicating that the type of substrate for secADH can influence the reaction optima.

Regarding the temperature optimum of secADH, the highest activity was measured at 18 °C and the lowest at 22 °C, where residual activity of 60% still remained, reflecting a rather broad range (Figure 5b).

The broad-range temperature optimum is beneficial for a one-pot reaction; however, the high pH optimum of secADH is problematic since the optimum of most OHs is rather in the acidic range, presumably due to an evolutionary adaptation to the acidic nature of the substrates. OhyPp [18] and OhyEm [16], for instance, have an optimum of 6. OhyRe, however, is an exception since it prefers rather basic pH environments [17].

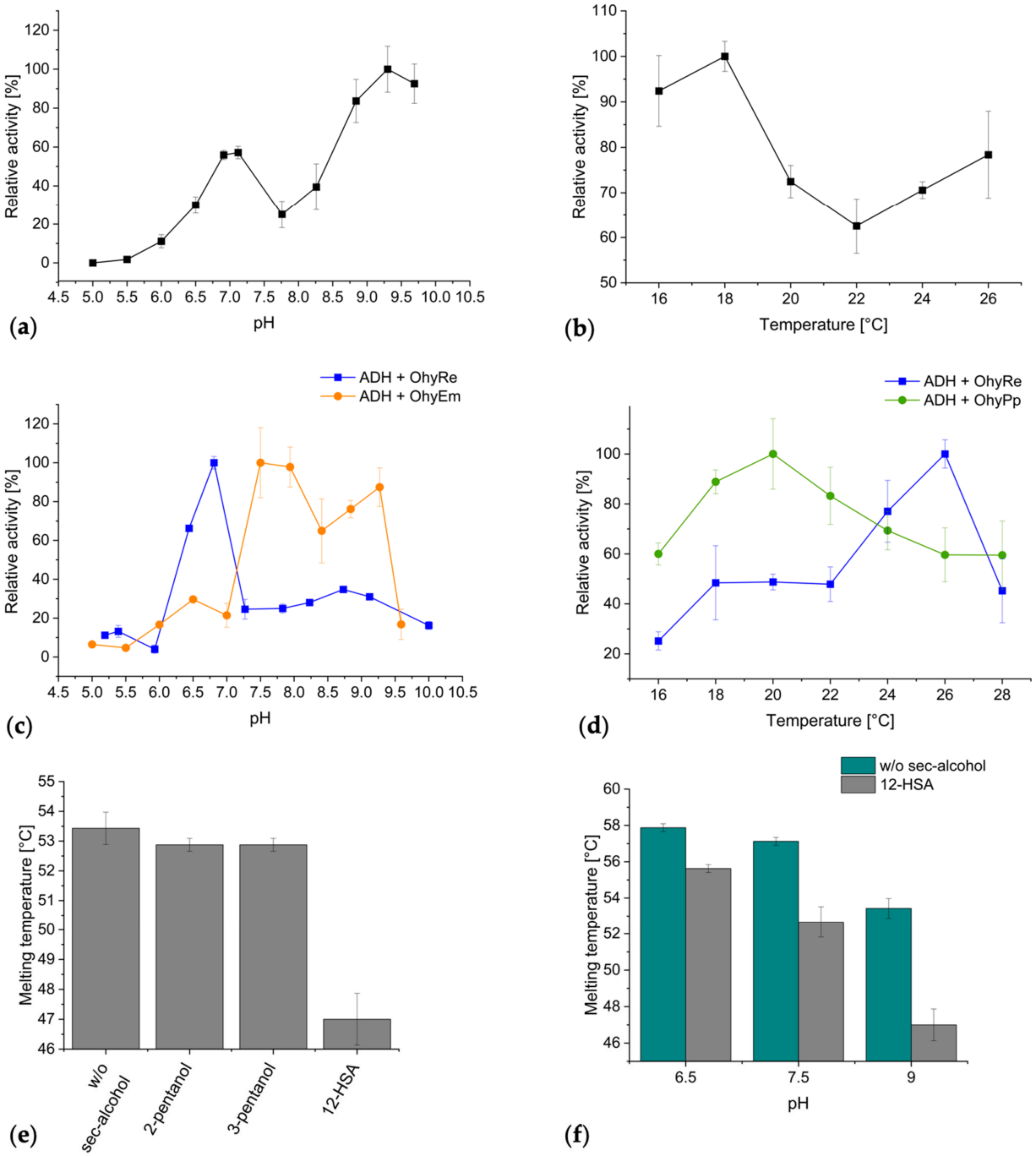

Figure 5. pH optima were analyzed using a multimode microplate reader, and temperature optima using GC-FID. Relative activities were given to the maximum of each respective curve. Experiments were conducted in triplicates; melting temperature analyses were conducted in quadruplicates. (**a**) pH optimum and (**b**) temperature optimum of secADH using 12-HSA as substrate. (**c**) Comparison of the pH optima of two cascade reactions with secADH and either OhyRe or OhyEm. (**d**) Comparison of the temperature optima of two cascade reactions with secADH and either OhyRe or OhyPp. (**e**) Analysis of the melting temperatures of secADH with and without secondary alcohols at pH 9 using 100 mM TAPS buffer. There was no statistically relevant difference between without sec-alcohol and 2- and 3-pentanol as calculated using a two-sided t-test. (**f**) Comparison of melting temperatures of secADH with and without 12-HSA at different pH values. $p < 0.01$. All variants were compared with each other using a *t*-test and show a *p*-value < 0.001, except for the comparison of pH 6.5 to 7.5, with a *p*-value < 0.01, as shown in the figure.

We analyzed the pH optima for the combination of secADH with two different OHs, OhyRe and OhyEm, since they hold varying pH optima (7.2 and 6, respectively). As shown in Figure 5c, the pH optimum was dependent on the type of OHs. In the cascade reaction with OhyRe and secADH, the optimum was measured to be around 6.5, which is close to the one from OhyRe alone [17]. On the other hand, in the cascade reaction with OhyEm, two optima were observed at around 7.5 and 9, which is more like the ones from secADH. Surprisingly, the combination of OhyRe and secADH showed a rather low conversion in basic environment despite OhyRe's robustness at elevated pH values [17] and secADH's optimum there.

The optimal temperature of the cascade reactions also depended on the type of OH used. Here, OhyPp was used, with its optimal temperature at 18 °C [18] and OhyRe at 28 °C [17]. For ADH and OhyRe, the optimum changed to 26 °C, and for ADH and OhyPp, to 20 °C (Figure 5d).

Next, the melting temperature of secADH was investigated at different pH values using protein thermal shift assays. SecADH is a stable enzyme, with its melting temperature measured to be 57.88 ± 0.22 °C at a pH of 6.5 (Table S2). Even though the highest activity was observed at pH 9, the general stability of secADH decreased with higher surrounding pH values (Figure 5f).

The stability was tested with protein thermal shift assays, where a bound ligand usually leads to a decrease in conformational protein flexibility, and thus, to an increase in its melting temperature [49]. For secADH, however, this was not the case since incubation with 3-pentanol and 2-pentanol did not lead to strong changes in the melting temperatures at pH values of 6.5, 7.5, or 9 (Table S2). On the contrary, when 12-HSA was used as the substrate, there was a significant decrease in the melting temperature at a pH of 9 from 53.43 ± 0.54 to 47.00 ± 0.87 °C (Figure 5e), which shows that the substrate strongly destabilized the protein at that pH. At the pH values of 6.5 and 7.5, secADH with 12-HSA showed only slight reductions in T_m, similar to the other substrates (Table S2).

In the coupled assay, secADH converted fatty acids, which are reported to behave differently depending on the environment, in particular, the pH value and the temperature [50]. Under basic conditions, they form mixtures of acid and soap, creating crystalline solids, which leads to non-accessible molecules and additionally might lead to the destabilization of proteins.

Most likely, the high pH and the soap attributes of the fatty acid, which became stronger at elevated pH values, had destabilizing effects on secADH. The OHs did not show these strong decreases in the melting temperatures during incubation with oleic acid, which suggests that they are evolutionarily better evolved to fatty acids as substrates (Table S3).

In summary, the temperature and pH optima cannot be concluded from the type of used OHs, but were different for every type of enzyme. The use of several enzymes within a cascade consequently led to higher complexity, and hence, the optimal parameters changed unpredictably. The results presented here show that either OH or secADH dominated the reaction conditions, which presumably depended on diverging kinetic behaviors, structural stability, or substrate access. The pH and temperature optima were closer to OhyRe's than to secADH's when they were combined in a cascade. In contrast, for OhyEm, the pH optimum followed the one for secADH more, which might have resulted from OhyEm being a faster enzyme compared to OhyRe, and hence, being the lesser rate-limiting factor within the cascade. To conclude, the conditions must be optimized separately for every type of OH.

2.6. ADH-Coupled Assay Reaction Parameter Optimization

Next, the effects of additives on the reaction cascade were tested. Oleic acid is insoluble in water, and OHs only have access to it when it is emulsified with water [15]. Additives like Tween 80 usually have positive effects on emulsification, and thus, on the activity [51,52]. Hence, the effect of the different additives (ethanol, Tween 80, dimethyl sulfoxide, and

1,5-pentanediol) in concentrations of 1, 2, 5, 10, and 20 % (v/v) on the cascade reaction was tested using OhyRe and secADH (Figure 6a). All additives showed positive effects only in low concentrations. At concentrations above 1% (v/v), the reactions started to be inhibited, except for ethanol, which led to the highest activity at 5% (v/v).

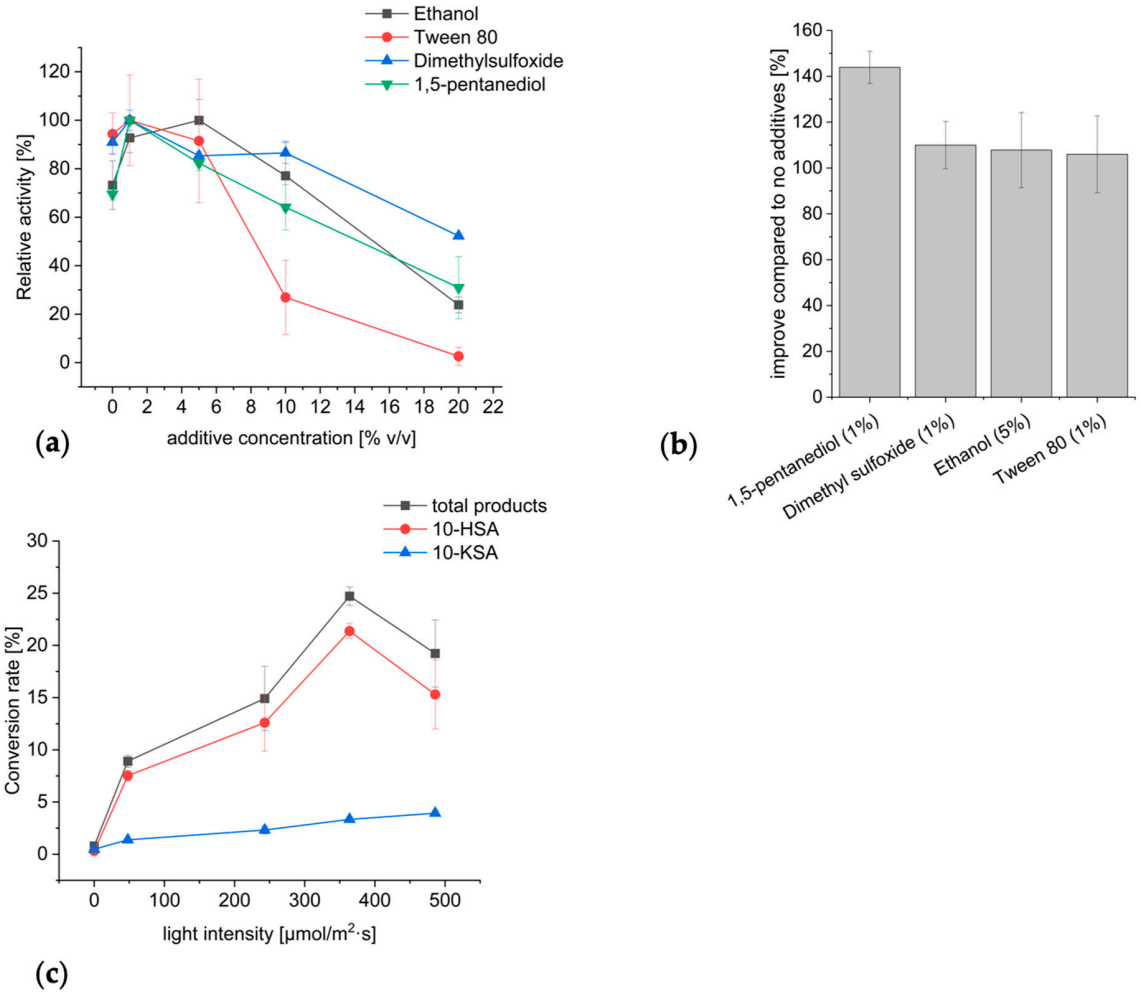

Figure 6. (**a**) Evaluating the effects of the four additives of ethanol, Tween 80, dimethyl sulfoxide, and 1,5-pentanediol at concentrations of 1, 2, 5, 10, and 20% (v/v) on a cascade reaction with OhyRe and secADH using oleic acid as substrate. (**b**) Fold improvement from reactions with no additives to those with additives for each of the optimal concentrations was used. (**c**) Evaluating different light intensities for the reduction of FAD. The same concentrations and volumes of reaction components were used as in (**a**) except for the additives, where the buffer volume was adjusted accordingly. Reactions were conducted for 3 h.

The effect was most profound for Tween 80, which, at 10% (v/v), led to a residual activity of only 30%. This is surprising since Tween 80 improved the activity of OhyRe alone strongly and at 10% (v/v), 96% residual activity, compared to the optimum at 5% (v/v), remained (Figure S4). The addition of Tween 80 to the reaction of secADH with 3-pentanol led to a decrease in activity as well, albeit not to such an extent as for the coupled assay. Tween 80 formed micellar structures with 10-HSA, potentially reducing the accessibility for secADH. The strongest increase, although still moderate compared to the control, could be observed for 1,5-pentanediol at 1% (v/v) (Figure 6b).

Since OhyRe's activity was found to be enhanced by a broadband white light at an optimal range between 243 and 364 µmol/m^2·s, the cascade reaction's performance with varying light intensities was tested (Figure 6c). As expected, a 30-fold increase in the

10-HSA yield was observed for the cascade reaction when comparing dark conditions with a light intensity of 364 µmol/m^2·s under broadband white light. The cascade reaction behaved differently on the light intensities compared to OhyRe alone since there was a sharp maximum at 364 µmol/m^2·s, whereas for OhyRe alone, there was rather a broad optimal range. Notably, the 10-KSA concentration also increased by a 14-fold factor, proving that the cascade benefitted from the light activation as well.

2.7. Optimization of Enzyme Concentrations

The combination of the two enzymes required harmonized protein concentrations. For this, different enzyme concentrations were tested. Interestingly, the concentration dependencies of secADH and OhyRe behaved differently in the coupled assay. For OhyRe, a typical saturation curve can be observed, where the v_{max}, in this experiment, was reached at 0.057 ± 0.007 U/mL, and the half-maximal concentration at 0.221 ± 0.065 g/L (Figure 7). For secADH, however, an inhibition course can be observed. Here, v_{max} was predicted to be at 0.057 ± 0.011 U/mL, and the half-maximal concentration at 0.012 ± 0.011 g/L by non-linear regression, which is 18-fold lower compared to OhyRe and Ki 0.953 ± 0.800 g/L.

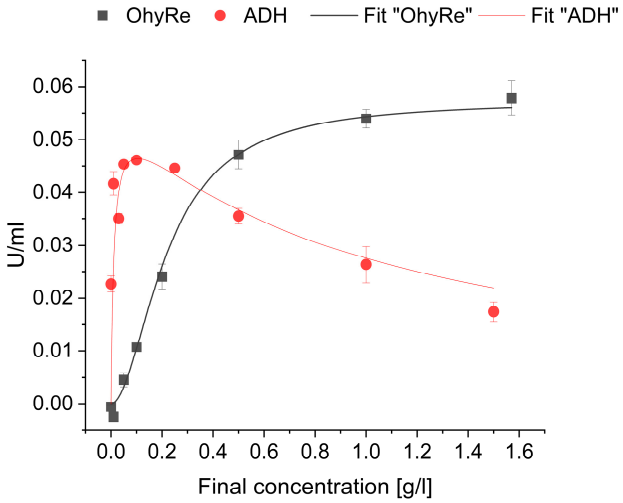

Figure 7. Evaluating different concentrations for secADH and OhyRe in a coupled assay. Dark grey curve: fixed secADH concentration (0.01 g/L). Red curve: fixed OhyRe concentration (1 g/L). The response for OhyRe was fitted using $y = Vmax \cdot x^n/(k^n + x^n)$; for secADH, using $y = Vmax \cdot x/(Km + x \cdot (1 + x/Ki))$.

Furthermore, the concentration dependency curve of secADH shows the behavior of substrate inhibition. This is surprising for an enzyme saturation curve since it usually behaves like OhyRe (dark grey curve in Figure 7). It might be that the increase in secADH led to an accumulation of 10-KSA, which led to the stronger product inhibition of OhyRe compared to 10-HSA. Furthermore, it might be that product inhibition of 10-KSA on secADH occurred, leading to the observed inhibition curves. The inhibition curve might additionally have resulted from a back reaction, which led to a decrease in the NADH/H$^+$ concentration.

2.8. Conversion of Cascade Reaction with OhyRe and secADH

With all of the optimized parameters, a long-time conversion was performed, investigating the conversion of substrates. In Figure 8a, the conversion over a period of 16 h is shown, which displays that the reaction was rather slow, as expected for OH despite the light-dependent activation. However, without that, the conversion might be even slower, as, in one study, a conversion was conducted over the course of 6 days [53]. The maximal conversion led to a residual substrate concentration of 20% of all measured fatty acids. 10-HSA was the predominant species among the products, and 10-KSA ranged only from

16 to 30% (Figure 8b and Table S4). This is surprising since OHs are often slow enzymes, as observable by their long turnover times [18,54], whereas the alcohol dehydrogenase was observed to act faster [55].

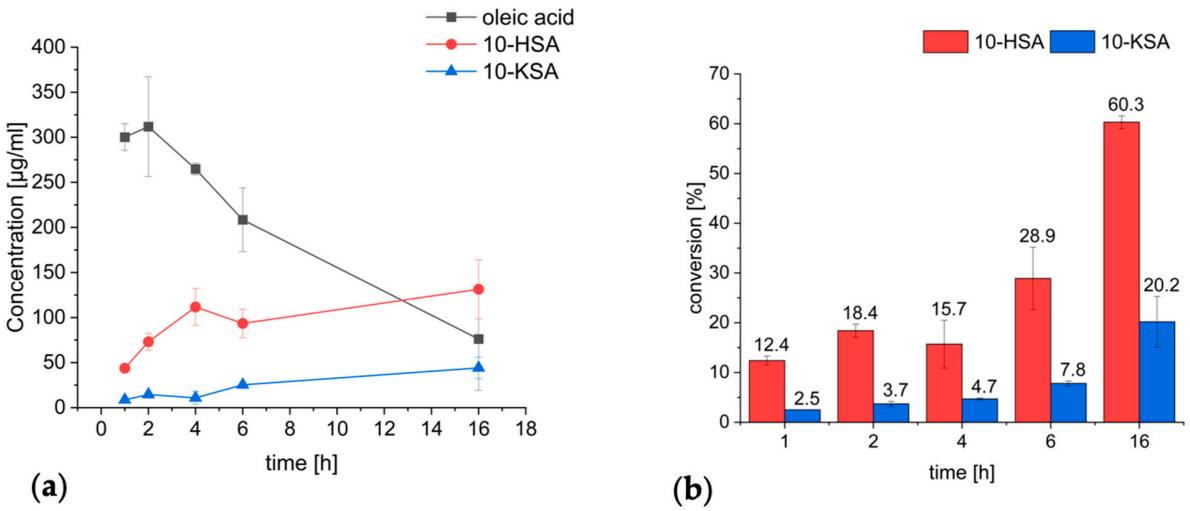

Figure 8. (**a**) Conversion of oleic acid into 10-HSA and 10-KSA using OhyRe and secADH over the course of 16 h. Reactions were performed in triplicates. Oleic acid was mixed with 50 mM MES buffer pH 6.5 to an emulsion of 10 mM, and 20 µL of it was added to a final concentration of 1 g/L OhyRe (with an equimolar concentration of FAD) and 0.01 g/L secADH, 20 µL NAD^+ (10 mM), 1% (*v*/*v*) 1,5-pentanediol, and 50 mM MES buffer pH 6.5 to a total volume of 200 µL. Reactions were stopped with 1 mL ethyl acetate. Samples were analyzed using GC-FID. (**b**) Conversions (%) of 10-HSA and 10-KSA of in (**a**) shown reactions.

An explanation might be the still-not-optimal conditions for secADH due to the undertaken compromises. Since Wu et al. also noticed that reaction conditions diverted between OH and their secADH from *Micrococcus luteus*, they decided to go for a consecutive conversion, where first 10-HSA was produced and then secADH and NAD^+-regenerating enzymes were added after pH adjustment [55]. Under these conditions, it was possible to reach a conversion of 95% of 10-HSA to 10-KSA. For the industrial production of 10-KSA on a large scale, the one-pot reaction is consequently rather unsuitable due to the low yield. 10-KSA, however, has less economic value compared to 10-HSA due to the unreactive 10-oxo group, and thus, this reaction is rather interesting for high-throughput screenings. However, for screening purposes, performing the reaction in a one-pot approach is strongly preferred since it saves time and consumables, and thus, the here-shown optimization of conditions can largely aid in its application. However, finding a 10-HSA converting secADH with a lower optimal pH might drastically increase the overall yield.

Finally, a combination of lipase, OhyRe, and secADH with oil from *C. oleaginosus* in an in vitro one-pot reaction was additionally conducted, and it was observed that around 80% of oleic acid was converted over 20 h, with around 60 % being 10-HSA, similar to the conversion shown in Figure 8. However, the complexity strongly increased with three different enzymes, and further optimization of this cascade is required to achieve the maximum output.

3. Materials and Methods

3.1. Chemicals

Chemicals were purchased from Thermo Fisher Scientific (Waltham, MA, USA), Merck (Darmstadt, Germany), and Carl Roth (Karlsruhe, Germany) at the highest available grade. *Candida rugosa* lipase was purchased from Merck. Commercially available olive, rapeseed, and linseed oils were purchased.

3.2. Cascade Reaction Using OhyRe and Lipase from C. rugosa

First, 1 µL of oil was added to 329 µL of buffer (20 mM Tris-Base, pH 7.2) and emulsified. Then, 50 µL of OhyRe (2 mg/mL with an equimolar concentration of FAD) and 20 µL of lipase (2 mg/mL) were added. Reactions were conducted for 20 h at 28 °C with 100 rpm of horizontal shaking. The samples were methylated and measured using GC-FID with a marine oil mix (Restek, Centre County, PA, USA) as an external standard.

3.3. Protein Expression

For protein expression, pet28a(+) containing secADH, OhyRe, OhyPp, and OhyEm was transformed into BL21DE3. Precultures were grown overnight in LB containing 50 µg/mL kanamycin. For the main culture, 500 mL of TB medium was inoculated to an OD_{600} of 0.05–0.1 and grown until they reached an OD_{600} of 0.6–0.8 in an Innova44R shaker (Eppendorf, Hamburg, Germany), after which the temperature was decreased to 16 °C, and gene expression was induced with a final concentration of 0.1 mM IPTG. After 16 h, the cells were harvested and resuspended in resuspension buffer (20 mM Tris-Base pH 7.2, 20 mM imidazole, 500 mM NaCl,). The cells were disrupted using a high-pressure homogenizer (EmulsiFlex-B15, AVESTIN, Ottawa, ON, Canada), and debris was removed by centrifugation at 20,000× *g* for 40 min at 4 °C. Finally, the proteins were purified using Ni^{2+}-NTA beads (Thermo Fisher Scientific), which were mixed and incubated overnight with the cell-free lysate. The beads were washed with resuspension buffer, proteins eluted using elution buffer (20 mM Tris-Base pH 7.2, 250 mM imidazole, 500 mM NaCl), and buffer exchanged with desalting columns (PD MidiTrap G-25; Cytiva, Marlborough, MA, USA). The final storage buffer was dependent on the type of enzyme and experiment and is described separately in the following paragraphs and underneath the figures. SecADH was stored in 20 mM Tris, pH 7.2. The protein concentrations were determined using ROTI®Quant with bovine serum albumin (both from Carl Roth).

3.4. Analytics

Assays were either analyzed using a multimode microplate reader (Enspire2; Perkin Elmer, Waltham, MA, USA) for 30 min at 340 nm or by GC-FID. The reactions were monitored for 30 min at 340 nm. For the calculation of U/mL, the initial linear slope of the absorbance curve of NADH, its extinction coefficient ε = 6.22 $mM^{-1} \cdot cm^{-1}$, and a plate thickness of 0.59 cm were used. U is defined as (initial slope·total volume)/(plate thickness·enzyme volume· ε). For GC-FID, the reactions were stopped, and the fatty acids were extracted with 1 mL ethyl acetate, which was evaporated afterward. All fatty acids and oils measured on GC-FID were methylated and measured as previously described [18].

3.5. Light Intensity Test

For the light intensity tests, reactions were performed in an incubation shaker equipped with LEDs of adjustable light intensity and color (TB2000, FutureLED, Berlin, Germany). For the light color test, reactions were conducted in broadband white, blue (425 nm), and red (680 nm) light at photosynthetic active radiation of 191 $\mu mol/m^2 \cdot s$ for each condition, and in the dark. For the light intensity tests, broadband white light was used at 48, 243, 364, and 486 $\mu mol/m^2 \cdot s$. Then, 1 µL oleic acid was emulsified with 149 µL buffer (20 mM Tris-Base pH 7.2, 200 mM NaCl), and 50 µL of OhyRe (30 µM with 30 µM FAD) was added. Reactions were conducted for 3 h at 28 °C and 100 rpm, followed by extraction with 1 mL of ethyl acetate with subsequent methylation. All following reactions were conducted in the LED shaker.

3.6. Optimal Conditions Test of secADH

For the pH optimum, 5 µL of 10 mM 12-HSA in ethanol was mixed with 10 µL of the secADH (0.2 g/L), 165 µL of each respective buffer, and 20 µL of NAD^+ (10 mM). The reactions were measured with a multimode microplate reader.

For the temperature optimum, 25 µL of 12-HSA (10 mg/mL), 100 µL of the secADH (2 mg/mL), 375 µL of 100 mM Tris-Base pH 8, and 20 µL NAD^+ (10 mM) were mixed and incubated for 10 min. The temperatures of 16, 18, 20, 22, 24, and 26 °C were tested. The samples were analyzed using GC-FID.

3.7. Optimal Conditions Test of Cascade Reaction with OH and secADH

For testing the pH optimum, oleic acid was emulsified with 20 mM Tris-Base buffer pH 7.2 to a concentration of 10 mM, and 20 µL of it was added to 20 µL of OhyRe or OhyEm (30 µM in 50 mM MES buffer pH 6.5, with an equimolar concentration of FAD for OhyRe), 20 µL NAD^+ (10 mM), 3 µL ADH (2 mg/mL), and the respective volume of each respective buffer to a total volume of 200 µL. The reactions were measured with a multimode microplate reader.

For testing the temperature optimum, 1 µL of oleic acid was added to 126 µL of 50 mM MES pH 6.5 and emulsified. Then, 50 µL OhyRe or OhyPp (30 µM in 50 mM MES buffer pH 6.5 for OhyRe and in 20 mM Tris-Base pH 7.2 for OhyPp, with an equimolar concentration of FAD), 20 µL NAD^+ (10 mM) and 3 µL of the secADH (2 mg/mL) were added. The experiments were conducted in triplicate for 15 min, and the samples were analyzed using GC-FID.

3.8. Buffer for pH-Tests

For the analysis of the pH optima, the following buffers were used: pH 5: citrate; pH 5.5-6.5: MES; pH 7-8.5: Tris-Base; pH 9-9.5: TAPS; pH 10: CAPS, all with a concentration of 100 mM.

3.9. Substrate Specificity Test for secADH

To initially investigate the substrate specificity, 10 µL of ethanol, tert.-butanol, and 2-propanol were mixed with 10 µL of ADH (2 mg/mL), 20 µL of NAD^+ (10 mM), and 160 µL of 20 mM Tris-Base, pH 7.2. For the conversion of diols, 1 M stocks, and for the secondary alcohols, 10 mM stocks, were prepared in ethanol. The reactions were conducted as described above and analyzed in a multimode microplate reader at 340 nm.

3.10. Determination of Melting Temperatures

First, 5 µL of ADH (2 mg/mL) was mixed with 2.5 µL SYPRO™ Orange (Thermo Fisher Scientific) (1:200), 1.3 µL of ethanol or 1.3 µL of 10 mM of each of the secondary alcohols dissolved in ethanol and 16.2 µL buffer in qPCR tubes with optically clear lids. For pH 6.5 MES, for pH 7.5 Tris-Base, and for pH 9, TAPS buffer was used (all with a concentration of 100 mM). After putting the samples on ice, they were transferred to an RT-PCR cycler (CFX Opus 96, Bio-Rad, Feldkirchen, Germany). The ramp went from 10 to 95 °C in 0.5 °C steps, holding for 10 s per cycle. The experiments were conducted in quadruplicate.

3.11. Testing of Different Additives

First, 10 mM oleic acid was mixed with 50 mM MES buffer pH 6.5 to an emulsion, and 20 µL of it was added to 20 µL OhyRe (30 µM with an equimolar concentration of FAD), 3 µL of the secADH (2 mg/mL), 20 µL NAD^+ (10 mM) of the respective volume of the additive, and 50 mM MES buffer pH 6.5 to a total volume of 200 µL. The reactions were monitored at 340 nm for 30 min.

3.12. Optimization of Enzyme Concentrations

For the fixed secADH concentrations (dark grey curve in Figure 7), the following conditions were used: oleic acid was mixed with 50 mM MES buffer pH 6.5 to an emulsion of 10 mM, and 20 µL of it was added to different final concentrations of OhyRe (stored with an equimolar concentration of FAD) and 0.01 g/L ADH, 20 µL NAD^+ (10 mM), and 50 mM MES buffer pH 6.5 to a total volume of 200 µL. For the fixed OhyRe concentrations (red

curve in Figure 7), a final concentration of OhyRe of 1 g/L was used. The reactions were monitored at 340 nm for 30 min.

4. Conclusions

In summary, rapid light-driven activation of OhyRe was presented with broadband white light at an intensity of 364 µmol/m^2·s, leading to the highest increase in activity. This most likely can be attributed to a partial reduction of FAD to $FADH_2$ without the utilization of anaerobic conditions.

Furthermore, two cascade reactions were presented, with one being upstream and one being downstream of OhyRe. For the upstream one, a lipase from *Candida rugosa* and OhyRe was presented, leading to the hydrolysis of triglyceride oils into free fatty acids and their subsequent hydroxylation. The yield was decreased with increasing amounts of oleic acid; however, other factors, such as remaining impurities, may also play a role.

The downstream cascade reaction comprised a novel alcohol dehydrogenase from *Deinococcus radiodurans*, which was functionally expressed, and its substrate specificity was investigated, proving a preference for long-carbon-chain secondary alcohols. It also converted hydroxylated fatty acids, which makes it an ideal candidate for high-throughput screenings of optimized OHs and large-scale conversions of 10-HSA. To be suitable for screenings, the optimal reaction conditions were investigated. The results show that the pH and temperature optima depended on the type of OHs and might either follow OH's or secADH's preferences. Furthermore, hydroxylated fatty acids destabilized secADH at elevated pH values and became more unstable with increasing pH despite showing the highest activity in basic environments. Since OHs prefer oleic acid as substrate in an emulsion, they had increased activity with emulsifiers such as ethanol or Tween 80. However, when using them together with secADH, the activity improvement was only marginal at low concentrations of these additives. At higher concentrations, a drastic decrease in activity occurred. Furthermore, it could be shown that a coupled assay can benefit from improvements in the OH reaction. The cascade reaction showed an increase in activity by a factor of 30 upon incubation under light. Still, the concentration of 10-KSA was rather low compared to 10-HSA. Additional optimizations can facilitate the achievement of further enhanced product concentrations, including the engineering of a secADH to enhance resistance to pH variations and additives.

We also showcased a proof-of-concept, indicating that a coupled assay using lipase, OhyRe, and a secADH to generate 10-KSA out of oil from *C. oleaginosus* is feasible.

In general, the utilization of cascade reactions in conjunction with OHs could potentially significantly impact catalyst optimization screenings and industrial applications in the future. This is due to their ability to reduce the number of processing steps, leading to savings in both time and costs. The data presented here represent initial strides toward the implementation of these cascade reactions.

In future activities, our group will validate and optimize the herein-described enzyme cascades at technical scales to generate data for a techno-economic analysis that will guide potential subsequent commercialization efforts.

In this context, fermentative enzyme production expenses are a main cost driver that may be an economic barrier in the industrialization process. The alleviation of these economic constraints requires the use of cost-efficient, complex feedstocks in enzyme production [56]. Significant progress has been made in achieving cost-efficient production of lipase, an industrially advanced enzyme system [57]. In follow-up experiments, lipase and OH can be produced from biomass residue streams, such as enzymatically hydrolyzed sunflower husks or wheat spelts, which are current milling by-products with little valorization. Our group has significant experience with these feedstocks and is in the process of developing economically viable processes in this respect.

Supplementary Materials: The following supporting information can be downloaded at: https://www.mdpi.com/article/10.3390/catal13091236/s1. Figure S1: SDS-page gel of the novel secADH from *Deinococcus radiodurans*. Predicted molecular weight is 32.4 kDa. Figure S1: Comparison of the conversion in U/ml of the diols 2,4-pentanediol, 2,5-hexanediol, 1,3-butanediol with the secondary alcohol 2-propanol. 1,2-butanediol didn't show any conversion. Figure S2: pH-optimum of secADH using 12-HSA compared with 3-pentanol as substrates. 5 µL of 10 mM 12-HSA in ethanol were mixed with 10 µL of secADH (0.2 mg/mL), 20 µL of NAD^+ (10 mM) and 165 µL of each respective buffer (100 mM concentrations). Figure S3: Effect of Tween 80 on the conversion of oleic acid using OhyRe. Oleic acid was mixed with 20 mM Tris-Base buffer pH 7.2 to an emulsion of 10 mM and 20 µL of it were added to 20 µL OhyRe (30 µM with an equimolar concentration of FAD), 20 µL NAD^+ (10 mM) the respective volume of the additive and 20 mM Tris-Base buffer pH 7.2 to a total volume of 200 µL. Table S1: Anticipated pH and actual (measured) pH using 5 µL of 10 mM 12-HSA in ethanol mixed with 10 µL of secADH (0.2 mg/mL in 20 mM Tris-Base pH 7.2), 20 µL of NAD^+ (10 mM in 20 mM Tris-Base pH 7.2) and 165 µL of each respective buffer (100 mM concentrations). Table S2: Melting temperatures (in °C) of secADH incubated with different secondary alcohols. Table S3: Melting temperatures (in °C) of OHs incubated with or without oleic acid in 200-molar excess. Oleic acid was dissolved in ethanol, which was evaporated prior the addition of the other components to assure an appropriate final concentration. The protein thermal shift assays were conducted at a pH of 7.2 for OhyRe and at a pH of 6 for OhyPp and OhyEm. Table S1: Conversion ratio of 10-KSA to total product concentration after 1, 2, 4, 6 and 16 h.

Author Contributions: Conceptualization, S.A.P., M.H. and F.M.; methodology, S.A.P., M.H. and M.R.; validation, S.A.P. and M.H.; formal analysis, S.A.P.; investigation, S.A.P. and M.R.; resources, S.A.P.; data curation, S.A.P.; writing—original draft preparation, S.A.P. and F.M.; writing—review and editing, S.A.P., M.H., M.R., F.M., D.G. and T.B.; supervision, D.G. and T.B.; project administration, D.G. and T.B.; funding acquisition, T.B. All authors have read and agreed to the published version of the manuscript.

Funding: We greatly acknowledge the German Federal Ministry of Education and Research (Bundesministerium für Bildung und Forschung), which funded this research project (grant number 03SF0577A).

Data Availability Statement: The data presented in this study are available upon request from the corresponding author.

Acknowledgments: We want to thank Maria Bandookwala for her support in the data acquisition. Furthermore, we appreciate Mahmoud Masri and Global Sustainable Transformation GmbH for providing microbial oil from *C. oleaginosus*. We would like to extend our sincere gratitude to FUCHS LUBRICANTS GERMANY GmbH for their generous provision of 12-HSA and HOSO for use in our research.

Conflicts of Interest: The authors declare no conflict of interest.

References

1. Claassens, N.J.; Burgener, S.; Vögeli, B.; Erb, T.J.; Bar-Even, A. A Critical Comparison of Cellular and Cell-Free Bioproduction Systems. *Curr. Opin. Biotechnol.* **2019**, *60*, 221–229. [CrossRef]
2. Siedentop, R.; Claaßen, C.; Rother, D.; Lütz, S.; Rosenthal, K. Getting the Most out of Enzyme Cascades: Strategies to Optimize in Vitro Multi-enzymatic Reactions. *Catalysts* **2021**, *11*, 1183. [CrossRef]
3. Hwang, E.T.; Lee, S. Multienzymatic Cascade Reactions via Enzyme Complex by Immobilization. *ACS Catal.* **2019**, *9*, 4402–4425. [CrossRef]
4. Lin, B.; Tao, Y. Whole-Cell Biocatalysts by Design. *Microb. Cell Fact.* **2017**, *16*, 1–12. [CrossRef] [PubMed]
5. Guterl, J.K.; Garbe, D.; Carsten, J.; Steffler, F.; Sommer, B.; Reiße, S.; Philipp, A.; Haack, M.; Rühmann, B.; Koltermann, A.; et al. Cell-Free Metabolic Engineering: Production of Chemicals by Minimized Reaction Cascades. *ChemSusChem* **2012**, *5*, 2165–2172. [CrossRef]
6. Voss, M.; Küng, R.; Hayashi, T.; Jonczyk, M.; Niklaus, M.; Iding, H.; Wetzl, D.; Buller, R. Multi-Faceted Set-up of a Diverse Ketoreductase Library Enables the Synthesis of Pharmaceutically-Relevant Secondary Alcohols. *ChemCatChem* **2020**, *13*, 1538–1545. [CrossRef]
7. Siedentop, R.; Rosenthal, K. Industrially Relevant Enzyme Cascades for Drug Synthesis and Their Ecological Assessment. *Int. J. Mol. Sci.* **2022**, *23*, 3605. [CrossRef]

8. Begander, B.; Huber, A.; Döring, M.; Sperl, J.; Sieber, V. Development of an Improved Peroxidase-Based High-Throughput Screening for the Optimization of d-Glycerate Dehydratase Activity. *Int. J. Mol. Sci.* **2020**, *21*, 335. [CrossRef]
9. Bub, O.; Jager, S.; Dold, S.M.; Zimmermann, S.; Hamacher, K.; Schmitz, K.; Rudat, J. Statistical Evaluation of Hts Assays for Enzymatic Hydrolysis of β-Keto Esters. *PLoS ONE* **2016**, *11*, e0146104. [CrossRef]
10. Kiianitsa, K.; Solinger, J.A.; Heyer, W.D. NADH-Coupled Microplate Photometric Assay for Kinetic Studies of ATP-Hydrolyzing Enzymes with Low and High Specific Activities. *Anal. Biochem.* **2003**, *321*, 266–271. [CrossRef]
11. Fang, X.; Zheng, Y.; Duan, Y.; Liu, Y.; Zhong, W. Recent Advances in Design of Fluorescence-Based Assays for High-Throughput Screening. *Anal. Chem.* **2019**, *91*, 482–504. [CrossRef] [PubMed]
12. Kozaeva, E.; Mol, V.; Nikel, P.I.; Nielsen, A.T. High-Throughput Colorimetric Assays Optimized for Detection of Ketones and Aldehydes Produced by Microbial Cell Factories. *Microb. Biotechnol.* **2022**, *15*, 2426–2438. [CrossRef] [PubMed]
13. Leippe, D.M.; Nguyen, D.; Zhou, M.; Good, T.; Kirkland, T.A.; Scurria, M.; Bernad, L.; Ugo, T.; Vidugiriene, J.; Cali, J.J.; et al. A Bioluminescent Assay for the Sensitive Detection of Proteases. *Biotechniques* **2011**, *51*, 105–110. [CrossRef] [PubMed]
14. Zegzouti, H.; Zdanovskaia, M.; Hsiao, K.; Goueli, S.A. ADP-Glo: A Bioluminescent and Homogeneous Adp Monitoring Assay for Kinases. *Assay Drug Dev. Technol.* **2009**, *7*, 560–572. [CrossRef]
15. Prem, S.; Helmer, C.P.O.; Dimos, N.; Himpich, S.; Brück, T.; Garbe, D.; Loll, B. Towards an Understanding of Oleate Hydratases and Their Application in Industrial Processes. *Microb. Cell Fact.* **2022**, *21*, 1–15. [CrossRef]
16. Engleder, M.; Pavkov-Keller, T.; Emmerstorfer, A.; Hromic, A.; Schrempf, S.; Steinkellner, G.; Wriessnegger, T.; Leitner, E.; Strohmeier, G.A.; Kaluzna, I.; et al. Structure-Based Mechanism of Oleate Hydratase from Elizabethkingia Meningoseptica. *ChemBioChem* **2015**, *16*, 1730–1734. [CrossRef]
17. Lorenzen, J.; Driller, R.; Waldow, A.; Qoura, F.; Loll, B.; Brück, T. Rhodococcus Erythropolis Oleate Hydratase: A New Member in the Oleate Hydratase Family Tree—Biochemical and Structural Studies. *ChemCatChem* **2018**, *10*, 407–414. [CrossRef]
18. Prem, S.A.; Helmer, C.P.O.; Loll, B.; Garbe, D.; Brück, T. Expanding the Portfolio by a Novel Monomeric Oleate Hydratase from Pediococcus Parvulus. *ChemCatChem* **2023**, *15*. [CrossRef]
19. Volkov, A.; Khoshnevis, S.; Neumann, P.; Herrfurth, C.; Wohlwend, D.; Ficner, R.; Feussner, I. Crystal Structure Analysis of a Fatty Acid Double-Bond Hydratase from Lactobacillus Acidophilus. *Acta Crystallogr. Sect. D Biol. Crystallogr.* **2013**, *69*, 648–657. [CrossRef]
20. Masri, M.A.; Garbe, D.; Mehlmer, N.; Brück, T.B. A Sustainable, High-Performance Process for the Economic Production of Waste-Free Microbial Oils That Can Replace Plant-Based Equivalents. *Energy Environ. Sci.* **2019**, *12*, 2717–2732. [CrossRef]
21. Ochsenreither, K.; Glück, C.; Stressler, T.; Fischer, L.; Syldatk, C. Production Strategies and Applications of Microbial Single Cell Oils. *Front. Microbiol.* **2016**, *7*. [CrossRef] [PubMed]
22. Fuchs, T.; Melcher, F.; Rerop, Z.S.; Lorenzen, J.; Shaigani, P.; Awad, D.; Haack, M.; Prem, S.A.; Masri, M.; Mehlmer, N.; et al. Identifying Carbohydrate-Active Enzymes of Cutaneotrichosporon Oleaginosus Using Systems Biology. *Microb. Cell Fact.* **2021**, *20*, 1–18. [CrossRef]
23. Shaigani, P.; Fuchs, T.; Graban, P.; Prem, S.; Haack, M.; Masri, M.; Mehlmer, N.; Brueck, T. Mastering Targeted Genome Engineering of GC-Rich Oleaginous Yeast for Tailored Plant Oil Alternatives for the Food and Chemical Sector. *Microb. Cell Fact.* **2023**, *22*, 1–14. [CrossRef] [PubMed]
24. Zhang, Y.; Eser, B.E.; Kristensen, P.; Guo, Z. Fatty Acid Hydratase for Value-Added Biotransformation: A Review. *Chin. J. Chem. Eng.* **2020**, *28*, 2051–2063. [CrossRef]
25. Schmid, J.; Steiner, L.; Fademrecht, S.; Pleiss, J.; Otte, K.B.; Hauer, B. Biocatalytic Study of Novel Oleate Hydratases. *J. Mol. Catal. B Enzym.* **2016**, *133*, S243–S249. [CrossRef]
26. Betancor, L.; Hidalgo, A.; Fernández-Lorente, G.; Mateo, C.; Rodríguez, V.; Fuentes, M.; López-Gallego, F.; Fernández-Lafuente, R.; Guisan, J.M. Use of Physicochemical Tools to Determine the Choice of Optimal Enzyme: Stabilization of D-Amino Acid Oxidase. *Biotechnol. Prog.* **2003**, *19*, 784–788. [CrossRef]
27. Hagedoorn, P.L.; Hoolmann, F.; Hanefeld, U. Novel Oleate Hydratases and Potential Biotechnological Applications. *Appl. Microbiol. Biotechnol.* **2021**, *105*, 6159–6172. [CrossRef]
28. Boratynski, F.; Szczepanska, E.; De Simeis, D.; Serra, S.; Brenna, E. Bacterial Biotransformation of Oleic Acid: New Findings on the Formation of γ-Dodecalactone and 10-Ketostearic Acid in the Culture of Micrococcus Luteus. *Molecules* **2020**, *25*, 3024. [CrossRef]
29. Huang, J.K.; Samassekou, K.; Alhmadi, H.B.; VanDerway, D.R.; Diaz, J.D.; Seiver, J.A.; McClenahan, S.W.; Holt, S.M.; Wen, L. Knockout of Secondary Alcohol Dehydrogenase in Nocardia Cholesterolicum NRRL 5767 by CRISPR/Cas9 Genome Editing Technology. *PLoS ONE* **2020**, *15*, e0230915. [CrossRef]
30. Sun, Q.F.; Zheng, Y.C.; Chen, Q.; Xu, J.H.; Pan, J. Engineering of an Oleate Hydratase for Efficient C10-Functionalization of Oleic Acid. *Biochem. Biophys. Res. Commun.* **2021**, *537*, 64–70. [CrossRef]
31. Chandra, P.; Enespa; Singh, R.; Arora, P.K. Microbial Lipases and Their Industrial Applications: A Comprehensive Review. *Microb. Cell Fact.* **2020**, *19*. [CrossRef] [PubMed]
32. Ranganathan, S.; Gärtner, T.; Wiemann, L.O.; Sieber, V. A One Pot Reaction Cascade of in Situ Hydrogen Peroxide Production and Lipase Mediated in Situ Production of Peracids for the Epoxidation of Monoterpenes. *J. Mol. Catal. B Enzym.* **2015**, *114*, 72–76. [CrossRef]
33. Van Dongen, S.F.M.; Nallani, M.; Cornelissen, J.J.L.M.; Nolte, R.J.M.; Hest, J.C.M. Van A Three-Enzyme Cascade Reaction through Positional Assembly of Enzymes in a Polymersome Nanoreactor. *Chemistry (Easton)* **2009**, *15*, 1107–1114. [CrossRef]

34. Srinivasamurthy, V.S.T.; Böttcher, D.; Bornscheuer, U.T. A Multi-Enzyme Cascade Reaction for the Production of 6-Hydroxyhexanoic Acid. *Zeitschrift fur Naturforsch.-Sect. C J. Biosci.* **2019**, *74*, 71–76. [CrossRef]
35. Serra, S.; De Simeis, D.; Marzorati, S.; Valentino, M. Oleate Hydratase from Lactobacillus Rhamnosus Atcc 53103: A Fadh2-Dependent Enzyme with Remarkable Industrial Potential. *Catalysts* **2021**, *11*, 1051. [CrossRef]
36. Lukacs, A.; Haigney, A.; Brust, R.; Zhao, R.K.; Stelling, A.L.; Clark, I.P.; Towrie, M.; Greetham, G.M.; Meech, S.R.; Tonge, P.J. Photoexcitation of the Blue Light Using FAD Photoreceptor AppA Results in Ultrafast Changes to the Protein Matrix. *J. Am. Chem. Soc.* **2011**, *133*, 16893–16900. [CrossRef] [PubMed]
37. Masuda, S.; Hasegawa, K.; Ishii, A.; Ono, T.A. Light-Induced Structural Changes in a Putative Blue-Light Receptor with a Novel FAD Binding Fold Sensor of Blue-Light Using FAD (BLUF); Slr1694 of Synechocystis Sp. PCC6803. *Biochemistry* **2004**, *43*, 5304–5313. [CrossRef]
38. Benjamin, S.; Pandey, A. Candida Rugosa Lipases: Molecular Biology and Versatility in Biotechnology. *Yeast* **1998**, *14*, 1069–1087. [CrossRef]
39. Macrae, A.R.; Hammond, R.C. Present and Future Applications of Lipases. *Biotechnol. Genet. Eng. Rev.* **1985**, *3*, 193–217. [CrossRef]
40. Melcher, F.; Ringel, M.; Vogelgsang, F.; Haack, M.; Masri, M.; Brück, T.; Garbe, D.; Roth, A. Lipase-Mediated Plant Oil Hydrolysis—Toward a Quantitative Glycerol Recovery for the Synthesis of Pure Allyl Alcohol and Acrylonitrile. *Eur. J. Lipid Sci. Technol.* **2023**, *2200196*, 1–12. [CrossRef]
41. Di Pietro, M.E.; Mannu, A.; Mele, A. NMR Determination of Free Fatty Acids in Vegetable Oils. *Processes* **2020**, *8*, 410. [CrossRef]
42. Ostojčić, M.; Budžaki, S.; Flanjak, I.; Bilić Rajs, B.; Barišić, I.; Tran, N.N.; Hessel, V.; Strelec, I. Production of Biodiesel by Burkholderia Cepacia Lipase as a Function of Process Parameters. *Biotechnol. Prog.* **2021**, *37*, e3109. [CrossRef]
43. Yiitolu, M.; Temoçin, Z. Immobilization of Candida Rugosa Lipase on Glutaraldehyde-Activated Polyester Fiber and Its Application for Hydrolysis of Some Vegetable Oils. *J. Mol. Catal. B Enzym.* **2010**, *66*, 130–135. [CrossRef]
44. Reis, P.; Holmberg, K.; Watzke, H.; Leser, M.E.; Miller, R. Lipases at Interfaces: A Review. *Adv. Colloid Interface Sci.* **2009**, *147–148*, 237–250. [CrossRef]
45. Huang, J.-K.; Park, J.K.; Dhungana, B.R.; Youngblut, N.D.; Lin, C.-T.; Wen, L. A Novel Secondary Alcohol Dehydrogenase from Micrococcus Luteus WIUJH20: Purification, Cloning, and Properties. *FASEB J.* **2010**, *24*, 835.5. [CrossRef]
46. Li, J.; Webster, T.J.; Tian, B. Functionalized Nanomaterial Assembling and Biosynthesis Using the Extremophile Deinococcus Radiodurans for Multifunctional Applications. *Small* **2019**, *15*, 1–15. [CrossRef]
47. Waterhouse, A.; Bertoni, M.; Bienert, S.; Studer, G.; Tauriello, G.; Gumienny, R.; Heer, F.T.; De Beer, T.A.P.; Rempfer, C.; Bordoli, L.; et al. SWISS-MODEL: Homology Modelling of Protein Structures and Complexes. *Nucleic Acids Res.* **2018**, *46*, W296–W303. [CrossRef] [PubMed]
48. Gasteiger, E.; Hoogland, C.; Gattiker, A.; Duvaud, S.; Wilkins, M.R.; Appel, R.D.; Bairoch, A. Protein Identification and Analysis Tools on the Expasy Server. In *The Proteomics Protocols Handbook*; Humana: Totowa, NJ, Canada, 2005; pp. 571–607.
49. Celej, M.S.; Montich, G.G.; Fidelio, G.D. Protein Stability Induced by Ligand Binding Correlates with Changes in Protein Flexibility. *Protein Sci.* **2003**, *12*, 1496–1506. [CrossRef]
50. Small, D.M. Physical Properties of Fatty Acids and Their Extracellular and Intracellular Distribution. *Polyunsaturated Fat. Acids Hum. Nutr. Nestlé Nutr. Work. Ser.* **1992**, *28*, 25–39.
51. Park, J.Y.; Lee, S.H.; Kim, K.R.; Park, J.B.; Oh, D.K. Production of 13S-Hydroxy-9(Z)-Octadecenoic Acid from Linoleic Acid by Whole Recombinant Cells Expressing Linoleate 13-Hydratase from Lactobacillus Acidophilus. *J. Biotechnol.* **2015**, *208*, 1–10. [CrossRef]
52. Kim, B.N.; Yeom, S.J.; Oh, D.K. Conversion of Oleic Acid to 10-Hydroxystearic Acid by Whole Cells of Stenotrophomonas Nitritireducens. *Biotechnol. Lett.* **2011**, *33*, 993–997. [CrossRef] [PubMed]
53. Busch, H.; Tonin, F.; Alvarenga, N.; van den Broek, M.; Lu, S.; Daran, J.M.; Hanefeld, U.; Hagedoorn, P.L. Exploring the Abundance of Oleate Hydratases in the Genus Rhodococcus—Discovery of Novel Enzymes with Complementary Substrate Scope. *Appl. Microbiol. Biotechnol.* **2020**, *104*, 5801–5812. [CrossRef]
54. Zhang, J.; Bilal, M.; Liu, S.; Zhang, J.; Lu, H.; Luo, H.; Luo, C.; Shi, H.; Iqbal, H.M.N.; Zhao, Y. Sustainable Biotransformation of Oleic Acid to 10-Hydroxystearic Acid by a Recombinant Oleate Hydratase from Lactococcus Garvieae. *Processes* **2019**, *7*, 326. [CrossRef]
55. Wu, Y.X.; Pan, J.; Yu, H.L.; Xu, J.H. Enzymatic Synthesis of 10-Oxostearic Acid in High Space-Time Yield via Cascade Reaction of a New Oleate Hydratase and an Alcohol Dehydrogenase. *J. Biotechnol. X* **2019**, *2*, 3–7. [CrossRef] [PubMed]
56. Sakhuja, D.; Ghai, H.; Rathour, R.K.; Kumar, P.; Bhatt, A.K.; Bhatia, R.K. Cost-Effective Production of Biocatalysts Using Inexpensive Plant Biomass: A Review. *3 Biotech* **2021**, *11*, 280. [CrossRef]
57. Abdelmoez, W.; Mostafa, N.A.; Mustafa, A. Utilization of Oleochemical Industry Residues as Substrates for Lipase Production for Enzymatic Sunflower Oil Hydrolysis. *J. Clean. Prod.* **2013**, *59*, 290–297. [CrossRef]

Supplementary Materials

Amino acid sequence of secADH from *Deinococcus radiodurans*

MSIKTVTVCGSGVLGSQIAFQTAFHGFDVHLYDINDAAIAKARETLGKLQARYQQDLKVDAQQTGDAFARISF
FTDIAEAVKGVDLVIEAIPENMDIKRKFYNQLGEVADPNTIFATNSSTLLPSQFMEETGRPEKFLALHFANEIWK
FNTAEIMRTPRTDDAVFDTVVQFAKDIGMVALPMYKEQAGYILNTLLVPLLGAALELVVKGIADPQTVDKTW
MIATGAPRGPFAFLDVIGLTTPYNINMASAETNPGSAAAAKYIKENYIDKGKLGTATGEGFYKYPNPAFESADF
LK

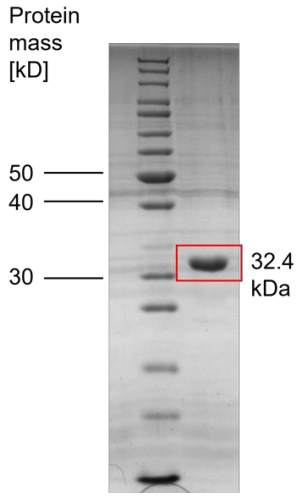

Figure S1. SDS-page gel of the novel secADH from *Deinococcus radiodurans*. Predicted molecular weight is 32.4 kDa.

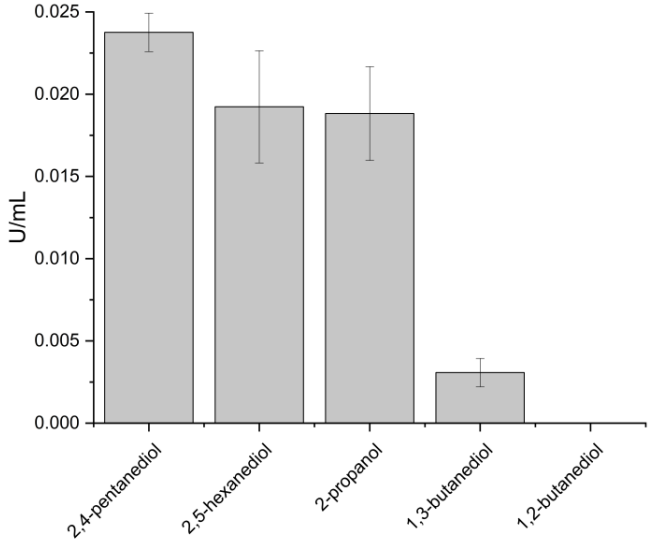

Figure S2. Comparison of the conversion in U/ml of the diols 2,4-pentanediol, 2,5-hexanediol, 1,3-butanediol with the secondary alcohol 2-propanol. 1,2-butanediol didn't show any conversion.

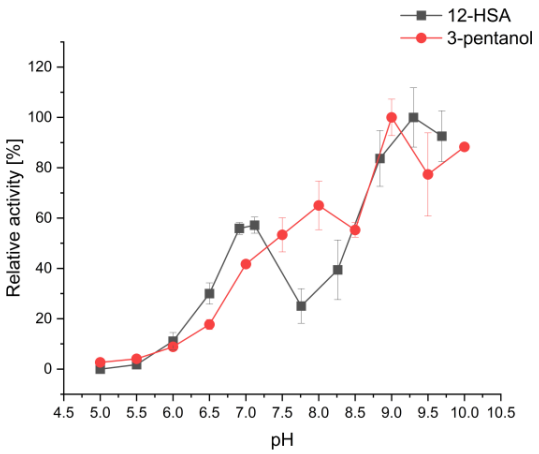

Figure S3. pH-optimum of secADH using 12-HSA compared with 3-pentanol as substrates. 5 µl of 10 mM 12-HSA in ethanol were mixed with 10 µl of secADH (0.2 mg/ml), 20 µl of NAD^+ (10 mM) and 165 µl of each respective buffer (100 mM concentrations).

Table S1. Anticipated pH and actual (measured) pH using 5 µl of 10 mM 12-HSA in ethanol mixed with 10 µl of secADH (0.2 mg/ml in 20 mM Tris-Base pH 7.2), 20 µl of NAD^+ (10 mM in 20 mM Tris-Base pH 7.2) and 165 µl of each respective buffer (100 mM concentrations).

Anticipated pH	5.00	5.50	6.00	6.50	7.00	7.50	8.00	8.50	9.00	9.50	10.00
Measured pH	5.00	5.50	6.00	6.50	6.91	7.12	7.76	8.26	8.84	9.30	9.69

Table S2. Melting temperatures (in °C) of secADH incubated with different secondary alcohols.

pH	w/o sec-alcohol	2-pentanol	3-pentanol	12-HSA
6.5	57.88 ± 0.22	56.75 ± 0.56	54.88 ± 1.34	55.63 ± 0.22
7.5	57.13 ± 0.22	56.25 ± 0.75	54.63 ± 0.41	54.00 ± 2.42
9	53.43 ± 0.54	52.88 ± 0.22	52.88 ± 0.22	47.00 ± 0.87

Table S3. Melting temperatures (in °C) of OHs incubated with or without oleic acid in 200-molar excess. Oleic acid was dissolved in ethanol, which was evaporated prior the addition of the other components to assure an appropriate final concentration. The protein thermal shift assays were conducted at a pH of 7.2 for OhyRe and at a pH of 6 for OhyPp and OhyEm.

	OhyRe	OhyPp	OhyEm

No oleic acid	45.00 ± 0.00	40.00 ± 0.00	48.50 ± 0.00
200 molar excess of oleic acid	44.64 ± 0.22	39.00 ± 0.00	49.00 ± 0.00

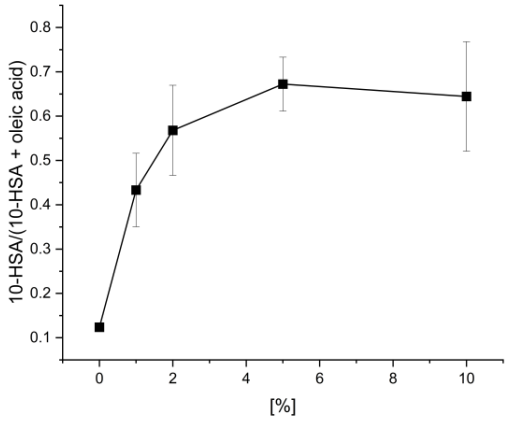

Figure S4. Effect of Tween 80 on the conversion of oleic acid using OhyRe. Oleic acid was mixed with 20 mM Tris-Base buffer pH 7.2 to an emulsion of 10 mM and 20 µl of it were added to 20 µl OhyRe (30 µM with an equimolar concentration of FAD), 20 µl NAD^+ (10 mM) the respective volume of the additive and 20 mM Tris-Base buffer pH 7.2 to a total volume of 200 µl.

Table S1. Conversion ratio of 10-KSA to total product concentration after 1, 2, 4, 6 and 16 h.

Time [h]	1	2	4	6	16
10-KSA/(10-KSA+ 10-HSA)	0.17 ± 0.08	0.17 ± 0.01	0.24 ± 0.05	0.22 ± 0.03	0.31 ± 0.05

4 Discussion and Outlook

4.1 Novel OhyPp and its characteristics

In this study, a novel OH has been elucidated and characterized originating from *Pediococcus parvulus*. OhyPp also holds a monomeric structure just as OhyRe and is the second characterized enzyme of the HFam3 family. Monomeric proteins, such as OhyPp might have advantages in immobilization strategies as they don't consist of subunits, which can dissociate. It was postulated that the dimeric structure of other OHs from HFam11 arises from N- and C-terminal extensions, which OhyRe doesn't carry, just as OhyPp, further confirming this theory.

The optimal reaction parameters of OhyPp differ from OhyRe's despite their close sequence comparison. The enzyme holds an optimal reaction temperature at 18 °C despite its bacteria's optimal growth being at 30 °C. Instead, OhyRe functions best at 28 °C consistent with *R. erythropolis* optimal growth temperature between 27 – 32 °C [87]. The slightly lower optimal reaction temperature might arise from the variance in overall stability since OhyPp has a lower melting temperature (45.0 ± 0.0 °C of OhyRe compared to 41.1 ± 0.2 °C of OhyPp). This was also observed during the conduction of the enzymatic assays with OhyPp, where white precipitates were occurring. These were not soluble in ethyl acetate thus indicating they were protein aggregates. OHs have a general issue with stability, as they are reported to quickly aggregate or lose function [16]. Since also many OHs are slow enzymes and full conversion often requires several hours [62,77], high stability over a long period is crucial. This needs to be addressed to ensure a stable industrial process by protein engineering means.

OhyPp's and OhyEm's stability was tested for an extended period at 4 °C and it could be observed that both enzymes were stable for at least 9 days. Consequently, the destabilization occurs mainly during the conversion, which potentially can be attributed to either the elevated temperature or effects from the substrate. Fatty acids have a soap-like character, particularly at elevated pH-values due to partial saponification [88,89] and this might lead to the destabilization and subsequent aggregation of proteins in general. Additionally, 10-HSA is a solid material and might lead to the precipitation of OH.

When comparing the two enzymes OhyPp and OhyEm, OhyEm showed particularly higher stability since it retained 80% of its initial activity after 27 days, whereas OhyPp only retained 20%. Consequently, the subunit dissociation is not the main factor for the loss of activity since OhyPp is monomeric, and most likely, the structural features of OHs contribute to the low stability. Studies, where mesophilic

enzymes were compared with thermophilic homologues, showed that the higher stability originates from many unique, small stabilizing interactions between single residues [90].

Increasing OH's stability is crucial since its aggregates further complicate downstream processing efforts. In another study (data not published), it could be observed that protein aggregates in lysates led to a massive decrease in the recovery rate of 10-HSA and oleic acid with ethyl acetate extraction. Consequently, large amounts of oleic acid and 10-HSA were interacting with the hydrophobic sites of aggregated proteins and were not extractable with an organic solvent. Furthermore, proteins can denature when being exposed to interfaces with high interfacial tension [91].

A solution might be a centrifugation step to precipitate converted 10-HSA, and the subsequent removal of the supernatant containing the remaining soluble protein prior to organic solvent extraction may drastically reduce the aggregation potential in future applications leading to higher yields.

However, potential solutions should also focus on the protein itself, which include the increase in turnover leading to a decrease in conversion time or finding or engineering OHs with elevated melting temperatures and stabilities to limit the aggregation potential during biocatalysis. Increased melting temperatures can be achieved using error-prone PCR and subsequent screening. This has, for instance, been performed with an esterase leading to more than 14 °C increased melting temperature [92]. Furthermore, site-directed mutagenesis was applied with the assistance of *in silico* tools such as FireProt or molecular dynamics. For instance, Cheng et al. used these tools to predict and engineer 10 sites in a nitrile hydratase leading to a 3.2 °C increase in melting temperature and a 2.1-fold increased activity [93].

So far, protein engineering efforts in OHs comprised mainly the expansion of the substrate spectrum and increased conversion efficiencies, but increased stability is crucial for an industrial application of OHs and thus might be a valuable target for future studies [94,95].

The saponification of fatty acids at elevated pH values might be one of the reasons, why most OHs have the lowest activity at pH values between 5 and 7 [43,51,61,62,65]. OhyPp for instance shows no activity at all at a pH of 7.5 and above [51]. OhyRe is an exception since its optimum is at 7.2 and there is still a 95 % residual activity at a pH of 8 [39]. The optimal temperature and pH are most likely also dependent on where each respective OH resides, which is still not fully understood and can either be within the cell, in extracellular vesicles or membrane associated [12,41,58].

Additionally, since some bacteria carry more than one OH, the varying characteristics and properties may complement their mode of action [60,61,63]. In future projects, an investigation of the localization of different OHs within one organism may reveal more on the function of OHs and their general place of action.

4.2 Structure and mechanism in HFam3 and HFam11

A variety of OHs have already been elucidated and their respective substrate specificity analyzed [18,39,41,57,61,63,64,96–98]. The majority of elucidated fatty acid hydratases can convert oleic acid and even use it as their main substrate, and a few have been found to be linoleate hydratases (LAH) [41,57,63,64]. Several fatty acid hydratases exhibit a lack of specificity regarding the length of the acyl chain. For example, OhyPp and OhyRe convert palmitoleic (16:1 (cis-9)), linoleic (18:2 (cis-9, 12)), and linolenic acid (18:3 (cis-9,12,15)) besides oleic acid, and OhyRe has recently been found to additionally convert longer carbon chains than oleic acid such as eicosenoic acid with one, two, three and four double bonds (20:1 (cis-11), 20:2 (cis-8,11), 20:3 (cis-8,11,14), 20:4 (cis-5,8,11,14)) and erucic acid (22:1 (cis-13)) [62]. This has evolutionary advantages since a large variety of occurring unsaturated long-chain fatty acids can be detoxified. Despite acting unspecifically for the type of substrate, OHs display a strong preference for specific stereoselectivity as they are known to be enantioselective for the 10-(R) isomer [99].

The variety of OHs is a chance to gain insights into mechanistic and functional properties, which can be particularly useful if, in addition to a sequence, a crystal structure is available. However, this has proven to be a difficult task, particularly including substrate, product, and FAD as cofactor [51]. So far, just a few crystal structures are available as shown in Table 1.

Table 1. List of available crystal structures of OHs including their enzyme name, originating organism, HFam-family, PDB ID and the corresponding reference. Table adapted from Zhang et al. [15].

Enzyme	organism	HFam	PDB ID	reference
LAH	*Lactobacillus acidophilus*	2	4ia5, 4ia6	[64]
OhyEm	*Elizabethkingia meningoseptica*	11	4uir	[65]
OhyRe	*Rhodococcus erythropolis*	3	5odo	[39]
OhySt	*Stenotrophomonas sp. KTCC 12332*	11	5z70	[40]
OhySa	*Staphylococcus aureus*	11	7kav, 7kaw, 7kax, 7kay	[66]

Amongst them is a linoleate hydratase of HFam2 and OHs with three members of the HFam11, and one of HFam3. The focus of this study was to investigate the FAD

binding properties in monomeric HFam3 members, which is why OhyPp was chosen as closest relative of OhyRe. The closer the relation between two enzymes, the easier it is to infer from the sequence to its function. However, in future studies, the focus should be laid on stability and structure elucidation using crystallization efforts. The crystallization success of proteins is associated with many factors such as adequate melting temperature, purity, and overall stability [51,100]. If these are not sufficient, means of protein engineering, creating truncations or co-crystallization might increase the chance of crystallization efforts [101,102]. Additionally, an HFam3 family member originating from a heat-resistant organism might also carry a more stable OH increasing the chance of crystallization success. In the hydratase database of Schmid et al. in the HFam3 family (https://hyed.biocatnet.de/hFam/3), no thermophile bacterium can be found, however, sequences from *Streptococci*, *Enterococci,* and *Staphylococci*, which often grow at elevated temperatures (38 – 45 °C) compared to *Rhodococcus erythropolis* und *Pediococcus parvulus* [87,103,104] . Three of these organisms that might be interesting for extracting and analyzing the respective OH are shown in **Table 2**.

Table 2. Putative OHs from HFam3 family extracted from the hyed database with the originating organism, growth temperature, and identifier possibly with higher stability and thermoresistance.

organism	Growth temp. of organism [°C]	Hyed identifier
Enterococcus faecium	42-45 [105]	S#1783
Staphylococcus epidermidis	30-37 [106]	S#1740
Streptococcus sobrinus	37 [107]	S#1742

A full structure including all relevant ligands for functioning is crucial for an understanding of HFam3 family members thus it will be necessary to apply these methods to achieve high-quality crystal structures.

Numerous hypotheses were put forward regarding the reaction mechanism of OHs. This can only be concluded from OhyEm including FAD, PEG as a fatty acid mimic [65] and from OhySa with a structure resolved with FAD, 10-HSA and oleic acid [66]. In both studies, a glutamic acid was suggested to be involved in the mode of action. For OhyEm, the mentioned glutamic acid (Glu122) and a tyrosine (Tyr241) were proposed to follow an acid base mechanism (compare **Fig. 6**). In Radka et al. [66], however, it was suggested that the corresponding glutamic acid (Glu82) stabilizes a hydronium ion, and that the tyrosine (Tyr201) stabilizes the 10-HSA hydroxy together with other amino acids.

This reaction mechanism can't easily be transferred to HFam3 members since they carry different amino acids at suggested positions. The glutamic acid in HFam11

members is equivalent to a methionine in HFam3 members such as OhyPp (Met72) or OhyRe (Met77) and since the HFam11 glutamic acid acts through stabilization with its side chains, HFam3 methionine aren't able to carry out the same ionic interactions (see **Fig. 6**). Consequently, the reaction mechanism of HFam3 is either different than of HFam11 or the mechanism in all OHs is carried out differently than suggested.

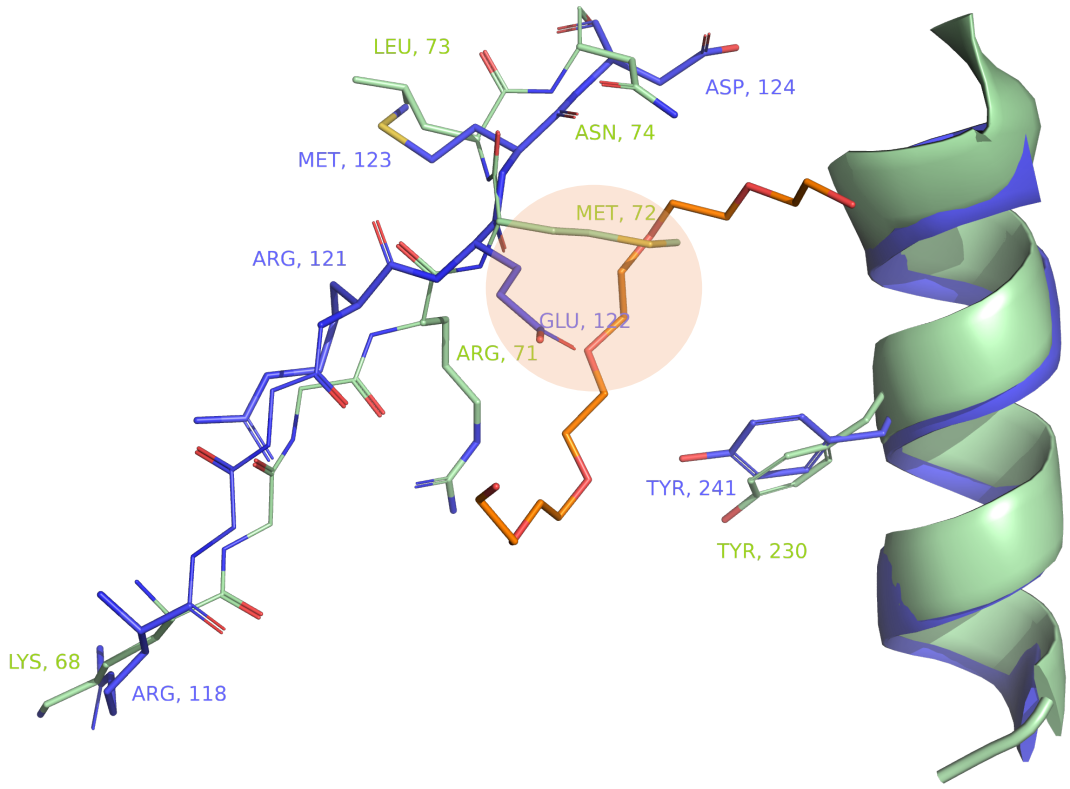

Fig. 6 Superposition of the putative active sites of OhyPp and OhyEm in stick representation. Highlighted in orange are the residues M72 (OhyPp) and E122 (OhyEm) subjected to mutagenesis. (A) Residues of OhyPp are shown as green sticks and residues of OhyEm in blue. Atoms are colored by the following scheme: red: oxygen, yellow: sulfur, backbone color: nitrogen and carbon. Shown in orange in stick representation is PEG, a potential placeholder for oleic acid/10-HSA. Structure of OhyEm originates from its crystal structure elucidation in Engleder et al. [65], whereas OhyPp has been modeled with the Robetta algorithm. Secondary structures were aligned.

Using sequence alignment comparisons, a region was found to be strongly conserved in OHs and it also was found in two other fatty acid converting enzymes, namely a hydroxylase [23] from *Ricinus communis* and a FAD2 fatty acid desaturase from *Arabidopsis thaliana* [108]. This region consists of the residues "GGRM", whereas the last

one is Met72 in OhyPp and Met77 in OhyRe being replaced by Glu122 in OhyEm and Glu82 in OhySa.

Oleate hydroxylases distinguish themselves from oleate hydratases in several ways. Firstly, they are membrane-bound enzymes that specifically convert fatty acids esterified to phosphatidylcholine [23]. Their catalytic activity relies on the presence of NADH and cytochrome b5 as cofactors. Moreover, the reaction mechanism involves a charge-transfer reaction, classifying hydroxylases as oxidoreductases. These hydroxylases possess a μ-oxo-bridged diiron cluster, which makes them reliant on oxygen and iron [109]. Although there are notable distinctions between these two types of enzymes responsible for fatty acid conversion, they share a common GGR motif. This motif displays a certain degree of evolutionary significance, potentially contributing to fatty acid or cofactor interactions or overall enzymatic activity.

Moreover, in that precise location, the region also features a methionine, a common characteristic shared by HFam3 members, while HFam11 members carry a glutamic acid, which is believed to play a pivotal role in catalysis. The differences between hydroxylases, desaturases and OHs by simultaneously sharing this motive, serve as additional hints to conclude that this residue probably is not involved in the reaction mechanism of OHs and that it might be different than suggested. Instead, it is more likely that the motive is involved in cofactor or fatty acid binding.

Until now, comprehending the reaction mechanism of HFam3 members including OhyPp based on the existing OhyRe crystal structure has proven challenging due to several reasons. Firstly, the depiction of the OhyRe's crystal structure is in its apo-state, as observed by water molecules within the inner cavity, where FAD is expected to reside, which normally is expected to displace these water molecules [66].

Additionally, FAD binding leads to a conformational change in an OhyEm region residing close to the reaction cavity, which contains the suggested active residues (R_{118}GGREM) as observed by a decrease in flexibility when FAD is bound [65]. This might also be the case for OhyRe and OhyPp and the rearrangements may lead to different positioning of residues within the reaction cavity. As a result, making predictions about reaction mechanisms based on the currently available information is challenging. This and a missing region in the crystal structure of OhyRe might furthermore be the reasons why *in silico* docking attempts were unsuccessful.

As already mentioned, the position of FAD in HFam3 can only be predicted based on OhyEm via structural alignments since the binding of FAD is highly conserved [110], suggesting a strong likelihood of similarity in FAD binding among members of the HFam3 and HFam11 protein families.

There is another striking difference in the sequence between HFam3 and HFam11 members. A region in OhySa was termed FAD lid by Radka et al. [66] and is expected to cover the entrance of the FAD-cavity (K_{60}AGGSL[…]R_{81}). This area could not be modeled in OhyRe's crystal structure due to its high flexibility. In HFam3 members, this region consists of an additional extension which is a striking difference compared to HFam11 members (compare to **Fig. 7**). HFam3 members have the disadvantage of a low affinity towards FAD, which is one of the main challenges to be tackled for a successful industrial application.

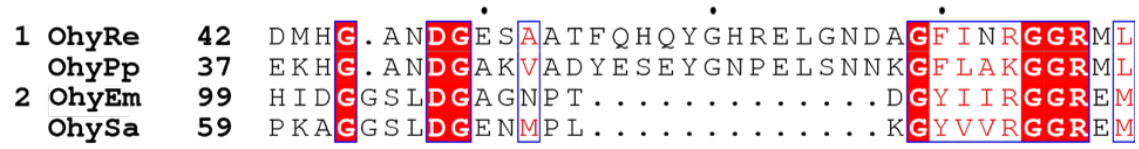

Fig. 7 Alignment between two members of the Hfam3 (OhyRe and OhyPp) and Hfam11 (OhyEm and OhySa) family using the Cobalt constraint alignment tool [111] and ESPript from the Endscript-server was used for visualization (https://espript.ibcp.fr) [112]. Red box, white character represents strict identity. Red character represents similarity in a group and a blue frame represents similarity across groups. There is a long insertion sequence visible in Hfam3 family enzymes starting at F_{55} in OhyRe, which does not occur in Hfam11 family members.

The affinity of FAD towards OhyRe, OhyPp, and OhyEm was measured and it could be observed that OhyEm holds a 200- and 500-fold higher affinity, respectively, towards the cofactor. OhyPp has a 50-fold higher affinity towards FAD compared to OhyRe. Since the extended flexible loop in HFam3 members is in close proximity to the FAD binding cleft and predicted to cover the FAD entrance in OhySa, this might be an explanation for the low binding affinity of HFam3 family members.

In future experiments, mutations within the loop or shortenings could provide valuable clues about which residues are engaged in FAD binding or which structural changes occur that contribute to the increased FAD affinity observed in OhyPp.

4.3 Stability of OhyPp and OhyEm

Finally, it is essential to address the overall stability of OHs to ensure their long-lasting integrity throughout a potential industrial process. Maintaining stability is crucial for maximizing the efficiency and reliability of OHs in industrial applications. So far, the dimeric dissociation applying mostly to HFam11 members, due to their dimeric nature, was suspected to be largely contributing to a loss of activity throughout process time [72]. However, OhyPp loses its activity much faster compared to OhyEm at 4 °C thus indicating that not the dimeric nature is responsible but rather the overall sequence and structure. More heat-stable enzymes have already been suggested here to increase the chance of crystallization efforts, however, they might additionally hold higher overall stability to ensure optimal process integrity for later application purposes. Furthermore,

certain types of oils with a high amount of saturated fatty acids only liquify at elevated temperatures, where liquefaction is crucial for substrate access and, thus conversion efficiency of OHs.

4.4 Cascade reactions with OhyRe, lipase and secADH

Additionally, a combined approach of OhyRe, a lipase and a secondary alcohol dehydrogenase was applied to increase the product spectrum by conducting a one-pot conversion with reduced processing steps and to additionally optimize the reaction for potential screening applications.

Numerous OHs with different properties have already been documented and studied [15,16,39,51,62]. Nevertheless, monomeric OHs offer the most promising potential for industrial use due to their ability to exclude subunit dissociation and to facilitate simpler adoption of immobilization strategies [39,67]. Hence, this study explored the application of OhyRe for the cascading reaction system, which represents the first known member of monomeric OHs.

As already mentioned, many OHs are slow enzymes, however, to a varying degree. For instance, in Busch et al. [62], reactions were conducted for 6 days. OhyPp has a half time of 3.7 h and maximum conversion was observed after 24 h [51]. For the planned cascade reaction, however, it was necessary to maximize OhyRe's yield and tackle the slow conversion.

4.5 Broadband white light enhances OhyRe's activity

Engleder et al. [65], described that a reducing environment led to an increase in k_{cat} by a factor of 6 to 7, concluding that effectively $FADH_2$ is the responsible cofactor as opposed to FAD. The cytoplasm comprises a reducing environment, which is strong enough to reduce FAD, even though within the cell, both species - reduced and oxidized FAD - occur [113–115]. The oxidizing environment upon cell lysis and during the conduction of the conversion assays leading to the oxidation of FAD was considered to be the reason for the observed slow conversion of OHs.

The reduction of FAD on a laboratory scale, on the other hand, is elaborate. For instance, photoreduction was described with 10 mM EDTA under anaerobic conditions and using white light [116]. Especially for OHs, Engleder et al. [65] used either photoreduction after adding 5 mM EDTA, 1 µM 5-deazariboflavin and 4 µM methyl viologen or chemical means with DTT, both under anaerobic conditions. Another group applied a cascade with glucose oxidase, FAD oxidoreductase and titanium citrate to reduce FAD for efficient oleic acid conversion [68].

To maximize the yield of OHs for the application of planned cascade reactions, a more rapid method to reduce FAD to $FADH_2$ would be required without maintaining an anaerobic environment. It was observed that white light had an effect on the OH activity even under aerobic conditions, and further experiments revealed that particularly blue light (425 nm) was responsible for the increase in activity.

Blue light is recognized as an activator for blue-light photoreceptors [117,118] and leads to changes in the redox state of FAD [119,120] by creating reduced species. Blue-light photoreceptors have functional roles in bacteria, plants, and animals, such as maintaining a circadian rhythm and for light-connected responses such as phototropism. It may be interesting to investigate whether blue light also has an effect on OHs within a cellular environment and, thus, whether its sensing has a functional aspect. For now, the blue light most likely leads to the partial reduction of FAD to $FADH_2$, which is the responsible species in OH conversion.

Additional experiments connected to light and $FADH_2$ on OH will help to gain more insights into their effects. For instance, it would be interesting to analyze the affinity of $FADH_2$ on OHs as compared to FAD, however, this can only be achieved under full reducing conditions. This is rather challenging since photobleaching can lead to partial photodegradation of FAD [121] and chemicals like DTT or titan citrate might have effects on the structure and binding site of the protein, which may impair the affinity measurements. The photodegradation of FAD most likely could also be observed in this study, where the activity at the highest tested light intensity at 486 µmol/m^2*s is reduced compared to the one at 364 µmol/m^2*s.

Furthermore, it might be interesting to analyze, which residues are interacting with FAD and whether structural changes occur within the protein upon light exposure or upon binding of $FADH_2$ instead of FAD.

4.6 OhyRe and lipase show highest 10-HSA yield for microbial oil

Since OH's only substrates are free fatty acids as opposed to protected ones for instance in the form of esters, a prior hydrolysis step of triglyceride oils into free fatty acids is crucial. This can be accomplished by using a lipase, which acts at the interface of the aqueous phase-oil bilayer [91]. This is rather challenging since OHs only convert their substrates when they are emulsified in the buffer. Since lipases show a low but still measurable decrease in conversion [91], the emulsification of triglyceride oil with buffer was applied for this study. Reasons for low conversion of OHs when the substrate is not emulsified with buffer might be either due to low substrate access of OHs or due to their denaturation as exposure to high interfacial tensions [91].

Thus, additional optimizations can be implemented to address the tradeoffs associated with the two different specifications of lipases and OHs when it comes to oil emulsification. One way to accomplish this is by examining the impact of surfactants or employing a two-step conversion process that involves an intermediate step of emulsification, as an example.

Even though the oil was emulsified with buffer, which is non-optimal for lipases, a range of 6-35% of oleic acid could be converted to 10-HSA when combining lipase and OH. This was, however, largely dependent on the used type of oil.

The highest conversion per oleic acid content was observed for oil from *C. oleaginosus*, and the lowest for linseed oil. The increase in yield is surprisingly alongside a decrease in oleic acid concentration. An explanation may be a substrate inhibition of OH. Linseed oil thereby is an exception since it showed the lowest yield of 10-HSA by also containing the lowest amounts of oleic acid. However, linseed oil consists of 15% linoleic and 54% linolenic acid. The latter two can be converted by many OHs as well, albeit to low extend, thus concluding that these unwanted side reactions might be responsible for the low yield of 10-HSA with linseed oil as substrate due to blocking of the active site. However, lipases also have varying substrate specificities [122–124] thus another explanation might be that the variance in yield is originating from the lipase rather than from OHs. This can be tested by analyzing the lipase conversion efficiency by measuring the amounts of free fatty acids compared to remaining mono-, di- and triacylglycerides. Also, rapeseed, olive, and linseed oil are not highly processed and their remaining contaminants may influence OH's and lipase's activity.

A recent study utilized the CRISPR/Cas system to create a knockout of the Δ12 Desaturase gene in *C. oleaginosus* [32]. This genetic modification resulted in an elevated concentration of oleic acid and the complete absence of polyunsaturated fatty acids in the oil produced, which has the potential to improve the overall yield of 10-HSA production by eliminating the undesired side reactions associated with the conversion of linoleic and linolenic acid. In particular, the mutant with a knockout of its ∆12-desaturase exhibited 64% oleic acid $w/w_{\text{total fatty acids}}$ instead of 52% in wild-type by simultaneously showing a total absence of C18:2 and C18:3. Additionally, the application of 10-HSA is of technical nature, indicating that utilizing oil derived from genetically modified organisms may be no regulatory obstacle. The conversion yield of lipase and OHs using this type of oil may be of interest to evaluate the effect of the heightened oleic acid concentration by a simultaneous absence of polyunsaturated fatty acids.

To summarize, oil from *C. oleaginosus* showed with 35% (10-HSA/(10-HSA+oleic acid)) the highest conversion of oleic acid to 10-HSA, thereby providing an initial proof of principle paving the way for further optimizations for a successful future application.

4.7 Characterization of a novel secADH

Next, a novel secondary alcohol dehydrogenase was applied to convert 10-HSA into its oxidized analog 10-keto stearic acid (10-KSA), which can serve as a precursor for further valuable molecules, as depicted in **Fig. 5**. In addition to its potential for large-scale production in downstream reactions, this promising fine chemical can also be utilized for high throughput screening purposes.

An ADH from *Deinococcus radioruans* was successfully identified (NCBI Reference Sequence: WP_027479748.1), which is an extremophile organism known for its superior properties in terms of pH and temperature ranges, as well as overall durability and stability [85].

The substrate specificity test of the ADH revealed that it prefers secondary alcohols and neither converts primary nor tertiary alcohols. Furthermore, it prefers long carbon chain alcohols as opposed to short ones and it can convert 10- and 12-HSA, which proves that it can be applied for the cascade with OH.

To further maximize the output signal of the reactions, the optimal reaction conditions of the secADH and the cascades had to be investigated. It could be shown that secADH has two pH optima, one at 7 and one 9.5, and a broad temperature range with 18 °C being the optimum. In combination with OHs, the optima change depending on which type of OH used. With OhyRe, the optimum is at 6.5, close to OhyRe's optimum, which is rather surprising since OhyRe and secADH show high activity in rather basic environments. In combination with OhyEm, two pH optima occur, one at 7.5 one at around 9, which are rather similar to secADH's. The temperature optimum changes to 26 °C for the combination with OhyRe and to 20 °C with OhyPp. It was observed that OhyEm is a faster enzyme compared to OhyRe (own analysis, data not shown) and OhyPp, thus OhyEm might be less rate limiting in a cascade reaction leading to secADH dictating the optimal conditions. This can be further investigated by applying more OHs with varying reaction conditions.

In summary, the optimal conditions depend on the OH used and on the combination and they need to be investigated for each OH individually.

Furthermore, the stability of secADH in form of melting temperatures was investigated. The melting temperatures depend on the pH applied and in general decrease with increasing pH. This effect was more profound with 12-HSA as a substrate,

consequently 12-HSA is most likely destabilizing secADH. And indeed, at a pH of 9, which is the optimum for secADH, there was nearly no effect on the melting temperature with 2-pentanol and 3-pentanol as substrates, but when 12-HSA was added, there was a strong decrease in melting temperature from 53.43 ± 0.54 to 47.00 ± 0.87 °C. Under basic conditions, fatty acids form mixtures of acid and soap leading to crystalline solids, which might affect secADH's stability.

4.8 Optimization of OhyRe and secADH cascade reaction

To further enhance the coupled assay, the effect of additives was tested. It is known that OHs benefit strongly from surfactants. In the form of whole-cell catalysts, surfactants lead to a higher dispersion of substrates and cell permeability, resulting in increased conversion yield [125]. In many other studies, Tween 80 or ethanol were used as surfactants to enhance isolated OH's activity [68,84,95,96,126].

Indeed, testing varying Tween 80 concentrations on the conversion of OhyRe showed an increase of activity up to 10% [v/v], thereby adjusting to a plateau. Instead, when Tween 80 was applied in the OH and secADH cascade reaction, small concentrations already led to a drastic decrease in activity. One of the challenges of applying this cascade reaction in high-throughput screenings, though, is the low solubility of oleic acid in water or aqueous buffers. High-throughput screenings serve the purpose of optimizing OHs to achieve higher conversion rates in a shorter time, higher ligand affinity, or increased stability and melting temperatures. Even when oleic acid is emulsified before being added to the reaction, local micellar structures can form over time or attach to vessel walls, resulting in a reduction of accessible substrate. A surfactant increases the overall stability of fatty acid-based molecules in aqueous solutions. Consequently, additives, which don't reduce the activity are already a great asset if applicable. Since 1,5-pentanediol led to the highest increase comprising 1.4-fold compared to no additive, this surfactant will aid in future applications in high-throughput assays or in other applications, where a more stable fatty-acid/water emulsion is needed.

Next, the improvements in activity using broadband white light with OhyRe were applied to the cascade-reaction. 10-HSA was the main species amongst the products and its concentration strongly reacted to the varying light intensities as observed by a 30-fold increase, where a 40-fold increase was observed for OhyRe alone. The optimum here is rather distinct as opposed to the reaction with OhyRe alone with a rather broad range. However, also the 10-KSA concentration benefited from the light-dependent activation of OhyRe since an increase of 14-fold was observed. As a result, the cascade reaction experiences significant advantages when activated by broadband white light.

It was observed that a high concentration of secADH in the cascade reaction led to a decrease in product yield. SecADH's and OhyRe's concentrations were increased, respectively, by simultaneously keeping the concentration of one player constant. For OhyRe, a saturation curve was observed, whereas on the other hand, the increase of secADH resulted in a substrate inhibition curve and an 18-fold lower half maximum concentration. One possible explanation for this observation could be the increase in 10-KSA level with higher concentrations of secADH. It is likely that 10-KSA binds to OhyRe but cannot undergo conversion, thereby inhibiting the activity of OhyRe. Furthermore, 10-KSA might inhibit secADH or a back reaction may occur with increasing secADH concentration. To confirm this hypothesis, the isolation and purification of 10-KSA can be carried out, followed by a detailed analysis of its inhibitory potential on OhyRe. This experiment will provide valuable insights into the inhibitory effects of 10-KSA and its role in the observed reduction of OhyRe activity in the presence of increasing secADH concentrations.

Lastly, the optimized reaction parameters were applied in a long-time conversion of oleic acid to 10-KSA. Even though the light activation led to an increase in 10-KSA of 14-fold, it still is the minor species within the products. Indeed, the observed results could be indicative of suboptimal conditions for secADH. For instance, Wu et al. [127] used a two-step approach with *M. luteus* secADH, which also has its optimum at a pH of 11 . For that, after 8 h of the OH conversion step, the reaction was adjusted to a pH of 8 and the secADH step was applied. This resulted in a 95% conversion of 10-HSA to 10-KSA. Consequently, a two-step one-pot conversion leads to higher yield in the case of large-scale 10-KSA production.

4.9 Concluding remarks

In conclusion, while the crystallization of the novel OhyPp didn't provide direct structural insights, its identification as the second confirmed member of the HFam3 family holds significant promise. Through a thoughtful comparison of its sequence with that of OhyRe and HFam11 members, we have garnered valuable information that contributes to our growing understanding of this protein family.

The difference in FAD affinity gives valuable information about the different cofactor binding characteristics in the two families and this might pave the way for future protein engineering strategies for the understanding and improvement of FAD binding.

Furthermore, a combined approach using OhyRe, a lipase, and a secondary alcohol dehydrogenase was explored to expand the product range and streamline the conversion process. Monomeric OHs were identified as the most promising enzymes for

industrial use due to their simplified immobilization strategies. The slow conversion rates of OHs were addressed by maximizing OhyRe's yield and investigating the effects of reducing agents and light activation. The substrate specificity of the secondary alcohol dehydrogenase from *Deinococcus radiodurans* was examined and the reaction conditions for the cascade reaction optimized. The addition of surfactants and the use of white light were found to enhance the overall activity of OhyRe and the cascade. The study demonstrated promising results for the conversion of oleic acid to valuable molecules, such as 10-HSA and 10-KSA, laying the foundation for further optimizations and potential applications in high-throughput screenings and sustainable large-scale production.

5 List of Publications

Prem, S.A.; Haack, M.; Melcher, F.; Ringel, M.; Garbe, D.; Brück, T. Two Cascade Reactions with Oleate Hydratases for the Sustainable Biosynthesis of Fatty Acid-Derived Fine Chemicals. *Catalysts* **2023**, *13*.

Prem, S.A.; Helmer, C.P.O.; Loll, B.; Garbe, D.; Brück, T. Expanding the Portfolio by a Novel Monomeric Oleate Hydratase from Pediococcus Parvulus. ChemCatChem 2023, e202300478, doi:10.1002/cctc.202300478.

Prem, S., Helmer, C.P.O., Dimos, N., Himpich, S., Brück, T., Garbe, D., Loll, B., 2022. Towards an understanding of oleate hydratases and their application in industrial processes. Microb. Cell Fact. 21, 1–15. https://doi.org/10.1186/s12934-022-01777-6

Shaigani, P., Fuchs, T., Graban, P., **Prem, S**., Haack, M., Masri, M., Mehlmer, N., Brueck, T., 2023. Mastering targeted genome engineering of GC-rich oleaginous yeast for tailored plant oil alternatives for the food and chemical sector. Microb. Cell Fact. 22, 1–14. https://doi.org/10.1186/s12934-023-02033-1

Fuchs, T., Melcher, F., Rerop, Z.S., Lorenzen, J., Shaigani, P., Awad, D., Haack, M., **Prem, S**.A., Masri, M., Mehlmer, N., Brueck, T.B., 2021. Identifying carbohydrate-active enzymes of Cutaneotrichosporon oleaginosus using systems biology. Microb. Cell Fact. 20, 1–18. https://doi.org/10.1186/s12934-021-01692-2

6 Reprint Permissions

Copyright and Licensing

For all articles published in MDPI journals, copyright is retained by the authors. Articles are licensed under an open access Creative Commons CC BY 4.0 license, meaning that anyone may download and read the paper for free. In addition, the article may be reused and quoted provided that the original published version is cited. These conditions allow for maximum use and exposure of the work, while ensuring that the authors receive proper credit.

In exceptional circumstances articles may be licensed differently. If you have specific condition (such as one linked to funding) that does not allow this license, please mention this to the editorial office of the journal at submission. Exceptions will be granted at the discretion of the publisher.

Reproducing Published Material from other Publishers

It is absolutely essential that authors obtain permission to reproduce any published material (figures, schemes, tables or any extract of a text) which does not fall into the public domain, or for which they do not hold the copyright. Permission should be requested by the authors from the copyright holder (usually the Publisher, please refer to the imprint of the individual publications to identify the copyright holder).

Permission **is required** for:

1. Your own works published by other Publishers and for which you did not retain copyright.
2. Substantial extracts from anyone's works or a series of works.
3. Use of Tables, Graphs, Charts, Schemes and Artworks if they are unaltered or slightly modified.
4. Photographs for which you do not hold copyright.

Permission **is not required** for:

1. Reconstruction of your *own* table with data already published elsewhere. Please notice that in this case you must cite the source of the data in the form of either "Data from..." or "Adapted from...".
2. Reasonably short quotes are considered *fair use* and therefore do not require permission.
3. Graphs, Charts, Schemes and Artworks that are completely redrawn by the authors and significantly changed beyond recognition do not require permission.

JOHN WILEY AND SONS LICENSE
TERMS AND CONDITIONS

Aug 03, 2023

This Agreement between Technische Universitaet Muenchen -- Sophia Prem ("You") and John Wiley and Sons ("John Wiley and Sons") consists of your license details and the terms and conditions provided by John Wiley and Sons and Copyright Clearance Center.

License Number	5601260137072
License date	Aug 03, 2023
Licensed Content Publisher	John Wiley and Sons
Licensed Content Publication	ChemCatChem
Licensed Content Title	Expanding the Portfolio by a Novel Monomeric Oleate Hydratase from Pediococcus parvulus
Licensed Content Author	Sophia A. Prem, Carl P. O. Helmer, Bernhard Loll, et al
Licensed Content Date	Jun 22, 2023
Licensed Content Volume	0
Licensed Content Issue	0
Licensed Content Pages	10
Type of use	Dissertation/Thesis

Requestor type	Author of this Wiley article
Format	Print and electronic
Portion	Full article
Will you be translating?	No
Title	Sustainable biosynthesis of fatty-acid derived molecules of industrial interest using oleate hydratases
Institution name	Technische Universitaet Muenchen
Expected presentation date	Nov 2023
Order reference number	SP12345
Requestor Location	Technische Universitaet Muenchen Lichtenbergstr. 4 Garching, 85748 Germany Attn: Technische Universitaet Muenchen
Publisher Tax ID	EU826007151
Total	0.00 EUR

Terms and Conditions

TERMS AND CONDITIONS

This copyrighted material is owned by or exclusively licensed to John Wiley & Sons, Inc. or one of its group companies (each a"Wiley Company") or handled on behalf of a society with which a Wiley Company has exclusive publishing rights in relation to a particular work (collectively "WILEY"). By clicking "accept" in connection with completing this licensing

transaction, you agree that the following terms and conditions apply to this transaction (along with the billing and payment terms and conditions established by the Copyright Clearance Center Inc., ("CCC's Billing and Payment terms and conditions"), at the time that you opened your RightsLink account (these are available at any time at http://myaccount.copyright.com).

Terms and Conditions

- The materials you have requested permission to reproduce or reuse (the "Wiley Materials") are protected by copyright.

- You are hereby granted a personal, non-exclusive, non-sub licensable (on a stand-alone basis), non-transferable, worldwide, limited license to reproduce the Wiley Materials for the purpose specified in the licensing process. This license, **and any CONTENT (PDF or image file) purchased as part of your order,** is for a one-time use only and limited to any maximum distribution number specified in the license. The first instance of republication or reuse granted by this license must be completed within two years of the date of the grant of this license (although copies prepared before the end date may be distributed thereafter). The Wiley Materials shall not be used in any other manner or for any other purpose, beyond what is granted in the license. Permission is granted subject to an appropriate acknowledgement given to the author, title of the material/book/journal and the publisher. You shall also duplicate the copyright notice that appears in the Wiley publication in your use of the Wiley Material. Permission is also granted on the understanding that nowhere in the text is a previously published source acknowledged for all or part of this Wiley Material. Any third party content is expressly excluded from this permission.

- With respect to the Wiley Materials, all rights are reserved. Except as expressly granted by the terms of the license, no part of the Wiley Materials may be copied, modified, adapted (except for minor reformatting required by the new Publication), translated, reproduced, transferred or distributed, in any form or by any means, and no derivative works may be made based on the Wiley Materials without the prior permission of the respective copyright owner.**For STM Signatory Publishers clearing permission under the terms of the STM Permissions Guidelines only, the terms of the license are extended to include subsequent editions and for editions in other languages, provided such editions are for the work as a whole in situ and does not involve the separate exploitation of the permitted figures or extracts,** You may not alter, remove or suppress in any manner any copyright, trademark or other notices displayed by the Wiley Materials. You may not license, rent, sell, loan, lease, pledge, offer as security, transfer or assign the Wiley Materials on a stand-alone basis, or any of the rights granted to you hereunder to any other person.

- The Wiley Materials and all of the intellectual property rights therein shall at all times remain the exclusive property of John Wiley & Sons Inc, the Wiley Companies, or their respective licensors, and your interest therein is only that of having possession of and the right to reproduce the Wiley Materials pursuant to Section 2 herein during the continuance of this Agreement. You agree that you own no right, title or interest in or to the Wiley Materials or any of the intellectual property rights therein. You shall have

no rights hereunder other than the license as provided for above in Section 2. No right, license or interest to any trademark, trade name, service mark or other branding ("Marks") of WILEY or its licensors is granted hereunder, and you agree that you shall not assert any such right, license or interest with respect thereto

- NEITHER WILEY NOR ITS LICENSORS MAKES ANY WARRANTY OR REPRESENTATION OF ANY KIND TO YOU OR ANY THIRD PARTY, EXPRESS, IMPLIED OR STATUTORY, WITH RESPECT TO THE MATERIALS OR THE ACCURACY OF ANY INFORMATION CONTAINED IN THE MATERIALS, INCLUDING, WITHOUT LIMITATION, ANY IMPLIED WARRANTY OF MERCHANTABILITY, ACCURACY, SATISFACTORY QUALITY, FITNESS FOR A PARTICULAR PURPOSE, USABILITY, INTEGRATION OR NON-INFRINGEMENT AND ALL SUCH WARRANTIES ARE HEREBY EXCLUDED BY WILEY AND ITS LICENSORS AND WAIVED BY YOU.

- WILEY shall have the right to terminate this Agreement immediately upon breach of this Agreement by you.

- You shall indemnify, defend and hold harmless WILEY, its Licensors and their respective directors, officers, agents and employees, from and against any actual or threatened claims, demands, causes of action or proceedings arising from any breach of this Agreement by you.

- IN NO EVENT SHALL WILEY OR ITS LICENSORS BE LIABLE TO YOU OR ANY OTHER PARTY OR ANY OTHER PERSON OR ENTITY FOR ANY SPECIAL, CONSEQUENTIAL, INCIDENTAL, INDIRECT, EXEMPLARY OR PUNITIVE DAMAGES, HOWEVER CAUSED, ARISING OUT OF OR IN CONNECTION WITH THE DOWNLOADING, PROVISIONING, VIEWING OR USE OF THE MATERIALS REGARDLESS OF THE FORM OF ACTION, WHETHER FOR BREACH OF CONTRACT, BREACH OF WARRANTY, TORT, NEGLIGENCE, INFRINGEMENT OR OTHERWISE (INCLUDING, WITHOUT LIMITATION, DAMAGES BASED ON LOSS OF PROFITS, DATA, FILES, USE, BUSINESS OPPORTUNITY OR CLAIMS OF THIRD PARTIES), AND WHETHER OR NOT THE PARTY HAS BEEN ADVISED OF THE POSSIBILITY OF SUCH DAMAGES. THIS LIMITATION SHALL APPLY NOTWITHSTANDING ANY FAILURE OF ESSENTIAL PURPOSE OF ANY LIMITED REMEDY PROVIDED HEREIN.

- Should any provision of this Agreement be held by a court of competent jurisdiction to be illegal, invalid, or unenforceable, that provision shall be deemed amended to achieve as nearly as possible the same economic effect as the original provision, and the legality, validity and enforceability of the remaining provisions of this Agreement shall not be affected or impaired thereby.

- The failure of either party to enforce any term or condition of this Agreement shall not constitute a waiver of either party's right to enforce each and every term and condition of this Agreement. No breach under this agreement shall be deemed waived or excused by either party unless such waiver or consent is in writing signed by the party

granting such waiver or consent. The waiver by or consent of a party to a breach of any provision of this Agreement shall not operate or be construed as a waiver of or consent to any other or subsequent breach by such other party.

- This Agreement may not be assigned (including by operation of law or otherwise) by you without WILEY's prior written consent.

- Any fee required for this permission shall be non-refundable after thirty (30) days from receipt by the CCC.

- These terms and conditions together with CCC's Billing and Payment terms and conditions (which are incorporated herein) form the entire agreement between you and WILEY concerning this licensing transaction and (in the absence of fraud) supersedes all prior agreements and representations of the parties, oral or written. This Agreement may not be amended except in writing signed by both parties. This Agreement shall be binding upon and inure to the benefit of the parties' successors, legal representatives, and authorized assigns.

- In the event of any conflict between your obligations established by these terms and conditions and those established by CCC's Billing and Payment terms and conditions, these terms and conditions shall prevail.

- WILEY expressly reserves all rights not specifically granted in the combination of (i) the license details provided by you and accepted in the course of this licensing transaction, (ii) these terms and conditions and (iii) CCC's Billing and Payment terms and conditions.

- This Agreement will be void if the Type of Use, Format, Circulation, or Requestor Type was misrepresented during the licensing process.

- This Agreement shall be governed by and construed in accordance with the laws of the State of New York, USA, without regards to such state's conflict of law rules. Any legal action, suit or proceeding arising out of or relating to these Terms and Conditions or the breach thereof shall be instituted in a court of competent jurisdiction in New York County in the State of New York in the United States of America and each party hereby consents and submits to the personal jurisdiction of such court, waives any objection to venue in such court and consents to service of process by registered or certified mail, return receipt requested, at the last known address of such party.

WILEY OPEN ACCESS TERMS AND CONDITIONS

Wiley Publishes Open Access Articles in fully Open Access Journals and in Subscription journals offering Online Open. Although most of the fully Open Access journals publish open access articles under the terms of the Creative Commons Attribution (CC BY) License only, the subscription journals and a few of the Open Access Journals offer a choice of Creative Commons Licenses. The license type is clearly identified on the article.

The Creative Commons Attribution License

The Creative Commons Attribution License (CC-BY) allows users to copy, distribute and transmit an article, adapt the article and make commercial use of the article. The CC-BY license permits commercial and non-

Creative Commons Attribution Non-Commercial License

The Creative Commons Attribution Non-Commercial (CC-BY-NC)License permits use, distribution and reproduction in any medium, provided the original work is properly cited and is not used for commercial purposes.(see below)

Creative Commons Attribution-Non-Commercial-NoDerivs License

The Creative Commons Attribution Non-Commercial-NoDerivs License (CC-BY-NC-ND) permits use, distribution and reproduction in any medium, provided the original work is properly cited, is not used for commercial purposes and no modifications or adaptations are made. (see below)

Use by commercial "for-profit" organizations

Use of Wiley Open Access articles for commercial, promotional, or marketing purposes requires further explicit permission from Wiley and will be subject to a fee.

Further details can be found on Wiley Online Library http://olabout.wiley.com/WileyCDA/Section/id-410895.html

Other Terms and Conditions:

v1.10 Last updated September 2015

Questions? customercare@copyright.com.

7 Figures and Tables

7.1 Figures

7.2 Tables

8 Literature

1. Hickel, J., O'Neill, D. W., Fanning, A. L. & Zoomkawala, H. National responsibility for ecological breakdown: a fair-shares assessment of resource use, 1970–2017. *Lancet Planet. Heal.* **6**, e342–e349 (2022).
2. International Resource Panel. Global Resources Outlook 2019: Summary for Policymakers. *United Nations Environ. Program.* 1–23 (2019).
3. Bagali, S. S. Optimization and Characterization of Castor Seed Oil Optimization and Characterization of Castor Seed Oil. *Leonardo J. Sci.* 59–70 (2016).
4. Akpan, U. G., Jimoh, A. & Mohammed, A. D. Extraction And Characterization Of Castor Seed Oil. *Internet J. Nutr. Wellness* **8**, 43–52 (2012).
5. Mubofu, E. B. Castor oil as a potential renewable resource for the production of functional materials. *Sustain. Chem. Process.* **4**, 1–12 (2016).
6. Soni, S. & Agarwal, M. Lubricants from renewable energy sources – a review. *Green Chem. Lett. Rev.* **7**, 359–382 (2014).
7. Bergfeld, W. F. *et al.* Safety Assessment of Hydroxystearic Acid as Used in Cosmetics. (2015).
8. Chauke, N. P., Mukaya, H. E. & Nkazi, D. B. Chemical modifications of castor oil: A review. *Sci. Prog.* **102**, 199–217 (2019).
9. Patel, V. R., Dumancas, G. G., Viswanath, L. C. K., Maples, R. & Subong, B. J. J. Castor oil: Properties, uses, and optimization of processing parameters in commercial production. *Lipid Insights* **9**, 1–12 (2016).
10. Borg, P., Lê, G., Lebrun, S. & Pées, B. Example of industrial valorisation of derivative products of Castor oil. *OCL - Ol. Corps Gras Lipides* **16**, 211–214 (2009).
11. Fameau, A. L. & Rogers, M. A. The curious case of 12-hydroxystearic acid — the Dr. Jekyll & Mr. Hyde of molecular gelators. *Curr. Opin. Colloid Interface Sci.* **45**, 68–82 (2020).
12. Prem, S. *et al.* Towards an understanding of oleate hydratases and their application in industrial processes. *Microb. Cell Fact.* **21**, 1–15 (2022).
13. Burrell, A. L., Evans, J. P. & De Kauwe, M. G. Anthropogenic climate change has driven over 5 million km2 of drylands towards desertification. *Nat. Commun.* **11**, 1–11 (2020).
14. Lorenzen, J. Enzymatic functionalization of bio based fatty acids and algae based triglycerides. (Technical University of Munich, 2019).
15. Zhang, Y., Eser, B. E., Kristensen, P. & Guo, Z. Fatty acid hydratase for value-added biotransformation: A review. *Chinese J. Chem. Eng.* **28**, 2051–2063 (2020).

16. Schmid, J. *et al.* Biocatalytic study of novel oleate hydratases. *J. Mol. Catal. B Enzym.* **133**, S243–S249 (2016).
17. Bevers, L. E., Pinkse, M. W. H., Verhaert, P. D. E. M. & Hagen, W. R. Oleate hydratase catalyzes the hydration of a nonactivated carbon-carbon bond. *J. Bacteriol.* **191**, 5010–5012 (2009).
18. Hirata, A. *et al.* A novel unsaturated fatty acid hydratase toward C16 to C22 fatty acids from Lactobacillus acidophilus. *J. Lipid Res.* **56**, 1340–1350 (2015).
19. Green, H. S. & Wang, S. C. Cis-vaccenic acid: New maker to detect seed oil adulteration in avocado oil. *Food Chem. Adv.* **1**, 1–5 (2022).
20. Nam, J. W. & Kappock, T. J. Cloning and transcriptional analysis of Crepis alpina fatty acid desaturases affecting the biosynthesis of crepenynic acid. *J. Exp. Bot.* **58**, 1421–1432 (2007).
21. Garba, L., Shukuri Mo, M., Nurbaya Os, S. & Noor Zalih, R. Review on Fatty Acid Desaturases and their Roles in Temperature Acclimatisation. *J. Appl. Sci.* **17**, 282–295 (2017).
22. Blacklock, B. J., Scheffler, B. E., Shepard, M. R., Jayasuriya, N. & Minto, R. E. Functional diversity in fungal fatty acid synthesis: The first acetylenase from the pacific golden chanterelle, cantharellus formosus. *J. Biol. Chem.* **285**, 28442–28449 (2010).
23. Van De Loo, F. J., Broun, P., Turner, S. & Somerville, C. An oleate 12-hydroxylase from Ricinus communis L. is a fatty acyl desaturase homolog. *Proc. Natl. Acad. Sci. U. S. A.* **92**, 6743–6747 (1995).
24. Sheldon, R. A. & Brady, D. Green Chemistry, Biocatalysis, and the Chemical Industry of the Future. *ChemSusChem* **15**, (2022).
25. Prem, S. A. *et al.* Two Cascade Reactions with Oleate Hydratases for the Sustainable Biosynthesis of Fatty Acid-Derived Fine Chemicals. *Catalysts* **13**, (2023).
26. Ochsenreither, K., Glück, C., Stressler, T., Fischer, L. & Syldatk, C. Production strategies and applications of microbial single cell oils. *Front. Microbiol.* **7**, (2016).
27. Masri, M. A., Garbe, D., Mehlmer, N. & Brück, T. B. A sustainable, high-performance process for the economic production of waste-free microbial oils that can replace plant-based equivalents. *Energy Environ. Sci.* **12**, 2717–2732 (2019).
28. Pinzi, S., Leiva-Candia, D., López-García, I., Redel-Macías, M. D. & Dorado, M. P. Latest trends in feedstocks for biodiesel production. *Biofuels, Bioprod. Biorefining* **8**, 126–143 (2014).
29. Chi, Z., Zheng, Y., Ma, J. & Chen, S. Oleaginous yeast Cryptococcus curvatus

culture with dark fermentation hydrogen production effluent as feedstock for microbial lipid production. *Int. J. Hydrogen Energy* **36**, 9542–9550 (2011).

30. Awad, D., Bohnen, F., Mehlmer, N. & Brueck, T. Multi-factorial-guided media optimization for enhanced biomass and lipid formation by the oleaginous yeast Cutaneotrichosporon oleaginosus. *Front. Bioeng. Biotechnol.* **7**, (2019).
31. Shaigani, P. *et al.* Oleaginous yeasts- substrate preference and lipid productivity: a view on the performance of microbial lipid producers. *Microb. Cell Fact.* **20**, 1–18 (2021).
32. Shaigani, P. *et al.* Mastering targeted genome engineering of GC-rich oleaginous yeast for tailored plant oil alternatives for the food and chemical sector. *Microb. Cell Fact.* **22**, 1–14 (2023).
33. T., J. A., Webb, J. P. & Kellock, T. D. The occurrence of unusual fatty acids in faecal lipids from human beings with normal and abnormal fat absorption. *Biochem. J.* **78**, 333–339 (1961).
34. Wallen, L. L., Benedict, R. G. & Jackson, R. W. The microbiological production of 10-Hydroxystearic acid from oleic acid. *Arch. Biochem. Biophys.* **99**, 249–253 (1962).
35. Thomas, P. J. Identification of Some Enteric Bacteria Which Convert Oleic Acid to Hydroxystearic Acid in Vitro. *Gastroenterology* **62**, 430–435 (1972).
36. Hudson, J. A., MacKenzie, C. A. M. & Joblin, K. N. Conversion of oleic acid to 10-hydroxystearic acid by two species of ruminal bacteria. *Appl. Microbiol. Biotechnol.* **44**, 1–6 (1995).
37. Koritala, S., Hou, C. T., Hesseltine, C. W. & Bagby, M. O. Microbial conversion of oleic acid to 10-hydroxystearic acid. *Appl. Microbiol. Biotechnol.* **32**, 299–304 (1989).
38. Bevers, L. E., Pinkse, M. W. H., Verhaert, P. D. E. M. & Hagen, W. R. Oleate hydratase catalyzes the hydration of a nonactivated carbon-carbon bond. *J. Bacteriol.* **191**, 5010–5012 (2009).
39. Lorenzen, J. *et al.* Rhodococcus erythropolis Oleate Hydratase: a New Member in the Oleate Hydratase Family Tree—Biochemical and Structural Studies. *ChemCatChem* **10**, 407–414 (2018).
40. Park, A. K. *et al.* Crystal structure of oleate hydratase from Stenotrophomonas sp. KCTC 12332 reveals conformational plasticity surrounding the FAD binding site. *Biochem. Biophys. Res. Commun.* **499**, 772–776 (2018).
41. Ortega-Anaya, J. & Hernández-Santoyo, A. Functional characterization of a fatty acid double-bond hydratase from Lactobacillus plantarum and its interaction with

biosynthetic membranes. *Biochim. Biophys. Acta - Biomembr.* **1848**, 3166–3174 (2015).

42. Tan, Y. S., Zhang, R. K., Liu, Z. H., Li, B. Z. & Yuan, Y. J. Microbial Adaptation to Enhance Stress Tolerance. *Front. Microbiol.* **13**, 1–9 (2022).
43. Subramanian, C., Frank, M. W., Batte, J. L., Whaley, S. G. & Rock, C. O. Oleate hydratase from Staphylococcus aureus protects against palmitoleic acid, the major antimicrobial fatty acid produced by mammalian skin. *J. Biol. Chem.* **294**, 9285–9294 (2019).
44. Desbois, A. P. & Smith, V. J. Antibacterial free fatty acids: Activities, mechanisms of action and biotechnological potential. *Appl. Microbiol. Biotechnol.* **85**, 1629–1642 (2010).
45. Greenway, D. L. A. & Dyke, K. G. H. Mechanism of the inhibitory action of linoleic acid on the growth of Staphylococcus aureus. *J. Gen. Microbiol.* **115**, 233–245 (1979).
46. Galbraith, H. & Miller, T. B. Effect of Metal Cations and pH on the Antibacterial Activity and Uptake of Long Chain Fatty Acids. *J. Appl. Bacteriol.* **36**, 635–646 (1973).
47. Parsons, J. B., Yao, J., Frank, M. W., Jackson, P. & Rock, C. O. Membrane disruption by antimicrobial fatty acids releases low-molecular-weight proteins from staphylococcus aureus. *J. Bacteriol.* **194**, 5294–5304 (2012).
48. Pande, S. V. & Mead, J. F. Inhibition of enzyme activities by free fatty acids. *J. Biol. Chem.* **243**, 6180–6185 (1968).
49. Zheng, C. J. *et al.* Fatty acid synthesis is a target for antibacterial activity of unsaturated fatty acids. *FEBS Lett.* **579**, 5157–5162 (2005).
50. McKain, N., Shingfield, K. J. & Wallace, R. J. Metabolism of conjugated linoleic acids and 18 : 1 fatty acids by ruminal bacteria: Products and mechanisms. *Microbiology* **156**, 579–588 (2010).
51. Prem, S. A., Helmer, C. P. O., Loll, B., Garbe, D. & Brück, T. Expanding the Portfolio by a Novel Monomeric Oleate Hydratase from Pediococcus parvulus. *ChemCatChem* **15**, (2023).
52. Rosberg-Cody, E. *et al.* Myosin-cross-reactive antigen (MCRA) protein from Bifidobacterium breve is a FAD-dependent fatty acid hydratase which has a function in stress protection. *BMC Biochem.* **12**, 9 (2011).
53. Bajerski, F., Wagner, D. & Mangelsdorf, K. Cell membrane fatty acid composition of Chryseobacterium frigidisoli PB4T, isolated from antarctic glacier forefield soils, in response to changing temperature and pH conditions. *Front. Microbiol.* **8**, 1–11

(2017).

54. Kil, K. S., Cunningham, M. W. & Barnett, L. A. Cloning and sequence analysis of a gene encoding a 67-kilodalton myosin- cross-reactive antigen of Streptococcus pyogenes reveals its similarity with class II major histocompatibility antigens. *Infect. Immun.* **62**, 2440–2449 (1994).
55. Radka, C. D., Batte, J. L., Frank, M. W., Rosch, J. W. & Rock, C. O. Oleate Hydratase (OhyA) Is a Virulence Determinant in Staphylococcus aureus. *Microbiol. Spectr.* **9**, 1–6 (2021).
56. Volkov, A. *et al.* Myosin cross-reactive antigen of Streptococcus pyogenes M49 encodes a fatty acid double bond hydratase that plays a role in oleic acid detoxification and bacterial virulence. *J. Biol. Chem.* **285**, 10353–10361 (2010).
57. Chen, Y. Y., Liang, N. Y., Curtis, J. M. & Gänzle, M. G. Characterization of linoleate 10-hydratase of Lactobacillus plantarum and novel antifungal metabolites. *Front. Microbiol.* **7**, 1–11 (2016).
58. Kengmo Tchoupa, A. & Peschel, A. Staphylococcus aureus Releases Proinflammatory Membrane Vesicles To Resist Antimicrobial Fatty Acids. *mSphere* **5**, (2020).
59. Malachowa, N. *et al.* Characterization of a staphylococcus aureus surface virulence factor that promotes resistance to oxidative killing and infectious endocarditis. *Infect. Immun.* **79**, 342–352 (2011).
60. Hirata, A. *et al.* A novel unsaturated fatty acid hydratase toward C16 to C22 fatty acids from Lactobacillus acidophilus. *J. Lipid Res.* **56**, 1340–1350 (2015).
61. Kang, W.-R., Seo, M.-J., Shin, K.-C., Park, J.-B. & Oh, D.-K. Comparison of Biochemical Properties of the Original and Newly Identified Oleate Hydratases from Stenotrophomonas maltophilia. *Appl. Environ. Microbiol.* **83**, 1–11 (2017).
62. Busch, H. *et al.* Exploring the abundance of oleate hydratases in the genus Rhodococcus—discovery of novel enzymes with complementary substrate scope. *Appl. Microbiol. Biotechnol.* **104**, 5801–5812 (2020).
63. Kim, K. R. *et al.* Unveiling of novel regio-selective fatty acid double bond hydratases from Lactobacillus acidophilus involved in the selective oxyfunctionalization of mono- and di-hydroxy fatty acids. *Biotechnol. Bioeng.* **112**, 2206–2213 (2015).
64. Volkov, A. *et al.* Crystal structure analysis of a fatty acid double-bond hydratase from Lactobacillus acidophilus. *Acta Crystallogr. Sect. D Biol. Crystallogr.* **69**, 648–657 (2013).
65. Engleder, M. *et al.* Structure-Based Mechanism of Oleate Hydratase from

Elizabethkingia meningoseptica. *ChemBioChem* **16**, 1730–1734 (2015).

66. Radka, C. D., Batte, J. L., Frank, M. W., Young, B. M. & Rock, C. O. Structure and mechanism of Staphylococcus aureus oleate hydratase (OhyA). *J. Biol. Chem.* **296**, (2021).
67. Betancor, L. *et al.* Use of physicochemical tools to determine the choice of optimal enzyme: Stabilization of D-amino acid oxidase. *Biotechnol. Prog.* **19**, 784–788 (2003).
68. Serra, S., De Simeis, D., Marzorati, S. & Valentino, M. Oleate hydratase from lactobacillus rhamnosus atcc 53103: A fadh2-dependent enzyme with remarkable industrial potential. *Catalysts* **11**, 1–14 (2021).
69. Ottaviano, F. G., Handy, D. E. & Loscalzo, J. Redox regulation in the extracellular environment. *Circ. J.* **72**, 1–16 (2008).
70. McDonald, A. G. & Tipton, K. F. Parameter Reliability and Understanding Enzyme Function. *Molecules* **27**, 1–18 (2022).
71. Small, D. M. Physical Properties of Fatty Acids and their Extracellular and Intracellular Distribution. *Polyunsaturated Fat. Acids Hum. Nutr. Nestlé Nutr. Work. Séries* **28**, (1992).
72. Todea, A. *et al.* Increase of stability of oleate hydratase by appropriate immobilization technique and conditions. *J. Mol. Catal. B Enzym.* **119**, 40–47 (2015).
73. Hauer, B. Embracing Nature's Catalysts: A Viewpoint on the Future of Biocatalysis. *ACS Catal.* **10**, 8418–8427 (2020).
74. Brück, T. & Lorenzen, J. A process for the cell-free enzymatic production of 10-hydroxystearic acid (10-HSA) from bio-based oils for lubricant formulation. (2019).
75. Federsel, H. J., Moody, T. S. & Taylor, S. J. C. Recent trends in enzyme immobilization—concepts for expanding the biocatalysis toolbox. *Molecules* **26**, (2021).
76. Hagedoorn, P. L., Hoolmann, F. & Hanefeld, U. Novel oleate hydratases and potential biotechnological applications. *Appl. Microbiol. Biotechnol.* (2021).
77. Song, J.-W. *et al.* Multistep Enzymatic Synthesis of Long-Chain α,ω-Dicarboxylic and ω-Hydroxycarboxylic Acids from Renewable Fatty Acids and Plant Oils. *Angew. Chemie* **125**, 2594–2597 (2013).
78. Marella, E. R. *et al.* A single-host fermentation process for the production of flavor lactones from non-hydroxylated fatty acids. *Metab. Eng.* **61**, 427–436 (2020).
79. Wood, P. L. Fatty acyl esters of hydroxy fatty acid (FAHFA) lipid families. *Metabolites* **10**, 1–8 (2020).

80. Awang, R., Azizan, A. N., Ahmad, S. & Yunus, Z. W. Characterization of estolides from dihydroxystearic acid. in (2007).
81. Isbell, T. A., Abbott, T. P. & Dworak, J. A. Shampoos and conditioners containing estolides. (2000).
82. National Center for Biotechnology Information (NCBI). Bethesda (MD): National Library of Medicine (US), National Center for Biotechnology Information. (1988). Available at: https://www.ncbi.nlm.nih.gov/.
83. Huang, J.-K. *et al.* A novel secondary alcohol dehydrogenase from Micrococcus luteus WIUJH20: purification, cloning, and properties. *FASEB J.* **24**, 835.5-835.5 (2010).
84. Wu, Y. X., Pan, J., Yu, H. L. & Xu, J. H. Enzymatic synthesis of 10-oxostearic acid in high space-time yield via cascade reaction of a new oleate hydratase and an alcohol dehydrogenase. *J. Biotechnol. X* **2**, 3–7 (2019).
85. Li, J., Webster, T. J. & Tian, B. Functionalized Nanomaterial Assembling and Biosynthesis Using the Extremophile Deinococcus radiodurans for Multifunctional Applications. *Small* **15**, 1–15 (2019).
86. Griffiths, M. J., Van Hille, R. P. & Harrison, S. T. L. Selection of direct transesterification as the preferred method for assay of fatty acid content of microalgae. *Lipids* **45**, 1053–1060 (2010).
87. De Carvalho, C. C. C. R. Adaptation of Rhodococcus erythropolis cells for growth and bioremediation under extreme conditions. *Res. Microbiol.* **163**, 125–136 (2012).
88. Small, D. M. Physical Properties of Fatty Acids and their Extracellular and Intracellular Distribution. *Polyunsaturated Fat. Acids Hum. Nutr. Nestlé Nutr. Work. Ser.* **28**, 25–39 (1992).
89. Cistola, D. P., Hamilton, J. A., Jackson, D. & Small, D. M. Ionization and Phase Behavior of Fatty Acids in Water: Application of the Gibbs Phase Rule. *Biochemistry* **27**, 1881–1888 (1988).
90. Wintrode, P. L., Zhang, D., Vaidehi, N., Arnold, F. H. & Goddard, W. A. Protein dynamics in a family of laboratory evolved thermophilic enzymes. *J. Mol. Biol.* **327**, 745–757 (2003).
91. Reis, P., Holmberg, K., Watzke, H., Leser, M. E. & Miller, R. Lipases at interfaces: A review. *Adv. Colloid Interface Sci.* **147**–**148**, 237–250 (2009).
92. Giver, L., Gershenson, A., Freskgard, P. O. & Arnold, F. H. Directed evolution of a thermostable esterase. *Proc. Natl. Acad. Sci. U. S. A.* **95**, 12809–12813 (1998).
93. Cheng, Z. *et al.* Computational design of nitrile hydratase from pseudonocardia

thermophila JCM3095 for improved thermostability. *Molecules* **25**, 1–18 (2020).

94. Gajdoš, M. *et al.* Chiral Alcohols from Alkenes and Water: Directed Evolution of a Styrene Hydratase. *Angew. Chemie - Int. Ed.* **62**, 1–6 (2023).
95. Sun, Q. F., Zheng, Y. C., Chen, Q., Xu, J. H. & Pan, J. Engineering of an oleate hydratase for efficient C10-Functionalization of oleic acid. *Biochem. Biophys. Res. Commun.* **537**, 64–70 (2021).
96. Joo, Y. C. *et al.* Biochemical characterization and FAD-binding analysis of oleate hydratase from Macrococcus caseolyticus. *Biochimie* **94**, 907–915 (2012).
97. Yang, B. *et al.* Myosin-cross-reactive antigens from four different lactic acid bacteria are fatty acid hydratases. *Biotechnol. Lett.* **35**, 75–81 (2013).
98. Takeuchi, M. *et al.* Characterization of the linoleic acid δ9 hydratase catalyzing the first step of polyunsaturated fatty acid saturation metabolism in Lactobacillus plantarum AKU 1009a. *J. Biosci. Bioeng.* **119**, 636–641 (2015).
99. Schroepfer, G. J. & Bloch, K. The Stereospecific Conversion of Stearic Acid to Oleic Acid. *J. Biol. Chem.* **240**, 54–63 (1965).
100. McPherson, A. & Gavira, J. A. Introduction to protein crystallization. *Acta Crystallogr. Sect. FStructural Biol. Commun.* **70**, 2–20 (2014).
101. Grob, P. *et al.* Crystal Contact Engineering Enables Efficient Capture and Purification of an Oxidoreductase by Technical Crystallization. *Biotechnol. J.* **15**, (2020).
102. Derewenda, Z. S. Rational protein crystallization by mutational surface engineering. *Structure* **12**, 529–535 (2004).
103. Immerstrand, T. *et al.* Characterization of the properties of pediococcus parvulus for probiotic or protective culture use. *J. Food Prot.* **73**, 960–966 (2010).
104. Fröhlich-Wyder, M.-T. *et al.* Swiss-Type Cheeses. in *Encyclopedia of Dairy Sciences (Third Edition)* (eds. McSweeney, P. L. H. & McNamara, J. P.) 386–399 (Academic Press, 2022). doi:https://doi.org/10.1016/B978-0-12-818766-1.00212-9
105. Zanoni, B., Garzaroli, C., Anselmi, S. & Rondinini, G. Modeling the growth of Enterococcus faecium in bologna sausage. *Appl. Environ. Microbiol.* **59**, 3411–3417 (1993).
106. Onyango, L. A., Dunstan, R. H., Gottfries, J., von Eiff, C. & Roberts, T. K. Effect of low temperature on growth and ultra-structure of staphylococcus spp. *PLoS One* **7**, 1–10 (2012).
107. Ma, Y. & Marquis, R. E. Thermophysiology of Streptococcus mutans and related lactic-acid bacteria. *Antonie van Leeuwenhoek, Int. J. Gen. Mol. Microbiol.* **72**, 91–

100 (1997).

108. Okuley, J. *et al.* Arabidopsis FAD2 gene encodes the enzyme that is essential for polyunsaturated lipid synthesis. *Plant Cell* **6**, 147–158 (1994).
109. Galliard, T. & Stumpf, P. K. Fat Metabolism in Higher Plants. *J. Biol. Chem.* **241**, 5806–5812 (1966).
110. Kleiger, G. & Eisenberg, D. GXXXG and GXXXA motifs stabilize FAD and NAD(P)-binding rossmann folds through Cα-H···O hydrogen bonds and van der Waals interactions. *J. Mol. Biol.* **323**, 69–76 (2002).
111. Papadopoulos, J. & Agarwala, R. COBALT: constraint-based alignment tool for multiple protein sequences. *Bioinformatics* **23**, 1073–79 (2007).
112. Robert, X. & Gouet, P. Deciphering key features in protein structures with the new ENDscript server. *Nucl. Acids Res.* **42**, W320–W324 (2014).
113. Debarbieux, L. & Beckwith, J. On the functional interchangeability, oxidant versus reductant, of members of the thioredoxin superfamily. *J. Bacteriol.* **182**, 723–727 (2000).
114. Chakraborty, S., Nian, F. S., Tsai, J. W., Karmenyan, A. & Chiou, A. Quantification of the Metabolic State in Cell-Model of Parkinson's Disease by Fluorescence Lifetime Imaging Microscopy. *Sci. Rep.* **6**, 1–9 (2016).
115. Prinz, W. A., Åslund, F., Holmgren, A. & Beckwith, J. The role of the thioredoxin and glutaredoxin pathways in reducing protein disulfide bonds in the Escherichia coli cytoplasm. *J. Biol. Chem.* **272**, 15661–15667 (1997).
116. Massey, V., Stankovich, M. & Hemmerich, P. Light-Mediated Reduction of Flavoproteins with Flavins as Catalysts. *Biochemistry* **17**, 1–8 (1978).
117. Yang, Z. *et al.* Cryptochromes Orchestrate Transcription Regulation of Diverse Blue Light Responses in Plants. *Photochem. Photobiol.* **93**, 112–127 (2017).
118. Grajek, H. Review - Flavins as photoreceptors of blue light and their spectroscopic properties. *Curr. Top. Biophys.* **34**, 53–65 (2012).
119. Bouly, J. P. *et al.* Cryptochrome blue light photoreceptors are activated through interconversion of flavin redox states. *J. Biol. Chem.* **282**, 9383–9391 (2007).
120. Lukacs, A. *et al.* Photoexcitation of the blue light using FAD photoreceptor AppA results in ultrafast changes to the protein matrix. *J. Am. Chem. Soc.* **133**, 16893–16900 (2011).
121. Cairns, W. L. & Metzler, D. E. Photochemical Degradation of Flavins. VI. A New Photoproduct and Its Use in Studying the Photolytic Mechanism. *J. Am. Chem. Soc.* **225**, 2772–2777 (1971).
122. Sagiroglu, A. Conversion of sunflower oil to biodiesel by alcoholysis using

immobilized lipase. *Artif. Cells, Blood Substitutes, Biotechnol.* **36**, 138–149 (2008).

123. Vanleeuw, E. *et al.* Substrate-Specificity of Candida rugosa Lipase and Its Industrial Application. *ACS Sustain. Chem. Eng.* **7**, 15828–15844 (2019).
124. Ostojčić, M. *et al.* Production of biodiesel by Burkholderia cepacia lipase as a function of process parameters. *Biotechnol. Prog.* **37**, 0–2 (2021).
125. Kim, B. S., Kim, H. R. & Hou, C. T. Effect of surfactant on the production of oxygenated unsaturated fatty acids by Bacillus megaterium ALA2. *N. Biotechnol.* **27**, 33–37 (2010).
126. Kim, B. N., Joo, Y. C., Kim, Y. S., Kim, K. R. & Oh, D. K. Production of 10-hydroxystearic acid from oleic acid and olive oil hydrolyzate by an oleate hydratase from Lysinibacillus fusiformis. *Appl. Microbiol. Biotechnol.* **95**, 929–937 (2012).
127. Wu, Y., Pan, J., Yu, H. & Xu, J. Enzymatic synthesis of 10-oxostearic acid in high space-time yield via cascade reaction of a new oleate hydratase and an alcohol dehydrogenase. 3–7 (2019). doi:10.1016/j.btecx.2019.100008